TABLE OF CONTENTS

SUMMARY	ii	1/A12
TABLE OF CONTENTS	iii	1/A1
LIST OF FIGURES	iv	1/A2
LIST OF TABLES	vi	1/A4
LIST OF SYMBOLS	vii	1/A5
§ 1. Introduction	1	1/A13
§ 2. History of the two dimensional problem	3	1/B1
§ 3. Theory of airfoil polynomials	21	1/C5
§ 4. Analytical and numerical properties of Bland's equation	28	1/C12
§ 5. Organization of the computer program	47	1/E3
§ 6. Some numerical considerations	51	1/E7
§ 7. Use of the TWODI program	63	1/F5
§ 8. Convergence characteristics of TWODI	68	1/F10
§ 9. Comparison with the Söhngen solution	71	1/F13
§10. Comparison with the Küssner-Schwarz solution	76	1/G4
§11. Verification and extension of Bland's results	85	1/G13
§12. Combined effects of depth to chord ratio and wall ventilation	90	2/A13
§13. Effect of wall ventilation of airfoil - tunnel acoustic resonance	107	2/C2
§14. Concluding remarks	111	2/C8
REFERENCES	113	2/C8
APPENDIX	119	2/C14

LIST OF FIGURES

1. Coordinate system and airfoil contour. 4 1/B2
2. Airfoil in a wind tunnel 15 1/B13
3. Airfoil polynomials. 22 1/C6
4. Interdigitation of zeros 25 1/C9
5. Calling hierarchy of the TWODI program 50 1/E6
6. The eigenvalue problem $\tan\lambda+\gamma\lambda=0$. 52 1/E8
7. Spectra of $\tan\lambda+\gamma\lambda=0$ vs. $\tan^{-1}\gamma$ 55 1/E11
8. $F(\delta)$ and $F'(\delta)$ for k=0 and $\gamma=0,1,\infty$ 59 1/F1
9. Parametric behavior of $F(\delta)$ vs. k for $M=0,\eta_H=10,\gamma=1$. 60 1/F2
10. Parametric behavior of $F(\delta)$ vs. M for $k=2\pi,\eta_H=10,\gamma=1$ 61 1/F3
11. Parametric behavior of $F'(\delta)$ vs. M for $k=2\pi,\eta_H=10,\gamma=1$. 62 1/F4
12. Deflections and pressures for the Söhngen comparison 75 1/G3
13. Pressures for the Küssner-Schwarz comparison with k=1. . . . . 84 1/G12
14. Lift coefficient vs. ventilation angle for M=.85,k=0 and $\eta_H=7.5$. . . . 87 2/A10
15. Moment coefficient vs. ventilation angle for M=.85,k=0 and $\eta_H=7.5$. . . 88 2/A11
16. Center of pressure vs. ventilation angle for M=.85,k=0 and $\eta_H=7.5$. . . 89 2/A12
17. Wind tunnel depth angle. 90 2/A13
18. Lift coefficient C_{L_α} vs. depth and ventilation for M=0 and k=0 . . . . 93 2/B2
19. Lift coefficient C_{L_α} vs. depth and ventilation for $M=\frac{1}{\sqrt{2}}$ and k=0. . . . 94 2/B3
20. Moment coefficient C_{M_α} vs. depth and ventilation for M=0 and k=0 . . . 95 2/B4
21. Moment coefficient C_{M_α} vs. depth and ventilation for $M=\frac{1}{\sqrt{2}}$ and k=0. . . 96 2/B5
22. Center of pressure $\bar{x}_{CP}$ vs. depth and ventilation for M=0 and k=0 . . . 97 2/B6
23. Center of pressure $\bar{x}_{CP}$ vs. depth and ventilation for $M=\frac{1}{\sqrt{2}}$ and k=0. . . 98 2/B7
24. Lift coefficient magnitude $|C_{L_h}|$ vs. depth and ventilation for M=0 and k=.1 . . . . . 99 2/B8
25. Lift coefficient magnitude $|C_{L_\alpha}|$ vs. depth and ventilation for M=0 and k=.1 . . . . . 100 2/B9
26. Moment coefficient magnitude $|C_{M_h}|$ vs. depth and ventilation for M=0 and k=.1 . . . . . 101 2/B10
27. Moment coefficient magnitude $|C_{M_\alpha}|$ vs. depth and ventilation for M=0 and k=.1 . . . . . 102 2/B11

28. Lift phase angle ϕ_{L_h} vs. depth and ventilation for M=0 and k=.1. . . . 103 **2/B12**

29. Lift phase angle ϕ_{L_α} vs. depth and ventilation for M=0 and k=.1. . . . 104 **2/B13**

30. Moment phase angle ϕ_{M_h} vs. depth and ventilation for M=0 and k=.1. . . 105 **2/B14**

31. Moment phase angle ϕ_{M_α} vs. depth and ventilation for M=0 and k=.1. . . 106 **2/C1**

32. Effect of ventilation on $|C_{L_\alpha}|$ vs. k with acoustic resonance effects . 109 **2/C4**

33. Effect of ventilation on ϕ_{L_α} vs. k with acoustic resonance effects . . 110 **2/C5**

LIST OF TABLES

1.	Convergence of function subroutine PICARD.	54	1/E10
2.	Accuracy of subroutine SUM for γ=k=0	58	1/E14
3.	Convergence of C_{L_α} vs. NP for M=0 and k=0.	68	1/F10
4.	Convergence of $\bar{x}_{CP}$ vs. NP for M=0 and k=0.	68	1/F10
5.	Convergence of P_{ψ_n} vs. NP for M=0, k=0 and η_H=10	69	1/F11
6.	Convergence of P_{ψ_n} vs. NP for M=.5, k=.1 and η_H=10	69	1/F11
7.	Pressures for the Söhngen comparison	73	1/G1
8.	Section coefficients for the Söhngen comparison.	73	1/G1
9.	Pressures for the Küssner-Schwarz comparison with k=1.	82	1/G10
10.	Section coefficients for the Küssner-Schwarz comparison with k=1 . .	83	1/G11
11.	Generalized aerodynamic forces for the Küssner-Schwarz comparison with k=1	83	1/G11
12.	Lift coefficient C_{L_α} vs. η_H and c_W for M=.85, and k=0.	86	1/G14
13.	Resonant frequencies vs. ventilation coefficient for M=$\frac{\sqrt{3}}{2}$ and η_H=10.	108	2/C3

LIST OF SYMBOLS

This section provides a partial list of frequently occurring symbols and their names. Places of first occurrence or definition are given by section number denoted with §, by equation number enclosed in parentheses, etc. In a few instances the same symbol is used for different meanings but it will be clear from the context which is correct. Any consistent system of physical units may be employed, although most quantities are nondimensional.

Symbol	Name	Place
$A, C(A)$	Complex matrix, condition number.	§4.5
A_{rs}	Components of generalized aerodynamic force matrix.	(3-39)
$\underline{a} = \{\hat{a}_n\}$	Matrix of unknowns with quadrature approximation.	(4-46), (4-47)
a_n	Coefficients of pressure basis functions.	(2-5)
b	Airfoil semichord.	(2-8)
b_n	Coefficients of downwash basis functions.	(2-6)
$C(k)$	Theodorsen's circulation function.	(2-17)
Ci	Cosine integral function.	(2-12)
$C_L, \lvert C_L \rvert$	Lift coefficient and magnitude.	(3-35)
$C_M, \lvert C_M \rvert$	Moment coefficient and magnitude.	(3-36)
C_{L_h}, C_{L_α}	Lift coefficients due to unit plunging and pitching motions.	§§8,12
C_{M_h}, C_{M_α}	Moment coefficients due to unit plunging and pitching motions.	§§11,12
C_{L_i}, C_{M_i}	Lift and moment coefficients due to ith deflection function.	§10
c_∞	Speed of sound.	(2-43)
c_W	Wall ventilation coefficient.	(2-49)
$E = [\varepsilon_{mn}]$	Matrix of quadrature errors.	§4.4

Symbol	Name	Place
F,F'	Function defined by infinite series, and its derivative.	(2-51)
f,f'	Function defined by infinite series, and its derivative.	(6-10),(6-11)
$\hat{f},\hat{f}'$	Closed form sums for infinite series and its derivative.	(6-12),(6-13)
G	Infinite series of Mathieu functions.	(2-40)
G	Matrix of inner products $\langle\psi_m,\chi_n\rangle_2$	§4.4
$[g_{mn}]$	Quadrature of $G = [\langle\psi_m,\chi_n\rangle_2]$.	§4.4
H_1,H_2	Hilbert spaces.	§4.2
$[H_1,H_2]$	Bounded linear operators from H_1 to H_2.	§4.2
H,H^{-1},H^*	Element of $[H_1,H_2]$, its inverse and adjoint.	§4.2
H,H^{-1}	Bland transforms.	(3-25),(3-26)
$H_n^{(2)}$	Hankel function of the second kind.	(2-18)
h	Airfoil profile function.	Figure 1
h_r	rth structural basis function.	(3-39)
h_{nr}	nth generalized Fourier coefficient of h_r.	(3-40)
I	Identity operator in a Hilbert space.	§4
Im	Imaginary part.	Table 9
I_n	Interval.	§6
i	Imaginary unit, $i^2 = -1$.	(2-9)
J_n	Bessel function of the first kind.	(2-18)
$K,\tilde{K}$	Kernel functions.	(2-1),(4-4)
K_C,K_{SC}	Continuous parts of kernel functions.	(4-3),(4-5)
K,K_i	Compact operators.	Definition 4.2
k	Reduced frequency. Also integer parameter.	(2-8)
$\hat{k}$	Reduced frequency under Küssner transformation.	(2-33)
k_n	Resonant reduced frequencies.	(2-44)
k_{max}	Maximum number of iterations.	(6-8)
L	Compact operator.	(4-28)

Symbol	Name	Place
$\underline{L} = [L_m(x_k)]$	Collocation matrix.	(4-48)
L_w^2, L_p^2	Spaces of Lebesgue square integrable functions for downwash and pressure.	(3-11), (3-12)
M	Mach number, v_∞/c_∞. Also integer parameter.	(2-30)
ND	Number of decimals of accuracy.	(6-18)
Ne_n	Mathieu function of the third kind.	(2-40)
NP	Number of pressure basis functions.	(2-5)
NQ	Number of quadrature points.	(2-24)
NT	Number of terms in an infinite series calculation.	(6-18)
n,N	Integer.	
P	Nonsingular factor of pressure. Also a matrix of polynomial values in §4.	(2-56), Theorem 4.10
P_{ψ_n}	Generalized Fourier coefficient of P.	(3-24)
P_{ns}	Generalized Fourier coefficient of P due to h_s.	(3-41)
P_N	Approximation to pressure function P.	(4-1)
P_N^C, P_N^G	Collocation and Galerkin approximation to pressure function P.	Theorem 4.12
$\hat{P}_N^C$	Quadrature approximation to P_N^G.	Theorem 4.12
P_n	Polynomials.	Theorem 4.10
Q_n	Orthogonal projection operator.	(4-12)
Re	Real part.	(2-9)
R_n, r_n	Residual errors.	(4-2), (4-32)
Si	Sine integral function.	(2-12)
se_n	Mathieu function of the first kind.	(2-40)
T, T_n	Compact operators.	§4
$T(k), T(\kappa,\hat{k})$	Functions used by Küssner that are related to Theodorsen's function.	(2-27), (2-41)
t	Time.	(2-9)
U_n	Span $\{\psi_k\}_1^n$.	Theorem 4.5
V	Vandermonde matrix.	Theorem 4.10
v_∞	Free stream velocity.	(2-8)

Symbol	Name	Place
$W, [\ W\ ]$	Diagonal matrices of quadrature weights.	(4-48),(2-24)
$\underline{W}, \{w(x_m)\}$	Column matrices of downwashes.	(4-47),(2-24)
$[w_n(x_m)]$	Rectangular matrix of induced downwashes.	(2-23),(2-24)
$w(x), w_n(x)$	Downwash functions.	(2-4),(2-22)
$\tilde{w}$	Downwash multiplied by $\frac{4}{\beta}$.	§4.2
$x, y, \hat{x}, \hat{y}$	Body coordinates.	Figure 1,(2-33)
x, y	Vectors in a Hilbert space.	Definition 4.3
$\bar{x}_{CP}$	Center of pressure as a fraction of chord, aft of leading edge.	Table 4
x_m	Quadrature nodes. Also collocation points.	(2-24)
x_j^n	Zero of χ_n.	(3-24)
Y_n	Bessel function of the second kind.	(2-18)
β	Co Mach number, $\sqrt{1-M^2}$.	(2-21)
γ	Wind tunnel parameter.	(2-55)
$\Delta p, \Delta p_s$	Pressure jump.	(2-1)
δ	Difference variable.	(2-51)
δ_{mn}	Kronecker delta: $\delta_{mn} = 1$ if $m = n$, $\delta_{mn} = 0$ if $m \neq n$.	(3-5)
δ_{min}	Smallest argument of F.	(6-15)
ε	Error tolerance.	§6
$\varepsilon_{[A]}$	Supremum error norm of generalized aerodynamic force matrix.	(10-17)
ε_{mn}	Quadrature errors.	§4.4
ζ_n	Frequency ratio.	(2-53)
η	Dummy variable. Also elliptic coord.	(2-26),(2-38)
η_H	Wind tunnel depth to airfoil chord ratio.	Figure 2
$\eta_x(\xi)$	$K_C(x-\xi)$.	§4.2
θ	Angular streamwise coordinate.	(2-14)
θ_H, θ_W	Tunnel depth angle and ventilation angle.	(12-1),(11-1)
κ	Compressibility frequency parameter.	(2-33)
$\Lambda(x,\xi)$	Symmetric logarithmic function in inverse kernel.	(2-29)

Symbol	Name	Place
$\lambda, \lambda_n, \lambda_n^{(k)}$	Eigenvalues and iterate.	(2-54), (6-1), (6-4)
$\hat{\lambda}_n$	Eigenvalue modified by frequency ratio.	(2-53)
ξ	Streamwise coordinate, also elliptic coordinate.	(2-3), (2-38)
ξ_i^n	Zero of ψ_n.	(3-25)
Π	Product symbol.	Theorem 4.10
π	Collocation matrix for polynomials. Also 3.14159...	Theorem 4.10
ρ_n	Convergence rate.	(6-5)
$\phi_{L_h}, \phi_{L_\alpha}$	Lift phase angles in plunging and pitching motions.	Figures 28,29
$\phi_{M_h}, \phi_{M_\alpha}$	Moment phase angles in plunging and pitching motions.	Figures 30,31
$\underline{X}$	Matrix of downwash polynomials.	(4-48)
X_n	Downwash polynomial.	(3-1)
ψ_n	Pressure polynomial.	(3-2)
ω	Frequency of oscillation (rad/sec).	(2-8)
f_{w_n}, g_{p_n}	Generalized Fourier coefficients with respect to downwash and pressure polynomials.	(3-15), (3-16)
$\langle f,g\rangle_1, \langle f,g\rangle_2$	Inner products on Hilbert spaces.	§4.2
$\langle f,g\rangle_w, \langle f,g\rangle_p$	Weighted inner products on function spaces.	(3-7), (3-8)
$\|f\|_1, \|f\|_2$	Hilbert space norms.	§4.2
$\|f\|_p, \|f\|_w$	Inner product norms.	(3-9), (3-10)
$\|\ \|$	Operator norm.	Theorem 4.2
$\|\ \|_{sup}$	Supremum norm.	(10-7)
$\rightarrow$	Implies, also limit.	§2
$\leftrightarrow$	Is equivalent to.	§3

MAY 8 1978

NAS1.26:2967

NASA Contractor Report 2967

COMPLETED
ORIGINAL

Unsteady Two Dimensional Airloads Acting on Oscillating Thin Airfoils in Subsonic Ventilated Wind Tunnels

Joseph Fromme and Michael Golberg

GRANT NSG-2140
MAY 1978

NASA

138

NAS1.26:2967

NASA Contractor Report 2967

Unsteady Two Dimensional Airloads Acting on Oscillating Thin Airfoils in Subsonic Ventilated Wind Tunnels

Joseph Fromme and Michael Golberg
University of Nevada at Las Vegas
Las Vegas, Nevada

Prepared for
Ames Research Center
under Grant NSG-2140

NASA
National Aeronautics
and Space Administration

Scientific and Technical
Information Office

1978

SUMMARY

The numerical calculation of unsteady two dimensional airloads which act upon thin airfoils in subsonic ventilated wind tunnels is studied. Neglecting certain quadrature errors, Bland's collocation method is rigorously proved to converge to the mathematically exact solution of Bland's integral equation, and a new three-way equivalence is established between collocation, Galerkin's method and least squares whenever the collocation points are chosen to be the nodes of the quadrature rule used for Galerkin's method. The computer program displays remarkable convergence with respect to the number of pressure basis functions employed, and agreement with known special cases is demonstrated. New results are obtained for the combined effects of wind tunnel wall ventilation and wind tunnel depth to airfoil chord ratio, including acoustic resonance between the airfoil and wind tunnel walls.

§1. Introduction[1]

Recent interest in aerodynamic testing at high subsonic and transonic speeds has increased the need for improved understanding of the phenomena involved, and for improved computational methods to guide experiments as well as to serve as a rational means for extrapolating wind tunnel test data to free flight conditions.

While fundamental differences exist between two and three dimensional flows, solutions of two dimensional problems provide advance insight into three dimensional flow phenomena. Calculations for two dimensional problems are significantly simpler, and testing can be performed using models with constant sections extending completely across the tunnel, or enclosed between splitter plates.

Aerodynamic interaction between the wind tunnel walls and the model, commonly termed interference, is present in all subsonic wind tunnels and becomes more complicated at higher subsonic and transonic speeds. Efforts to utilize opposing interference effects associated with closed wall and open jet tunnels have resulted in the development of ventilated wind tunnels at various facilities. Whereas theories of interference are highly developed for steady subsonic flow in fully closed or open jet tunnels, relatively little is known about unsteady flow, especially in ventilated tunnels.[2,3]

---

[1]The authors wish to acknowledge the help of Dr. Sanford S. Davis, Ms. Sara Alfont, Messrs. Tuli Haromy, Charles Doughty and Karl Kuopus.

[2]A comprehensive survey of the state of the art may be found in the work by Garner, Rogers, Acum and Maskell [1,1966]. See also Goethert [2,1961], Glauert [3,1933] and Pope and Harper [4,1966].

[3]Numbers in square brackets refer to the bibliography in the order of citation, followed by the year of publication, and possibly the page, section or chapter of interest.

This work addresses the problem of predicting unsteady airloads on oscillating thin planar airfoils in subsonic ventilated wind tunnels, and extends the earlier work of Bland [5,1970] which is based on an approximate ventilation boundary condition that is exact for only the closed wall and open jet conditions.

We rigorously establish in Section 4 that Bland's collocation method must converge to the mathematically exact solution of his integral equation. The analysis is made using two sets of orthogonal polynomials, one for downwash the other for pressure. These polynomials, called airfoil polynomials, enable an elegant formulation in terms of dual generalized Fourier series. The known closed form Söhngen and Küssner-Schwarz solutions are reformulated in terms of airfoil polynomials, and used to evaluate the accuracy of the computer calculations.

The computer program developed during this study is called TWODI and will calculate pressures, section coefficients and generalized aerodynamic forces for arbitrary combinations of Mach number, reduced frequency, tunnel depth to airfoil chord ratio, ventilation coefficient and downwash. TWODI is shown to be in accurate agreement with known closed form results and extends previous results of unsteady flow to ventilated tunnels. Various calculations are presented, including predictions of the combined effects of depth to chord ratio, and of acoustic resonance between the wind tunnel walls and the airfoil.

While the reader who wishes to avoid theoretical considerations cannot help but be at some disadvantage, it is possible to use the TWODI program by proceeding directly to Section 7. Other sections may then be read as the interest arises.

§2. History of the two dimensional problems

This section presents an extensive although not complete history of developments in the problem of predicting airloads in unsteady two dimensional subsonic flow. Attention is given to the emergence of exact closed form solutions because these provide permanent and enduring standards of comparison for numerical as well as theoretical considerations. The integral equations relating downwash and pressure in linearized potential flow are especially emphasized.

Three dimensional results are generally excluded except insofar as they relate to the two dimensional problem. Nevertheless we note that one of the most important uses of two dimensional theories is to provide insight into the practical matters of three dimensional problems.

The most important engineering application of unsteady aerodynamics traditionally has been to calculate forcing functions for structural dynamics and aeroelasticity. This interest is readily apparent in the earliest papers, and it may be observed that a recurring practical problem has been to maintain acceptable accuracy at higher frequencies. While the physical conditions which justify linearized inviscid theories are not satisfied at arbitrarily high frequencies, an arbitrary frequency capability is worthy because the ability to analyze arbitrary time dependence demands it mathematically.

We begin with a brief description of the airfoil equation. By 1918, Prandtl at Göttingen had completed the theory of bound vortices, and Ackermann had performed calculations for steady lift on airfoils at low speed. However, Ackermann's work was interrupted by the war and was not reported until afterward by Birnbaum [6,1923], then only at Prandtl's request. Comparable calculations were performed in the United States by Munk [7,1922], [8,1924]. Restated in terms of pressure jump rather than vorticity, it was necessary to solve an integral equation of the form

$$w(x) = \int_{-1}^{1} K(x-\xi)\Delta p(\xi)d\xi \qquad (2\text{-}1)$$

where the kernel is given by

$$K(x) = \frac{1}{4\pi x}, \qquad (2\text{-}2)$$

and subject to the Kutta condition that the pressure jump vanish at the trailing edge

$$\lim_{\xi \to 1} \Delta p(\xi) = 0^{1}. \tag{2-3}$$

The downwash, assumed known, is given for steady flow by the streamwise derivative of the vertical coordinate of the airfoil contour:

$$w(x) = \frac{dh}{dx} \tag{2-4}$$

The coordinate system and airfoil contour are shown in Figure 1.

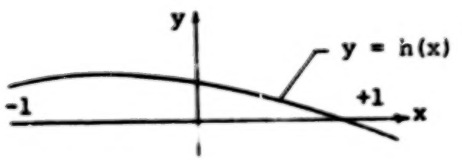

Figure 1. Coordinate system and airfoil contour

We shall refer to the integral equation (2-1) with kernel given by equation (2-2) and subject to the Kutta condition (2-3) as the airfoil equation. It may be observed that the airfoil equation is a singular Fredholm integral equation of the first kind and its kernel is of difference type with a Cauchy singularity.[2] Much of the difficulty encountered in

---

[1]We shall generally, but not always, follow the practice of stating values of the downwash function in terms of x and values of the pressure function in terms of ξ for the purpose of emphasizing certain symmetries.

[2]An integral equation of the form

$$f(x) = \int_a^b K(x,\xi)u(\xi)d\xi$$

where f is a known function and K is a known function (called the kernel function) is said to be a Fredholm integral equation for u of the first kind. An integral equation of the form

$$f(x) = u(x) + \int_a^b K(x,\xi)u(\xi)d\xi$$

is said to be a Fredholm integral equation of the second kind. If the kernel depends upon the difference $x-\xi$, it is said to be of difference type and we write $K(x-\xi)$. If the kernel is bounded for all values of x and ξ, the integral equation is said to be nonsingular, otherwise singular. If the kernel is of difference type and of the form

$$K(x-\xi) = \frac{C}{x-\xi}$$

where C is a constant, it is singular and is said to have a Cauchy singularity.

solving the airfoil equation and related equations in aerodynamics may be attributed to the fact that until recently, no general theory existed for the solution to integral equations of the first kind. The translation and publication of Ivanov's book [9,1976] indicates that substantial activity has been taking place in the Soviet Union in this area, much of it unreported in the Western literature. Without detailed examination of this work its relationship (if any) to ours remains unclear.

The airfoil equation, based upon classical linear potential flow theory, is rigorously valid for zero Mach number steady two dimensional flow about an airfoil with profile differing infinitesimally from the x-axis. Noting the linearity of the airfoil equation, Birnbaum calculated the first order effect of thickness by using the difference between the upper and lower surface profiles, and calculated the lift and moment using the centerline profile, for profiles described by third degree polynomials. The pressure functions

$$\sqrt{\frac{1-\xi}{1+\xi}}, \qquad \sqrt{1-\xi^2}, \qquad \xi\sqrt{1-\xi^2}$$

when substituted into the airfoil equation produce downwash functions that are constant, linear and quadratic, respectively, and satisfy the Kutta condition. The Birnbaum-Ackermann calculations consist of integrating in closed form each of the above basis functions (Grundfunktionen) to obtain an induced downwash (induzierte Vertikalgeschwindigkeit), which is integrated in turn to produce a profile function. These profile functions are then superimposed to represent an arbitrary profile of third degree. The general procedure is to represent the pressure as a linear combination of NP prescribed pressure basis functions

$$\Delta p(\xi) = a_1\sqrt{\frac{1-\xi}{1+\xi}} + a_2\sqrt{1-\xi^2} + \ldots + a_{NP}\xi^{NP-2}\sqrt{1-\xi^2} \qquad (2\text{-}5)$$

and to determine the unknown coefficients according to a prescribed profile which is given by a corresponding linear combination of basis functions, in this case, powers of x,

$$h(x) = b_1x + b_2x^2 + \ldots + b_{NP}x^{NP}. \qquad (2\text{-}6)$$

Although no discussion was made of collocation, residual error or convergence, the method of solution appearing in the Birnbaum-Ackermann paper of 1923 is a forerunner of modern collocation solutions to the integral equations of aerodynamics.

The first published calculations for unsteady flow are due to Birnbaum [10,1922] and are closely connected with the Birnbaum-Ackermann paper. Birnbaum was a doctoral student of Prandtl's and his dissertation was devoted to extending Prandtl's theory of bound vortices to the more difficult problem of unsteady flow. Through an analysis of free and bound vortex sheets, Birnbaum was led to infinite series of the form

$$\sum_{m \geq n} c_{mn} k^n (\log k)^n \tag{2-7}$$

which did not converge well even for small values of reduced frequency near $k = 0.10$. Birnbaum apparently coined the term reduced frequency,[3] and defined it in terms of the semichord as

$$k = \frac{\omega b}{v_\infty}. \tag{2-8}$$

He noted that the numerical limitation

$$k < .1$$

corresponded physically to less than one structural oscillation per thirty chordlengths of flow, and referred to this as a quasi-steady oscillation (quasi-stationäre Schwingungen). Birnbaum analyzed time dependence with complex Fourier series and introduced into unsteady aerodynamics the concept of complex amplitude of motion

$$h(x,t) = \mathrm{Re}[h(x)e^{i\omega t}] \tag{2-9}$$

for the particular cases of plunging and pitching, but did not use complex downwash nor complex pressure

$$w(x,t) = \mathrm{Re}[w(x)e^{i\omega t}] = \mathrm{Re}[(\frac{d}{dx} + ik)h(x)e^{i\omega t}], \tag{2-10}$$

$$\Delta p(\xi,t) = \mathrm{Re}[\Delta p(\xi)e^{i\omega t}]. \tag{2-11}$$

Lift and moment were graphed as complex vectors parameterized by reduced frequency from $k = .00$ to $k = .12$. Birnbaum's interest in structural dynamics was clear. He treated the static and dynamic stability of an elastically suspended wind tunnel model using the concept of energy transfer and presented damped and divergent experimental response curves together with theoretically calculated frequencies.

---

[3] "reduzierte Frequenz", Birnbaum [10,1922, p.12], [11,1924, p.270].

It is significant that Birnbaum did not find the integral equation between pressure and downwash for unsteady incompressible flow. This equation is the same as the airfoil equation (2-1) except that the downwash and pressure are complex as in (2-9) and (2-10), and the kernel[4] is given by

$$K(x,k) = \frac{1}{4\pi x} - \frac{ik}{4\pi} e^{-ikx}[Ci(k|x|) + iSi(kx) + \frac{i\pi}{2}] \tag{2-12}$$

where Ci and Si are the cosine and sine integrals.[5] This equation was not derived until 1938 by Possio as a limiting case of what we now call Possio's integral equation for compressible subsonic unsteady flow.

The next work on unsteady flow after Birnbaum's was published by Wagner [20,1925][6] based on his doctoral dissertation at Berlin under Hoff and Hamel. Wagner used the method of conformal mapping to solve the two transient problems of a flat plate accelerating from rest to constant velocity, and of a step change in angle of attack. Glauert [21,1929] used the same method to compute lift and moment on an oscillating airfoil for reduced frequencies up to k = .5. Küssner [22,1929] extended the frequency range further to k = 1.5, avoiding the slowly convergent series[7] of Birnbaum and expressing the pressure as

$$\Delta p(\xi) = a_0\sqrt{\frac{1-\xi}{1+\xi}} + a_1\sqrt{1-\xi^2} + a_2\xi\sqrt{1-\xi^2} + a_3(4\xi^2-1)\sqrt{1-\xi^2} + \ldots \tag{2-13}$$

By making the coordinate transformation,

$$\xi = -\cos\vartheta, \tag{2-14}$$

Küssner was able to simultaneously recast the pressure basis functions as a Fourier sine series except for the first term

$$\Delta p(\vartheta) = a_0\cot\frac{\theta}{2} + 2\sum_{n=1}^{\infty} a_n \sin n\theta \tag{2-15}$$

---

[4]See, e.g., Bland [12,1968,§4.1], [5,1970,§8].

[5]See, e.g., Abramowitz and Stegun [13,1964,§5.2]. The complex setting in Abramowitz and Stegun does not render Ci an even function. To avoid error in the logarithmic term, the absolute value sign is necessary in (2-12), and in this regard, it could be considered as missing or at least ambiguous in Possio [14,1938,p.448], Dietze [15,1946,p.22], Watkins, Runyan and Woolston [16,1955, App. B] Bisplinghoff, Ashley and Halfman [17,1955,p.325], Garrick [18,1957,p.710], and Fung [19,1969,p.429].

[6]For further discussion, see, e.g., Y.C. Fung [19,1969,§§5.8,6.7,15.1] or Bisplinghoff, Ashley and Halfman [17,1955,§5.7].

[7]See, H.G. Küssner [23,1953,§3] for further information.

and the downwash as a Fourier cosine series

$$w(\theta) = b_0 + 2\sum_{n=1}^{\infty} b_n \cos n\theta. \tag{2-16}$$

He analyzed the oscillating flat plate and approximated the discontinuous downwash of a flap with a fifth degree polynomial.

Theodorsen [24,1935] obtained the first closed form solution for the force and moment on a flat plate undergoing pitch rotation, vertical translation and aileron rotation. Theodorsen's solution, though restricted to rigid body motions, was valid for an arbitrary frequency range. He used the method of conformal mapping employed earlier by Wagner. The flutter solution for the three degree of freedom system was thus reduced to a non-Hermitian three by three matrix eigenvalue problem, and the three special cases called torsion-aileron, aileron-deflection, and deflection-torsion were solved in closed form, producing flutter velocity curves vs. in vacuo frequency ratios. Theodorsen improperly expressed his intermediate results in terms of a quotient of nonconvergent integrals

$$C(k) = \frac{\int_1^{\infty} e^{-ik\xi} \frac{\xi}{\sqrt{\xi^2-1}}\, d\xi}{\int_1^{\infty} e^{-ik\xi} \frac{\xi+1}{\sqrt{\xi^2+1}}}$$

which he identified in terms of Hankel functions of the second kind

$$C(k) = \frac{H_1^{(2)}(k)}{H_1^{(2)}(k) + iH_0^{(2)}(k)} \tag{2-17}$$

where

$$H_n^{(2)}(k) = J_n(k) - iY_n(k) \tag{2-18}$$

and where J_n and Y_n are standard Bessel functions of the first and second kinds.[8] The function C(k) is called Theodorsen's circulation function. Although his derivation of it was faulty, the result was shown later by Schwarz to be correct.[9]

---

[8]See, e.g., Abramowitz and Stegun [13,1964].

[9]Schwarz [25,1940,§4]. See also the discussion in Bisplinghoff, Ashley and Halfman [17,1955,p.272].

Shortly after Theodorsen's solution in 1934 for three downwash functions, the same problem for arbitrary downwash functions was solved independently by Cicala [26,1935] and Küssner [27,1936]. They showed that the coefficients of the downwash and pressure basis functions appearing in equations (2-15) and (2-16) are related recursively:

$$a_0 = \frac{b_0 H_1^{(2)}(k) + i b_1 H_0^{(2)}(k)}{H_1^{(2)}(k) + i H_0^{(2)}(k)}, \tag{2-19}$$

$$a_n = \frac{ik}{2n} b_{n-1} - b_n - \frac{ik}{2n} b_{n+1}; \; n \geq 1. \tag{2-20}$$

The importance of the Cicala-Küssner extension to arbitrary downwash functions is notable. While rigid body motions as discussed by Theodorsen are important, higher flexible modes are essential to the theory of aeroelasticity. Whereas chordwise flexibility is typically insignificant in two dimensional flow, it has long been recognized as significant in the design of modern airplanes,[10] and the ability of a two dimensional aerodynamic method to shed practical light on three dimensional methods requires that it possess an arbitrary chordwise downwash capability.

The problem of unsteady airloads on an airfoil entering a sharp-edged gust was solved for incompressible flow by von Kármán and Sears [29,1938] using conformal mapping. In the same year, Possio [14,1938] obtained the kernel relating the downwash and pressure for compressible subsonic flow about an oscillating airfoil:

$$K(x,k,M) = \frac{k}{8\beta} e^{-ikx}\{\exp(\frac{ikx}{\beta^2})[iM \operatorname{sgn}(x) H_1^{(2)}(\frac{kM|x|}{\beta^2}) + H_0^{(2)}(\frac{kM|x|}{\beta^2})]$$
$$+ \frac{2i}{\pi}\beta \log\frac{1+\beta}{M} + ik\int_0^x \exp(\frac{ik\lambda}{\beta^2}) H_0^{(2)}(\frac{kM|\lambda|}{\beta^2})\,d\lambda\}. \tag{2-21}$$

Although Possio did not explicitly write down the integral equation,[11] he performed numerical calculations for lift and moment on an oscillating flat plate at values of reduced frequency up to k = .6 and at four values of Mach number, M = 0,.25,.50, and .70. Using the same pressure basis

---

[10] See, e.g., Turner, Clough, Martin and Topp [28,1956,p.805].

[11] The Possio integral equation first appears in Küssner's Allgemeine Tragflächentheorie [30,1940,§7] as a special case of the Küssner integral equation for three dimensional flow.

functions as Birnbaum, Possio observed that the solution to the integral equation required that the linear combination of downwashes induced by the pressure basis functions must equal the prescribed downwash at all points on the airfoil; i.e.,

$$w(x) = \sum_{n=1}^{NP} a_n w_n(x), \tag{2-22}$$

which is in general not possible. Possio resolved this difficulty by collocating (2-22) at an equal number of discrete points according to the system of linear algebraic equation

$$\sum_{n=1}^{NP} w_n(x_m) a_n = w(x_m);\ m = 1,\ldots,NP. \tag{2-23}$$

This is the earliest use we have found of the method of collocation to solve an integral arising in aerodynamics.

We note that a least square error solution of equation (2-22) in which the overall error is integrated numerically and then minimized results in the matrix equation

$$\underset{NPxNQ}{[w_n(x_m)]^*}\underset{NQxNQ}{[\ W_m\ ]}\underset{NQxNP}{[w_n(x_m)]}\underset{NPx1}{\{a_n\}} = \underset{NPxNQ}{[w_n(x_m)]^*}\underset{NQxNQ}{[\ W_m\ ]}\underset{NQx1}{\{w(x_m)\}}, \tag{2-24}$$

where x_m; $m = 1,\ldots,NQ$ are the nodes of the quadrature rule and W_m; $m = 1,\ldots,NQ$ are its weights, and where * denotes the complex conjugate of the transposed matrix, a fact sometimes missed.[12]

Under fairly restrictive assumptions, Söhngen [32,1939] proved that the solution to the airfoil equation is given by

$$\Delta p(\xi) = \frac{4}{\pi}\sqrt{\frac{1-\xi}{1+\xi}}\int_{-1}^{1}\sqrt{\frac{1+x}{1-x}}\ \frac{w(x)}{\xi-x}\,dx, \tag{2-25}$$

which is called the <u>Söhngen inversion formula</u> and is a particular case of a more general formula given in [33,1953,Ch 11]. These restrictions were later weakened by Söhngen [34,1954] to include all downwash functions of class $L^p, p>1$.[13] A weaker proof based on the stronger assumption that $p>\frac{4}{3}$ was given by Tricomi [35,1951] and appears in his book on integral equations

---

[12]Since the error is a real valued nonconstant function of several complex variables, it is not differentiable. A rigorous proof of (2-24) is given by Fromme [31,1964, Appendix A].

[13]A function f belongs to class L^p over the interval I if $\int_I |f(x)|^p dx$ is finite.

[36,1957]. Söhngen's later proof and Tricomi's proof both identify the integral equation (2-1) with the difference kernel (2-2) as a finite Hilbert transform.[14] We point out that these mathematical results make essential use of the condition that the pressure be finite at the trailing edge (and hence zero, thereby satisfying the Kutta condition (2-3)), for otherwise the finite Hilbert transform has no unique solution in the L^p space, $p>1$, and contains an additional term of the form

$$\frac{C}{\sqrt{1-\xi^2}}$$

where C is an arbitrary constant. Therefore, if the Kutta condition is denied, the solution to the airfoil equation is not unique.

Five important papers appeared in 1940: 1) Küssner published the integral equation relating pressure and downwash in unsteady three dimensional flow;[15] (2) Küssner and Schwarz [39], [40] analytically summed the series (2-15), (2-16), (2-19) and (2-20) to provide in closed form the pressure in terms of downwash for oscillatory flow as

$$\Delta p(\theta) = \frac{4}{\pi}\int_0^{\pi}\Big\{\frac{\sin\theta}{\cos\theta-\cos\eta} + \frac{ik}{2}\sin\eta\,\log\frac{1-\cos(\eta+\theta)}{1-\cos(\eta-\theta)} + \cot\frac{\theta}{2}[1+\cos\eta+(1-\cos\eta)T(k)]\Big\}w(\eta)\,d\eta \qquad (2\text{-}26)$$

where

$$T(k) = \frac{H_1^{(2)}(k) - i\,H_0^{(2)}(k)}{H_1^{(2)}(k) + i\,H_0^{(2)}(k)} = 2C(k) - 1; \qquad (2\text{-}27)$$

(3) Küssner [41,1940] used the method of Laplace transforms to extend the solution (2-25) to arbitrary time dependence; (4) Schwarz [25,1940] used the Söhngen inversion formula to obtain the solution (2-26) by an independent approach; and (5) Söhngen [42,1940] used the inversion formula (2-25),

---

[14] The finite Hilbert transform of ϕ is the function f with values given by

$$f(x) = \frac{1}{\pi}\int_{-1}^{1}\frac{\phi(\xi)}{\xi-x}\,d\xi.$$

See also Sneddon [37,1971,p.238,p.467].

[15] H.G. Küssner [30,1940], [38,1940]. However, the kernel was not put into a computationally tractable form until fifteen years later by Watkins, Runyan and Woolston [16,1955].

together with Birnbaum's method and Laplace transforms to derive the solution for the oscillating airfoil and for an airfoil starting from rest. Equation (2-26) is called the Küssner-Schwarz solution and in Cartesian coordinates it is given by

$$\Delta p(\xi) = \frac{4}{\pi}\sqrt{\frac{1-\xi}{1+\xi}}\int_{-1}^{1}\left\{\sqrt{\frac{1+x}{1-x}}\left[\frac{1}{\xi-x}+1-C(k)\right]-ik\Lambda(x,\xi)\sqrt{\frac{1+\xi}{1-\xi}}\right\}w(x)\,dx, \tag{2-28}$$

where

$$\Lambda(x,\xi) = \log\left|\frac{\sqrt{\frac{1+\xi}{1-\xi}}+\sqrt{\frac{1+x}{1-x}}}{\sqrt{\frac{1+\xi}{1-\xi}}-\sqrt{\frac{1+x}{1-x}}}\right|. \tag{2-29}$$

Taking advantage of the theoretical developments principally by Theodorsen and Küssner, Smilg and Wasserman [43,1942] published their AFTR 4798 which was to serve for years as the standard reference in the United States on flutter. The kernel to Possio's equation was tabulated by Schwarz [44,1943], and Possio's numerical calculations based on the method of collocation were extended by Fraser [45,1941], Fraser and Skan [46,1942], and Schade.[16] Dietze,[17] working under the supervision of Söhngen, introduced an iteration method to solve Possio's integral equation approximately, making use of the known Küssner-Schwarz solution. Dietze's iteration method consists of, given the downwash, calculating the pressure according to the Küssner-Schwarz solution for incompressible flow, and calculating the downwash required by that pressure according to Possio's integral equation. The residual error in downwash furnishes the starting point for successive iterations. Dietze's calculations were for values of reduced frequency up to k = 1.0 for pitch rotation, vertical translation and flap rotation. In a major review of the two dimensional problem, done in two parts by Karp, Shu and Weil [52,1947], and Karp and Weil [53,1948], it is observed that in the case of a discontinuity in downwash the Dietze iteration will not eliminate the logarithmic singularity at the discontinuity so that slow pointwise convergence might be found in the neighborhood of a discontinuity. Additional calculations with Dietze's method by Turner and Rabinowitz [54,1950] indicated that numerical values of overall section

---

[16] T. Schade [47,1944]. An English translation is available as [48,1946].

[17] F. Dietze [49,1943], [50,1944]. English translations are available as [15,1946] and [51,1947]. A description of Dietze's method may be found in Y.C. Fung [19,1969,§14.5].

coefficients appeared to be acceptable, but that the rate of convergence deteriorated for larger values of Mach number and reduced frequency. Apparently no mathematical proof of convergence of Dietze's method has ever been given. A compilation of tables from various references was given by Luke [55,1950], and another method which approximated the continuous part of Possio's kernel by a polynomial was introduced by Pettis [56,1952].

The next major advance comparable to the Küssner-Schwarz solution is a general solution to Possio's integral equation using elliptic coordinates and Mathieu functions. It is obtained by starting from the basic differential field equations and boundary conditions

$$\nabla^2\phi - M^2(\frac{\partial}{\partial x} + ik)^2\phi = 0 \tag{2-30}$$

$$p = -2(\frac{\partial}{\partial x} + ik)\phi, \tag{2-31}$$

$$w(x) = \lim_{y\to 0} \frac{\partial\phi}{\partial y}, \quad |x| \leq 1. \tag{2-32}$$

Upon making the Küssner transformation in the form[18]

$$\hat{x} = x, \ \hat{y} = \frac{y}{\beta}, \ \hat{k} = \frac{k}{\beta^2}, \ \kappa = \frac{kM}{\beta^2}, \tag{2-33}$$

$$\phi = \beta e^{i\kappa x}\hat{\phi}, \ w = \beta e^{i\kappa x}\hat{w}, \ p = e^{i\kappa x}\hat{p}, \tag{2-34}$$

there results

$$\hat{\nabla}^2\hat{\phi} + \kappa^2\hat{\phi} = 0, \tag{2-35}$$

$$\hat{p} = -2(\frac{\partial\hat{\phi}}{\partial\hat{x}} + i\hat{k}\,\hat{\phi}), \tag{2-36}$$

$$\hat{w}(\hat{x}) = \lim_{\hat{y}\to 0} \frac{\partial\hat{\phi}}{\partial\hat{y}}, \quad |\hat{x}| \leq 1. \tag{2-37}$$

Applying Green's identities, integrating (2-36), and introducing elliptic coordinates (ξ,η) according to

$$x = -\cosh\xi\cos\eta, \ y = \sinh\xi\sin\eta, \tag{2-38}$$

---

[18]This transformation, valid for arbitrary time dependence in three dimensional flow, was first used in aerodynamics by Küssner [30,1940,§3], and is a combination of the Galilean and Lorentz transformations. See, e.g., Miles [57,1959,§§2.3,2.4]. For the special case of steady flow, Küssner's transformation reduces to the Prandtl-Glauert transformation.

Küssner [23,1953,§§2-4] showed that

$$\hat{p}(\xi,\theta) = \frac{2}{\pi}\int_0^{\pi}\{G,_{\eta}(\kappa,\xi,0,\theta)\ [G,_{\theta}(\kappa,0,\eta,\pi)T(\kappa,\hat{k})-G,_{\theta}(\kappa,0,\eta,0)]$$
$$+\ (i\hat{k}-\frac{1}{\sin\eta}\frac{\partial}{\partial\eta})G(\kappa,\xi,\eta,\theta)\}\hat{w}(\eta)\sin\eta\,d\eta, \qquad (2\text{-}39)$$

where

$$G(\kappa,\xi,\eta,\theta) = \sum_{n=1}^{\infty}\frac{Ne_n^{(2)}(\frac{\kappa^2}{4},\xi)}{Ne_n^{(2)}(\frac{\kappa^2}{2},0)}se_n(\frac{\kappa^2}{4},\eta)se_n(\frac{\kappa^2}{4},\theta), \qquad (2\text{-}40)$$

and

$$T(\kappa,\hat{k}) = \frac{\int_{-\infty+i\pi/2}^{\infty-i\pi/2}\exp(-i\hat{k}\cosh\xi)G,_{\eta\theta}(\kappa,\xi,0,\pi)d\xi}{\int_{-\infty+i\pi/2}^{\infty-i\pi/2}\exp(-i\hat{k}\cosh\xi)G,_{\eta\theta}(\kappa,\xi,0,0)d\xi}. \qquad (2\text{-}41)$$

In the above, partial differentiation is denoted with a comma followed by a subscript, and se_n and $Ne_n^{(2)}$ denote Mathieu functions of the first and third kind, respectively.[19] Equations (2-39), (2-40) and (2-41) reduce in the case M = 0 to equations (2-26) and (2-27).

The application of elliptic coordinates and Mathieu functions to the unsteady flow equations was undertaken first by Reissner and Sherman [59,1944], followed with apparently independent work by Biot [60,1946], Timman [61,1946], and Haskind [62,1947].[20] Among these, Timman's was the most successful. Further work was done by Billington [64,1949], Timman and van de Vooren [65,1949], Reissner [66,1951] and [67,1951], Timman, van de Vooren and Griedanus [68,1951], Küssner [23,1953],[21] van Spiegel and van de Vooren [69,1953], de Jager [70,1954], and Williams [71,1955]. Despite its success, the method of elliptic coordinates and Mathieu functions has been slow in gaining the recognition it merits.

Using successive conformal mappings and Jacobian elliptic functions, Timman [72,1951] obtained in closed form the exact solution for pressure on

---

[19] See, e.g., N.W. McLachlan [58,1947].

[20] In Russian. An English translation is available as [63,1947].

[21] This contains a comprehensive and elegant discussion of the two dimensional problem up to that time.

an oscillating airfoil in a wind tunnel with parallel closed walls. Timman's solution is for incompressible flow and reduces to the Küssner-Schwarz solution in the limiting case of infinite tunnel depth. The analysis applies to a centrally located airfoil as shown in Figure 2.

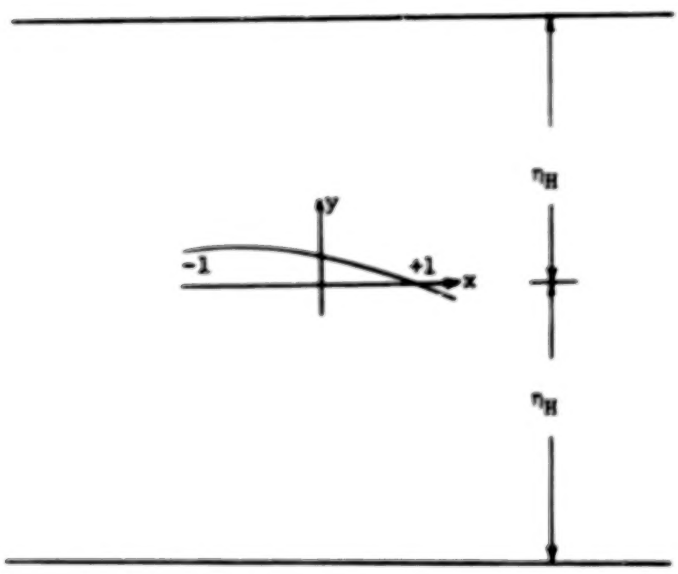

Figure 2. Airfoil in a wind tunnel

The condition that the tunnel wall be closed is the kinematical one that the component of velocity normal to the wall vanish at the wall.

$$\frac{\partial}{\partial y}\,\phi(x,\pm\eta_H) = 0. \tag{2-42}$$

For incompressible flow, wind tunnel wall effects tend to become maximum at some small value of reduced frequency and to diminish as the frequency is increased further. Disturbances produced by an oscillating airfoil are reflected by the walls instantaneously in the sense that the acoustic transit time for a given distance is much less than the flow transit time for the same distance. Mathematically this ratio of transit times is zero because $\frac{v}{c} = M = 0$. However, when the fluid is compressible, a nonzero

transit time is required and it is possible for the frequency of airfoil oscillation to be such that succeeding disturbances arrive back at the airfoil so as to reinforce one another, thereby causing an acoustic resonance. Runyan and Watkins [73,1953] predicted that this resonance phenomenon would occur at frequencies given by

$$\omega_n = \frac{\pi\beta c_\infty}{b\eta_H}(n-\frac{1}{2});\ n = 1,2,... \tag{2-43}$$

These resonant frequencies are finite for all subsonic Mach numbers in a compressible fluid, and become lower as the Mach increases. The resonant reduced frequencies are

$$k_n = \frac{\pi\beta}{M\eta_H}(n-\frac{1}{2});\ n = 1,2,... \tag{2-44}$$

and decrease rapidly at higher Mach numbers. For example,

$$M = \frac{\sqrt{3}}{2}\ \&\ \eta_H = 10 \rightarrow k_1 = .090690. \tag{2-45}$$

Thus, acoustic resonance between the airfoil and the tunnel becomes an important phenomenon at high subsonic speeds because it occurs at relatively low values of reduced freqvency. Furthermore, these resonant frequencies are the same for all downwashes.

Runyan and Watkins also showed that the pressure and downwash are related for subsonic compressible flow in a closed wind tunnel by an integral equation of the form (2-1) where the kernel may be expressed as the sum of the Possio kernel (2-21) plus an incremental part representing the presence of the walls. The incremental kernel becomes singular at the resonant frequencies (2-44) and since the kernel may be interpreted physically as the downwash at one point due to unit pressure at another point, the pressure should drop to zero at resonance. This effect is entirely analogous to the elementary spring-mass system in which vanishingly small forces can produce large amplitudes when the excitation frequency is sufficiently close to the resonant frequency.

The above theoretical predictions were verified experimentally and computationally by Runyan, Woolston and Rainey [74,1956]. The kernel function was approximated by assuming the tunnel depth to chord ratio to be large, the pressure was represented by the first three terms of the

series (2-15), and the integral equation was collocated at three points. Good agreement was obtained between theory and experiment for phase angles and fair agreement was obtained for magnitudes. Resonant frequencies were predicted accurately by the theory, and the expected drop in lift at resonance appeared to be quite abrupt.

Bland, Rhyne and Pierce [75,1967] extended the theory to include narrow channel flow in connection with destructive oscillations in nuclear rocket engines. The kernel obtained previously by Runyan and Watkins was expressed as a single function in a simpler form without using the deep tunnel approximation:

$$K(x,k,M,\eta_H) = \frac{k}{8}(1+\operatorname{sgn} x)e^{-ikx}\tanh k\eta_H$$

$$+ \exp\left(\frac{ikM^2x}{\beta^2}\right)\sum_{n=1}^{\infty}\left(\frac{\operatorname{sgn} x}{4\eta_H} + \frac{ik}{\pi\beta R_n}\right)\frac{\exp\left[-\frac{\pi R_n|x|}{\beta\eta_H}\right]}{1 + \left[\frac{k\eta_H}{\pi(n-\frac{1}{2})}\right]^2}, \qquad (2\text{-}46)$$

where

$$R_n = \sqrt{(n-\tfrac{1}{2})^2 - \left(\frac{Mk\eta_H}{\pi\beta}\right)^2}. \qquad (2\text{-}47)$$

At the resonant frequencies given by (2-44), the kernel (2-46) becomes infinite because $R_n = 0$. The kernel is singular at $x = 0$ and the infinite series in (2-46) behaves in the neighborhood of 0 like a slowly convergent geometric series. The pressure was represented in the form

$$\Delta p(\xi) = \sqrt{\frac{1-\xi}{1+\xi}}\sum_{n=1}^{\infty} a_n \frac{\sin\left[(n-\frac{1}{2})\cos^{-1}\xi\right]}{\sin\left[\frac{1}{2}\cos^{-1}\xi\right]} \qquad (2\text{-}48)$$

but no elaboration was offered for the reason behind this choice. Nevertheless, for continuous downwash functions, this marks the first basic improvement in the choice of pressure basis functions since 1929,[22] and as we shall see, leads to an elegant closed form generalized Fourier solution for pressure in certain special cases.

Because the physical problem of interest to Bland, Rhyne and Pierce involved low speed flow, numerical calculations were performed only with

---

[22]Cf. equation (2-15). The singularities in pressure that must accompany downwash discontinuities have been given by White and Landahl [76,1968], Landahl [77,1968] and Rowe, Sebastian and Redman [78,1976].

$M = 0$ using a form of the kernel (2-46) in which certain of the series could be summed in closed form. The integral equation was collocated using Hsu's technique [79,1958] in which collocation points are interdigitated with the quadrature points so as to minimize the error in lift on the average. Flutter calculations using two degrees of freedom were performed for depth to chord ratios from 0.06 to 2.00 and verified by experiment.

The problem of unsteady flow in ventilated wind tunnels was undertaken by Bland in his doctoral thesis [12,1968] and subsequently published in the open literature [5,1970]. Bland approximated the boundary condition at a ventilated wall by a linear combination of the boundary conditions for open and closed walls,

$$p + c_W \frac{\partial p}{\partial y} = 0 \text{ at } y = \pm\eta_H, \tag{2-49}$$

where the semi-empirical constant c_W is called the wall ventilation coefficient (D. Davis and D. Moore [80,1953] discuss an approximation of c_W for a wall with longitudinal slots.). The boundary condition (2-49) is exact only for the two limiting cases; (1) $c_W = 0$, which corresponds to an open jet and, (2) $c_W = \infty$, which corresponds to a closed wall. Treating the pressure as an odd function of y for a centrally located airfoil, Bland applied the method of Fourier transforms to derive the kernel for the integral equation between downwash and pressure. Bland's kernel can be expressed as

$$\begin{aligned} K(x,k,M,\eta_H,c_W) = {} & \frac{\beta}{4\pi x} - \frac{ik}{4\pi\beta}\log|x| + \frac{1+\operatorname{sgn}(x)}{8}\frac{1+c_W k\tanh k\eta_H}{c_W+\frac{1}{k}\tanh k\eta_H}e^{-ikx} \\ & - \frac{1}{4\eta_H}\left[\operatorname{sgn}(x)F'\left(\frac{|x|}{\beta\eta_H}\right) - \frac{ik\eta_H}{\beta}F\left(\frac{|x|}{\beta\eta_H}\right)\right]\exp\frac{ikM^2x}{\beta^2} \\ & + \frac{1}{8\eta_H}\left[\operatorname{csch}\frac{\pi x}{2\beta\eta_H} - \frac{2\beta\eta_H}{\pi x} + \left(\exp\frac{ikM^2x}{\beta^2}-1\right)\operatorname{csch}\frac{\pi x}{2\beta\eta_H}\right] \\ & - \frac{ik}{4\pi\beta}\left[\log\left(\frac{1}{x}\tanh\frac{\pi x}{4\beta\eta_H}\right) + \left(\exp\frac{ikM^2x}{\beta^2}-1\right)\log\tanh\frac{\pi|x|}{4\beta\eta_H}\right], \end{aligned} \tag{2-50}$$

where

$$F(\delta) = \sum_{n=1}^{\infty} \{\frac{a_n}{\hat{\lambda}_n} \exp(-\hat{\lambda}_n \delta) - \frac{1}{\pi(n-\frac{1}{2})} \exp[-(n-\frac{1}{2})\pi\delta]\}, \tag{2-51}$$

$$a_n = \frac{1}{[1 + \frac{\gamma}{1+(\gamma\lambda_n)^2}][1 + (\frac{k\eta_H}{\lambda_n})^2]}, \tag{2-52}$$

$$\hat{\lambda}_n = \lambda_n\sqrt{1-\zeta_n^2}, \quad \zeta_n = \frac{Mk\eta_H}{\beta\lambda_n}, \tag{2-53}$$

$$\tan \lambda_n + \gamma\lambda_n = 0, \tag{2-54}$$

$$\gamma = \frac{c_W}{\eta_H}. \tag{2-55}$$

Equations (2-50) to (2-55) are slightly modified from the form originally given. Bland used two functions in place of F and F', and we have identified one of them as the derivative of the other, resulting in a numerical simplification. The series (2-51) has been accelerated by subtracting asymptotic terms which can be summed analytically. Even with this improvement, due to Bland, the series are poorly convergent for very small values of the argument, especially for unsteady flow.

The singularities of the kernel are confined to the first two terms. The first term, a Cauchy singularity, is the dominant one and is present in all two dimensional subsonic kernels. The second term is a weaker, integrable singularity of logarithmic type and is present in all the unsteady kernels. The remaining terms are bounded and can be accurately integrated using an appropriate Gaussian quadrature rule. Bland's complete kernel reduces in special cases to all kernels given previously.

The method of solution employed by Bland is unique and is particularly interesting. From the Söhngen inversion formula, Bland observed that the function

$$P(\xi) = \sqrt{\frac{1+\xi}{1-\xi}}\, \Delta p(\xi) \tag{2-56}$$

results in an integral equation of the form

$$w(x) = \int_{-1}^{1} \sqrt{\frac{1-\xi}{1+\xi}}\, K(x-\xi)P(\xi)d\xi \tag{2-57}$$

and that in the special case of the airfoil equation if w is a polynomial, then P is a polynomial of the same degree. This property is based on the Bland integral transforms and will be discussed further in Section 3. Using this result as a starting point for equations with more complicated kernels, Bland introduced airfoil polynomials and used them to evaluate integrals of the singular part of the kernel in closed form and integrals of the bounded part using Jacobi-Gaussian quadrature. Collocation and quadrature points were interdigitated following Hsu's technique, and remarkably good numerical convergence with respect to the number of pressure basis functions was obtained. Numerical results including flutter calculations were presented for several problems of interest.

Of the methods considered in this study, Bland's is the most germane to the problem of unsteady two dimensional subsonic flow in ventilated wind tunnels, it has superior numerical characteristics, and it is the most general.

Convergence of Bland's method is proved for the first time in Section 4. We note that the proof of convergence of Bland's method hinges on the Cauchy singularity and is largely independent of the particular form of the remaining part of the kernel.

§3. Theory of airfoil polynomials[1]

The theory of airfoil polynomials springs from the solution to the airfoil equation for steady incompressible flow using the Bland transform, and may be applied to the numerical solution of any problem for which the linear transformation from pressure to downwash is a singular integral equation of the first kind whose kernel is dominated by a Cauchy singularity.

Let

$$\chi_n(x) = \frac{\cos[(n-\frac{1}{2})\cos^{-1}x]}{\cos[\frac{1}{2}\cos^{-1}x]}; \quad n = 1,2,... \tag{3-1}$$

$$\psi_n(\xi) = \frac{\sin[(n-\frac{1}{2})\cos^{-1}\xi]}{\sin[\frac{1}{2}\cos^{-1}\xi]}; \quad n = 1,2,... \tag{3-2}$$

be defined on the open interval (-1,1). These functions, shown in Figure 3, are polynomials of degree n-1:

$$\chi_1(x) = 1,\ \chi_2(x) = -1+2x,...,\ \chi_{n+2}(x) = 2x\chi_{n+1}(x)-\chi_n(x),\ ... \tag{3-3}$$

$$\psi_1(\xi) = 1,\ \psi_2(\xi) = 1+2\xi,...,\ \psi_{n+2}(\xi) = 2\xi\psi_{n+1}(\xi)-\psi_n(\xi),\ ... \tag{3-4}$$

The above recursion formulas are neutrally stable so that computational errors are neither damped nor magnified with increasing n.

These polynomials are orthogonal with respect to reciprocal weight functions

$$\frac{1}{\pi}\int_{-1}^{1}\sqrt{\frac{1+x}{1-x}}\,\chi_m(x)\chi_n(x)dx = \delta_{mn}, \tag{3-5}$$

$$\frac{1}{\pi}\int_{-1}^{1}\sqrt{\frac{1-\xi}{1+\xi}}\,\psi_m(\xi)\psi_n(\xi)d\xi = \delta_{mn}, \tag{3-6}$$

---

[1]Proofs of most of the results stated in this section may be found in Bland [12,1968, pp.79-90].

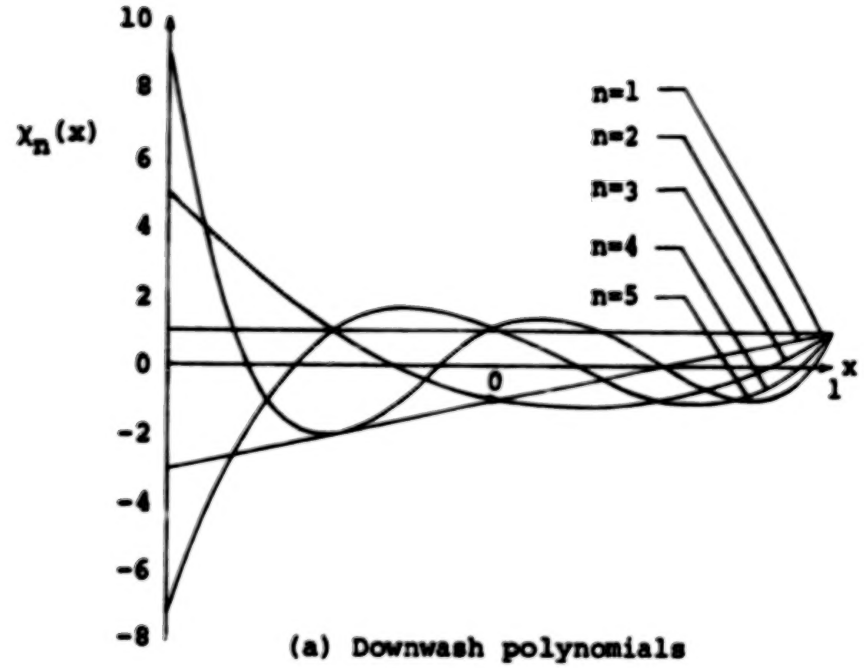

(a) Downwash polynomials

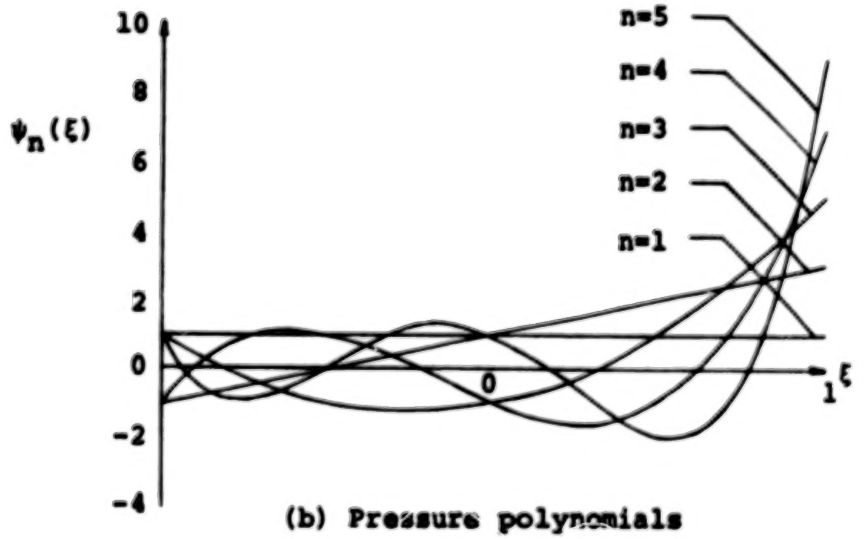

(b) Pressure polynomials

Figure 3. Airfoil polynomials

and lead to two generalized Fourier series, one for downwash, the other for pressure. Let

$$\langle f,g\rangle_w \equiv \frac{1}{\pi}\int_{-1}^{1}\sqrt{\frac{1+x}{1-x}}\,f(x)\bar{g}(x)dx, \tag{3-7}$$

$$\langle f,g\rangle_p \equiv \frac{1}{\pi}\int_{-1}^{1}\sqrt{\frac{1-\xi}{1+\xi}}\,f(\xi)\bar{g}(\xi)d\xi \tag{3-8}$$

denote complex inner products with respect to the above weight functions, let

$$\|f\|_w = \sqrt{\langle f,f\rangle_w}, \tag{3-9}$$

$$\|f\|_p = \sqrt{\langle f,f\rangle_p} \tag{3-10}$$

denote their inner product norms, and let

$$L_w^2 = \{f:\|f\|_w<\infty\}, \tag{3-11}$$

$$L_p^2 = \{f:\|f\|_p<\infty\}. \tag{3-12}$$

The equivalence classes of L_w^2 and L_p^2 induced by these norms[2] are Hilbert spaces and the polynomials $\{\chi_n\}_1^\infty$ and $\{\psi_n\}_1^\infty$ can be shown to be respective bases for them. Thus, if $f\epsilon L_w^2$ and $g\epsilon L_p^2$, then

$$f = \sum_{n=1}^{\infty} f_{\chi_n}\,\chi_n, \tag{3-13}$$

$$g = \sum_{n=1}^{\infty} g_{\psi_n}\,\psi_n, \tag{3-14}$$

where we adopt the abbreviated notation

$$f_{\chi_n} \equiv \langle f,\chi_n\rangle_w = \frac{1}{\pi}\int_{-1}^{1}\sqrt{\frac{1+x}{1-x}}\,f(x)\chi_n(x)dx, \tag{3-15}$$

$$g_{\psi_n} \equiv \langle g,\psi_n\rangle_p = \frac{1}{\pi}\int_{-1}^{1}\sqrt{\frac{1-\xi}{1+\xi}}\,g(\xi)\psi_n(\xi)d\xi \tag{3-16}$$

for the generalized Fourier coefficients. Since these polynomials are complete, the only functions which are orthogonal to all of them are null;

---

[2]The equivalence class of $f\epsilon L_w^2$ is the set of all functions g such that $\|f-g\|_w = 0$, and similarly for $f\epsilon L_p^2$. In general the Fourier series of a function need not converge everywhere to the value of the function itself, particularly in the case of a flap where the downwash function is discontinuous. The notion of an equivalence class enables functions and their Fourier series to be treated as essentially the same. Henceforth, unless stated to the contrary, we shall not distinguish between different representatives of equivalence classes.

i.e.,

$$f \in L_w^2 \;\&\; f_{\chi_n} = 0 \;\forall\; n \rightarrow f = 0, \tag{3-17}$$

$$g \in L_p^2 \;\&\; g_{\psi_n} = 0 \;\forall\; n \rightarrow g = 0. \tag{3-18}$$

The role of airfoil polynomials in aerodynamics stems from their being integral transform pairs of one another:

$$\frac{1}{\pi} \int_{-1}^{1} \sqrt{\frac{1+x}{1-x}}\, \frac{\chi_n(x)}{x-\xi}\, dx = \psi_n(\xi), \tag{3-19}$$

$$\frac{1}{\pi} \int_{-1}^{1} \sqrt{\frac{1-\xi}{1+\xi}}\, \frac{\psi_n(\xi)}{x-\xi}\, d\xi = \chi_n(x) \tag{3-20}$$

and from recognizing that the airfoil equation and the Söhngen inversion formula can be recast in the same form:

$$P(\xi) = \frac{1}{\pi} \int_{-1}^{1} \sqrt{\frac{1+x}{1-x}}\, \frac{4w(x)}{x-\xi}\, dx, \tag{3-21}$$

$$4w(x) = \frac{1}{\pi} \int_{-1}^{1} \sqrt{\frac{1-\xi}{1+\xi}}\, \frac{P(\xi)}{x-\xi}\, d\xi. \tag{3-22}$$

From the above, it follows that

$$w = \sum_{n=1}^{\infty} w_{\chi_n} \chi_n \;\&\; P \in L_p^2 \leftrightarrow P = 4\sum_{n=1}^{\infty} w_{\chi_n} \psi_n \;\&\; w \in L_w^2. \tag{3-23}$$

In other words, for steady incompressible flow, the generalized Fourier coefficients of the nonsingular pressure function P with respect to $\{\psi_n\}_1^\infty$ are equal to four times the generalized Fourier coefficients of the downwash function w with respect to $\{\chi_n\}_1^\infty$: i.e.,

$$P_{\psi_n} = \langle P, \psi_n \rangle_p = 4 \langle w, \chi_n \rangle_w = 4 w_{\chi_n}. \tag{3-24}$$

For this reason, the functions χ_n are called <u>downwash polynomials</u> and the functions ψ_n are called <u>pressure polynomials</u>.

The integral transforms appearing in (3-19)-(3-22) are central to the theory of airfoil polynomials. They appear to have been first discovered by N.I. Akhiezer in 1945 and are discussed briefly in [9,1976,Ch 2,p.133]. However, since these insights were apparently initially applied to the solution of practical aerodynamics problems by Bland in his thesis [12,1968], we shall define the integral transforms

$$Hf(x) = \frac{1}{\pi} \int_{-1}^{1} \sqrt{\frac{1-\xi}{1+\xi}} \frac{f(\xi)}{x-\xi} \, d\xi, \tag{3-25}$$

$$H^{-1}f(\xi) = \frac{1}{\pi} \int_{-1}^{1} \sqrt{\frac{1+x}{1-x}} \frac{f(x)}{x-\xi} \, dx \tag{3-26}$$

as Bland transforms.

The functions χ_n and ψ_n are related to Chebyshev polynomials and can be shown to be constant multiples of Jacobi polynomials.[3] Their n-1 zeros are given by

$$\chi_n(x_i^n) = 0; \; x_i^n = -\cos \frac{2i\pi}{2n-1}; \; i = 1,\ldots,n-1; \; n \geq 2, \tag{3-27}$$

$$\psi_n(\xi_i^n) = 0; \; \xi_i^n = \cos \frac{2i\pi}{2n-1}; \; i = 1,\ldots,n-1; \; n \geq 2, \tag{3-28}$$

are antisymmetric in the sense that $\xi_i^n = -x_i^n$, and are interdigitated according to

$$-1 < \xi_{n-1}^n < x_1^n < \ldots < \xi_1^n < x_{n-1}^n < 1, \tag{3-29}$$

as shown in Figure 4.

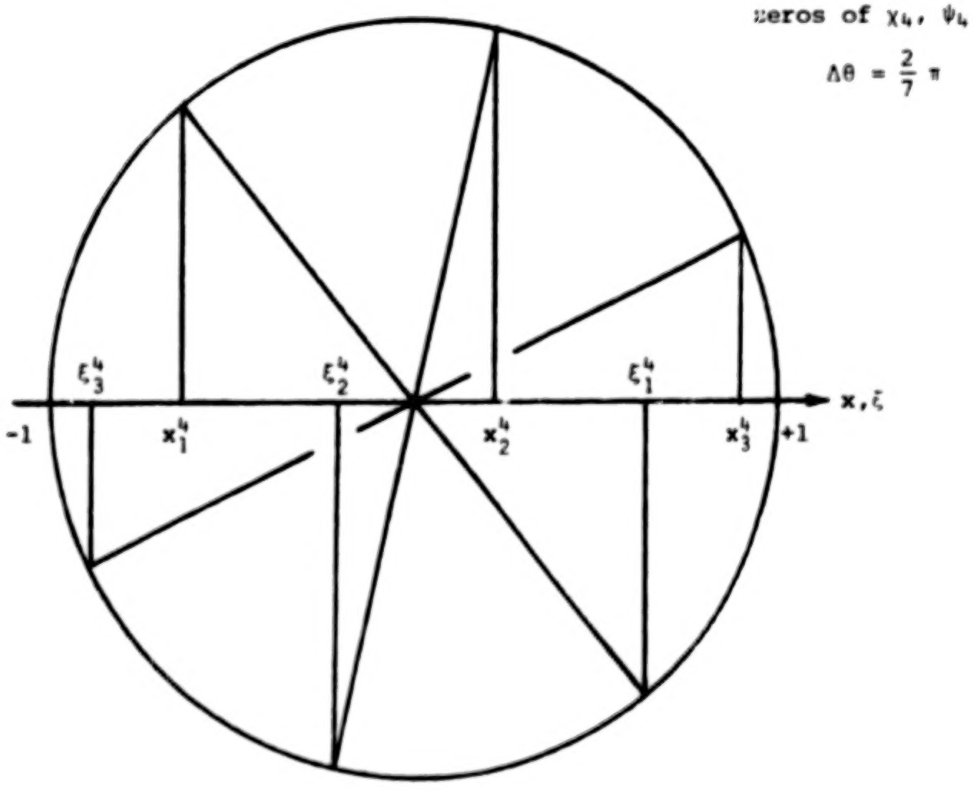

Figure 4. Interdigitation of zeros

[3] See, Bland [12,1968,pp. 79-80] and Abramowitz and Stegun [13,1964,Ch. 22].

The logarithmic transforms

$$\frac{1}{\pi}\int_{-1}^{1}\sqrt{\frac{1+x}{1-x}}\,\chi_n(x)\log|x-\xi|\,dx = \begin{cases} -\dfrac{\psi_2(\xi)+(1+\log 2)\psi_1(\xi)}{2}, & n=1 \\ -\dfrac{\psi_{n+1}(\xi)-\psi_n(\xi)}{2n}-\dfrac{\psi_n(\xi)-\psi_{n-1}(\xi)}{2(n-1)}, & n\geq 2 \end{cases} \tag{3-30}$$

$$\frac{1}{\pi}\int_{-1}^{1}\sqrt{\frac{1-\xi}{1+\xi}}\,\psi_n(\xi)\log|x-\xi|\,d\xi = \begin{cases} \dfrac{\chi_2(x)+(1+\log 2)\chi_1(x)}{2}, & n=1 \\ \dfrac{\chi_{n+1}(x)+\chi_n(x)}{2n}-\dfrac{\chi_n(x)+\chi_{n-1}(x)}{2(n-1)}, & n\geq 2 \end{cases} \tag{3-31}$$

permit closed form integrations of a logarithmic singularity appearing in the kernel, and the continuous part of the kernel may be integrated according to the following NQ-point Jacobi-Gaussian quadrature rule:

$$\int_{-1}^{1}\sqrt{\frac{1+x}{1-x}}\,f(x)\,dx \approx \frac{2\pi}{2NQ+1}\sum_{i=1}^{NQ}(1+x_i^{NQ+1})f(x_i^{NQ+1}), \tag{3-32}$$

$$\int_{-1}^{1}\sqrt{\frac{1-\xi}{1+\xi}}\,f(\xi)\,d\xi \approx \frac{2\pi}{2NQ+1}\sum_{i=1}^{NQ}(1-\xi_i^{NQ+1})f(\xi_i^{NQ+1}). \tag{3-33}$$

If the generalized Fourier coefficients for the continuous factor of pressure are known,

$$P = \sum_{n=1}^{\infty} P_{\psi_n}\,\psi_n \tag{3-34}$$

then the lift and pitching moment coefficients[4]

$$C_L \equiv \frac{1}{2}\int_{-1}^{1}\Delta p(\xi)\,d\xi, \tag{3-35}$$

$$C_M \equiv \frac{1}{2}\int_{-1}^{1}(\xi+\tfrac{1}{2})\Delta p(\xi)\,d\xi \tag{3-36}$$

are given exactly by the first two Fourier coefficients alone:

$$C_L = \frac{1}{2}\int_{-1}^{1}\sqrt{\frac{1-\xi}{1+\xi}}\,\psi_1(\xi)\sum_{n=1}^{\infty}P_{\psi_n}\,\psi_n(\xi)\,d\xi = \frac{\pi}{2}P_{\psi_1}, \tag{3-37}$$

$$C_M = \frac{1}{4}\int_{-1}^{1}\sqrt{\frac{1-\xi}{1+\xi}}\,\psi_2(\xi)\sum_{n=1}^{\infty}P_{\psi_n}\,\psi_n(\xi)\,d\xi = \frac{\pi}{4}P_{\psi_2}. \tag{3-38}$$

---

[4]In this definition lift is positive upward, and pitching moment is positive counterclockwise (leading edge down) about the quarter chord and is based on the semichord.

Exact closed form expressions similar to (3-37) and (3-38) may be obtained for the generalized aerodynamic force matrix. The components A_{rs} of this matrix are defined as the virtual work done as the structure deforms in mode r against the pressure corresponding to mode s:

$$A_{rs} \equiv \frac{1}{2}\int_{-1}^{1} h_r(\xi)\Delta p_s(\xi)d\xi;\ r,\ s = 1,2,... \tag{3-39}$$

where $\{h_r\}_{r=1}^{\infty}$ are structural basis functions, commonly selected in practice as the in vacuo vibrational eigenfunctions. Expand the structural basis functions and their corresponding pressure functions in the pressure polynomials

$$h_r(\xi) = \sum_{n=1}^{\infty} \langle h_r,\psi_n\rangle_p\ \psi_n(\xi) = \sum_{n=1}^{\infty} h_{nr}\ \psi_n(\xi);\ r = 1,2,... \tag{3-40}$$

$$\Delta p_s(\xi) = \sqrt{\frac{1-\xi}{1+\xi}}\ \sum_{n=1}^{\infty} \langle p_s,\psi_n\rangle_p\ \psi_n(\xi) = \sqrt{\frac{1-\xi}{1+\xi}}\ \sum_{n=1}^{\infty} P_{ns}\ \psi_n(\xi);\ s = 1,2,... \tag{3-41}$$

and obtain

$$A_{rs} = \frac{1}{2}\ \sum_{n=1}^{\infty} \langle h_r,\psi_n\rangle_p \langle p_s,\psi_n\rangle_p = \frac{\pi}{2}\ \sum_{n=1}^{\infty} h_{nr}\ P_{ns};\ r,\ s = 1,2,... \tag{3-42}$$

The generalized aerodynamic force matrix may be considered to be the single most important aerodynamic quantity in aeroelasticity because it completely determines the aeroelastic coupling.

§4. Analytical and numerical properties of Bland's equation

In this section we discuss some of the theoretical aspects of the collocation method developed by Bland for the solution of (2-57). In particular it will be shown that the apparent numerical convergence observed by Bland and ourselves can be established theoretically. In order to do this it is necessary to take a somewhat different viewpoint toward collocation than has been done in the past. We regard, as did Bland, collocation as only a secondary numerical method arising out of somewhat different procedures. Bland, in his thesis, proposed a generalized least squares method for the solution of (2-57), which was shown under certain conditions (to be discussed later) to be equivalent to collocation. In the same spirit we approach Bland's equation by a projection method analogous to Galerkin's method for equations of the second kind. Here again it can be shown that this technique is numerically equivalent to collocation. Reversing the argument, we prefer to regard the Galerkin method as primary, since it will be shown that the theory appears to emerge best from this viewpoint.

4.1 Collocation

For completeness and ease of reference Bland's collocation method is now reviewed. Since the space L_p^2 is spanned by the pressure polynomials $(\psi_n)_1^\infty$, P can be expanded as

$$P = \sum_{n=1}^{\infty} \langle P, \psi_n \rangle_p \, \psi_n .$$

because of this one seeks an approximate solution P_N of the form

$$P_N = \sum_{n=1}^{N} a_n \, \psi_n , \tag{4-1}$$

where a_n; $n = 1,2,\ldots,N$ are to be determined. Letting

$$r_N(x) = w(x) - \int_{-1}^{1} \sqrt{\frac{1-\xi}{1+\xi}} \, K(x-\xi) P_N(\xi) d\xi , \tag{4-2}$$

and setting $r_N(x)$ equal to zero at the zeros of $\chi_{N+1}(x)$ gives N linear equations in the N unknowns $(a_n)_1^N$. Solving for these determines the approximation P_N to the pressure coefficient P. This is Bland's collocation method. The numerical examples given by Bland and by us appear to indicate that P_N converges to P.

To establish this it is convenient to regard (2-57) as an operator equation acting between the two spaces L_p^2 and L_w^2 defined in Section 3. Making use of the properties of the airfoil polynomials given by (3-15), (3-16), (3-30) and (3-31) enables us to show that this equation has interesting analytic properties which permit a detailed analysis of the above numerical method.

4.2. Analytical properties

To set the stage for our theoretical treatment of (2-57) we make some simple preliminary observations. From (2-50) the kernel can be written as

$$K(x-\xi) = \left(\frac{\beta}{4\pi}\right)\frac{1}{x-\xi} - \left(\frac{ik}{4\pi\beta}\right)\log|x-\xi| + K_C(x-\xi), \tag{4-3}$$

where $K_C(x-\xi)$ is the bounded part. Multiplying both sides of (2-57) by $\frac{4}{\beta}$ allows us to rewrite it as

$$\tilde{w}(x) = \int_{-1}^{1} \sqrt{\frac{1-\xi}{1+\xi}}\, \tilde{K}(x-\xi)P(\xi)d\xi, \tag{4-4}$$

where $\tilde{w}(x) = \left(\frac{4}{\beta}\right)w(x)$ and $\tilde{K}(x-\xi) = \left(\frac{4}{\beta}\right)K(x-\xi)$. This transformation obviously has no effect on the solutions of (2-57). The key observation, and one that was made by Bland in his thesis is that (4-4) is actually equivalent to an equation of the second kind. To see this decompose $\tilde{K}(x-\xi)$ as

$$\tilde{K}(x-\xi) = \frac{1}{\pi(x-\xi)} + K_{SC}(x-\xi). \tag{4-5}$$

This first term in (4-5) leads to the integral operator

$$HP(x) = \frac{1}{\pi}\int_{-1}^{1} \sqrt{\frac{1-\xi}{1+\xi}}\, \frac{P(\xi)}{x-\xi}\, d\xi$$

which is just the Bland transform (3-25). From (3-19) and (3-20) it is seen that H maps the orthonormal basis $(\psi_n)_1^\infty$ onto the orthonormal basis $(\chi_n)_1^\infty$, and thus can be extended to a bounded invertible operator from L_p^2 to L_w^2. If one then operates on both sides of (4-4) by H^{-1} it takes the form of an equation of the second kind in L_p^2. This leads one to suspect that the well developed numerical methods for such equations would be useful in solving (2-57) which, as we shall see, is the case.

To proceed further, it is necessary to develop some of the analytical properties of (4-4). For this we digress slightly and state some definitions and theorems from functional analysis.

Notation: Let H_1 and H_2 be Hilbert spaces. The inner products on $H_i, i = 1,2$ will be denoted by $\langle\ ,\ \rangle_i$ and the corresponding norm by $\|\ \|_i$. The set of bounded linear operators from H_1 to H_2 will be denoted by $[H_1,H_2]$.

Definition 4.1. Let H_1 and H_2 be Hilbert spaces. Let $H \in [H_1,H_2]$. If $\|Hx\|_2 = \|x\|_1$ for all $x \in H$, we say that H is an isometry. In addition if H has a bounded inverse we say that H is unitary.

Theorem 4.1. Let H_1 be a Hilbert space with a complete orthonormal basis $\{\psi_n\}_1^\infty$. A necessary and sufficient condition that $H \in [H_1,H_2]$ be unitary is that the set $\{H\psi_n\}_1^\infty$ be a complete orthonormal basis in H_2.

Proof. See [81].

Definition 4.2. Let H_1 and H_2 be Hilbert spaces. Let $K \in [H_1,H_2]$. We say that K is compact if for every bounded sequence $\{x_n\}_1^\infty$ in H_1 the sequence $\{Kx_n\}_1^\infty$ has a convergent subsequence.

Theorem 4.2. (Properties of compact operators.) Let $K_i \in [H_1,H_2]$; i = 1,2 be compact. Then

(i) $K_1 + K_2$ is compact.

(ii) If $T \in [H_1,H_2]$ then $T K_i$; i = 1,2 are compact.

(iii) If C is a complex number then CK_i; i = 1,2 are compact.

(iv) If K_1 has finite dimensional range then K_1 is compact.

(v) Let $\| \ \|$ denote the operator norm on $[H_1,H_2]$. Let $\{K_n\}_1^\infty$ be a sequence of compact operators from H_1 to H_2 such that $\lim_{n\to\infty} \|K_n-K\| = 0$ where $K \in [H_1,H_2]$. Then K is compact.

(iv) It follows from (iv) that if $\{K_n\}_1^\infty$ is a sequence of operators each having finite dimensional range, and $\lim_{n\to\infty} \|K-K_n\| = 0$ then K is compact.

Proof. See [81].

Definition 4.3. Let $H \in [H_1,H_2]$. The adjoint of H denoted by H^* is the bounded linear operator defined by

$$\langle H^*x,y\rangle_1 = \langle x,Hy\rangle_2, \tag{4-6}$$

where x and y are arbitrary vectors in H_2 and H_1 respectively.

Theorem 4.3. Let $H \in [H_1,H_2]$. Then H has a unique adjoint $H^* \in [H_2,H_1]$.

Proof. See [81].

Theorem 4.4. Let H be a unitary operator from H_1 to H_2. Then $H^* = H^{-1}$. (H^{-1} denotes the inverse of H.)

Proof. Note first of all that since H is an isometry it preserves inner products; i.e., $\langle Hx,Hy\rangle_2 = \langle x,y\rangle_1$ for all $(x,y) \in H_1$. In fact $\|H(x+y)\|_2^2 = \|(x+y)\|_1^2$. But

$$\|H(x+y)\|_2^2 = \langle Hx,Hx\rangle_2 + 2\ \mathrm{Re}\ \langle Hx,Hy\rangle_2 + \langle Hy,Hy\rangle_2$$

$$= \langle x,x\rangle_1 + 2\ \mathrm{Re}\ \langle Hx,Hy\rangle_2 + \langle y,y\rangle_1. \tag{4-7}$$

Similarly

$$\|(x+y)\|_1^2 = \langle x,x\rangle_1 + 2\ \mathrm{Re}\ \langle x,y\rangle_1 + \langle y,y\rangle_1. \tag{4-8}$$

Equating (4-7) and (4-8) along with replacing x+y by x+iy gives the result. Now

$$\langle Hx,Hy\rangle_2 = \langle H^*Hx,y\rangle_1 = \langle x,y\rangle_1, \tag{4-9}$$

by the definition of adjoint and the above observation. Since (4-9) holds for all $y\in H_1$ we get that

$$H^*Hx = x,\ \forall x\in H_1. \tag{4-10}$$

Let $y\in H_1$. Then, since H^{-1} exists, $y = Hx$ for some $x\in H_1$. Therefore $y = Hx = H(H^*Hx) = (HH^*)Hx = HH^*y$. Thus $y = HH^*y$ for all $y\in H_2$, and this with (4-10) shows that H^* is both a left and right inverse of H so that $H^{-1} = H^*$.

<u>Theorem 4.5.</u> <u>Let H_1 and H_2 be Hilbert spaces. Let $T\in[H_1,H_2]$. Let $\{\psi_n\}_1^\infty$ be a complete orthonormal basis for H_1. Assume that</u>

$$\sum_{n=1}^{\infty} \|T\psi_n\|_2^2 < \infty. \tag{4-11}$$

<u>Then T is compact.</u>

(Note: <u>Operators satisfying (4-11) are said to have finite double or Hilbert-Schmidt norm. See [82] for a discussion of their properties.</u>)

<u>Proof.</u> From Theorem 4.2 it suffices to show that there exists a sequence of operators $\{T_n\}_1^\infty$, each having finite range, such that $\lim_{n\to\infty} \|T-T_n\| = 0$. Let $U_n = \mathrm{span}\ \{\psi_k\}_1^n$ and define Q_n by

$$Q_n x = \sum_{k=1}^{n} \langle x,\psi_k\rangle_1\ \psi_k,\ x\in H_1. \tag{4-12}$$

Q_n is the operator of orthogonal projection onto U_n. Let $T_n = TQ_n$. From (4-12) it is seen that

$$T_n x = \sum_{k=1}^{n} \langle x,\psi_k\rangle_1\ T\psi_k,\ x\in H_1. \tag{4-13}$$

Letting U_n = span $\{T\psi_k\}_1^n$, we see that T_n has finite range. Now

$$\|Tx-T_nx\|_2 = \|\sum_{k=n+1}^{\infty} \langle x,\psi_k\rangle_1 \, T\psi_k\|_2 \leq \sum_{k=n+1}^{\infty} |\langle x,\psi_k\rangle_1| \, \|T\psi_k\|_2. \tag{4-14}$$

By the Cauchy-Schwarz inequality (4-14) becomes

$$\|Tx-T_nx\|_2 \leq (\sum_{k=n+1}^{\infty} |\langle x,\psi_k\rangle_1|^2)^{\frac{1}{2}} (\sum_{k=n+1}^{\infty} \|T\psi_k\|_2^2)^{\frac{1}{2}} \leq \|x\|_1 (\sum_{k=n+1}^{\infty} \|T\psi_k\|_2^2)^{\frac{1}{2}}. \tag{4-15}$$

From (4-15) it is seen that

$$\|T-T_n\| \leq (\sum_{k=n+1}^{\infty} \|T\psi_k\|_2^2)^{\frac{1}{2}}. \tag{4-16}$$

Since $\sum_{k=1}^{\infty} \|T\psi_k\|_2^2$ converges the right hand side of (4-16) can be made arbitrarily small for n large. Thus $\lim_{n\to\infty} \|T-T_n\| = 0$ and the theorem is proved.

The results of the above theorems are now applied to (2-57) (or equivalently (4-4)). As was stated in §4.1 we wish to regard (2-57) as an operator equation acting between L_p^2 and L_w^2. Using the equivalent form (4-4) the kernel decomposition gives rise to three operators H, K_1 and K_2 defined by

$$H\,P(x) = \frac{1}{\pi} \int_{-1}^{1} \sqrt{\frac{1-\xi}{1+\xi}} \, \frac{P(\xi)}{x-\xi} \, d\xi, \tag{4-17}$$

$$K_1P(x) = -\frac{ik}{\pi\beta^2} \int_{-1}^{1} \sqrt{\frac{1-\xi}{1+\xi}} \log|x-\xi| P(\xi) d\xi, \tag{4-18}$$

and

$$K_2P(x) = \int_{-1}^{1} \sqrt{\frac{1-\xi}{1+\xi}} \, K_C(x-\xi) P(\xi) d\xi, \tag{4-19}$$

where the integral in (4-17) is taken in the sense of a Cauchy principal value. The basic properties of these operators are summarized in Theorem 4.6 below.

Theorem 4.6. H, K_1 and K_2 define bounded linear operators from L_p^2 to L_w^2. In addition H is unitary and K_1 and K_2 are compact.

Proof. As stated above H is just the Bland transform (3-25). Since $H\psi_k = \chi_k$ where $\{\psi_k\}_1^{\infty}$ and $\{\chi_k\}_1^{\infty}$ are defined by (3-1) and (3-2) respectively, H can be uniquely extended as a bounded operator from L_p^2 to L_w^2 by

$$HP(x) = \sum_{k=1}^{\infty} \langle P,\psi_k\rangle_p H\psi_k(x) = \sum_{k=1}^{\infty} \langle P,\psi_k\rangle_p \chi_k.$$

Since $\{\chi_k\}$ is a complete orthonormal basis in L^2_w it follows from Theorem 4.1 that H is unitary.

From (3-31) we see that

$$K_1\psi_n = -\frac{ik}{\pi\beta^2}\begin{cases}\dfrac{\chi_2(x) + (1+\log 2)\chi_1(x)}{2}, & n = 1\\ \dfrac{\chi_{n+1}+\chi_n}{2n} - \dfrac{(\chi_n+\chi_{n-1})}{2(n-1)}, & n \geq 2\end{cases}.$$

Since K_1 is well defined on the basis elements $\{\psi_n\}_1^\infty$ it can be extended as an operator to all of L^2_w by the formula

$$K_1P(x) = \sum_{k=1}^{\infty} \langle P,\psi_k\rangle_p \, K_1\psi_k, \tag{4-20}$$

provided that the sum in (4-20) converges in the L^2_w norm. To verify this observe that

$$\|K_1\psi_n\|_w^2 = \langle K_1\psi_n, K_1\psi_n\rangle_w = \frac{k^2}{\pi\beta^4}\begin{cases}\dfrac{2 + 2\log 2 + (\log 2)^2}{4}, & n = 1\\ \dfrac{(n^2-n+1)}{2n^2(n-1)^2}, & n \geq 2\end{cases}.$$

Thus (4-20) converges, and since $\|K_1\psi_n\|_w^2$ is of order $\frac{1}{n^2}$ the series $\sum_{n=1}^{\infty} \|K_1\psi_n\|_w^2$ converges and thus by Theorem 4.5 K_1 is compact.

Now

$$|K_2P(x)| \leq \int_{-1}^{1} \sqrt{\frac{1-\xi}{1+\xi}}\, |K_C(x-\xi)| \, |P(\xi)|\,d\xi$$
$$\leq \left[\int_{-1}^{1} \sqrt{\frac{1-\xi}{1+\xi}}\, |P(\xi)|^2 d\xi\right]^{\frac{1}{2}} \left[\int_{-1}^{1} \sqrt{\frac{1-\xi}{1+\xi}}\, |K_C(x-\xi)|^2 d\xi\right]^{\frac{1}{2}}$$

by the Cauchy-Schwarz inequality. Thus

$$\|K_2P\|_w^2 \leq \|P\|_p^2 \int_{-1}^{1} \sqrt{\frac{1+x}{1-x}} \left[\int_{-1}^{1} \sqrt{\frac{1-\xi}{1+\xi}}\, |K_C(x-\xi)|^2 d\xi\right] dx, \tag{4-21}$$

where the integral in (4-21) exists since $K_C(x-\xi)$ is bounded and the function $\sqrt{\frac{1+x}{1-x}}$ is integrable on $[-1,1]$. From this it is seen that $\|K_2P\|_w \leq C\|P\|_p$ and so K_2 is bounded. To establish compactness we again resort to Theorem 4.5 by showing that $\sum_{k=1}^{\infty} \|K_2\psi_n\|_w^2$ converges. For this observe that

$$\sum_{k=1}^{\infty} |K_2\psi_k|^2 = \sum_{k=1}^{\infty} \left|\int_{-1}^{1} \sqrt{\frac{1-\xi}{1+\xi}}\, K_C(x-\xi)\psi_k(\xi)\,d\xi\right|^2. \tag{4-22}$$

But

$$\int_{-1}^{1} \sqrt{\frac{1-\xi}{1+\xi}}\, K_C(x-\xi)\psi_k(\xi)d\xi = \pi \langle \eta_x, \psi_k \rangle_p, \tag{4-23}$$

where $\eta_x(\xi) = K_C(x-\xi)$. Thus the right hand sum in (4-22) can be written as

$$\pi^2 \sum_{k=1}^{\infty} |\langle \eta_x, \psi_k \rangle_p|^2. \tag{4-24}$$

By Parseval's Theorem this is equal to $\pi \int_{-1}^{1} \sqrt{\frac{1-\xi}{1+\xi}}\, |\eta_x(\xi)|^2 d\xi$. Multiplying both sides of (4-22) by $\sqrt{\frac{1+x}{1-x}}$ and integrating with respect to x gives

$$\sum_{k=1}^{\infty} \int_{-1}^{1} \sqrt{\frac{1+x}{1-x}} |K_2\psi_k|^2 dx = \pi \sum_{k=1}^{\infty} \|K_2\psi_k\|_w^2 = \pi \int_{-1}^{1} \sqrt{\frac{1+x}{1-x}} \left[\int_{-1}^{1} \sqrt{\frac{1+\xi}{1-\xi}} |K_C(x-\xi)|^2 d\xi\right]. \tag{4-25}$$

The integral in (4-25) is finite since $K_C(x-\xi)$ is bounded and $\sqrt{\frac{1+x}{1-x}}$ is integrable. Thus K_2 is compact since it has finite double norm.

From the results of Theorems 4.5 and 4.6, (4-4) can be written in operator form as

$$(H + K)P = \tilde{w} \tag{4-26}$$

where $H + K \in [L_p^2, L_w^2]$ and $K = K_1 + K_2$ is compact. A solution to (4-4) will now mean an element $P \in L_p^2$ solving (4-26). In general such a solution will satisfy (2-57) or (4-4) almost everywhere. If the solution is sufficiently smooth it will satisfy (2-57) in the usual pointwise sense. Since physically one is interested in weighted integrals of P such generalized solutions are perfectly reasonable.

From Theorem 4.4 we know that H has an inverse. Applying H^{-1} to both sides of (4-26) gives the equivalent equation

$$P + H^{-1} K P = H^{-1} \tilde{w}. \tag{4-27}$$

From Theorem 4.5 $H^{-1} K$ is a compact operator and (4-27) has the form

$$(I + L)P = H^{-1} \tilde{w} \tag{4-28}$$

where I is the identity operator on L_p^2 and $L = H^{-1}K$. Equation (4-28) is now in the standard form of equations of the second kind [83]. From this it is possible to obtain solvability theorems by appealing to the Fredholm theory. We state only one such theorem.

<u>Theorem 4.7. Bland's integral equation has a solution in L_p^2 iff -1 is not an eigenvalue of $H^{-1} K$.</u>

Proof. This is just the usual Fredholm alternative for operators of the form I + L where L is compact. See [84] for more details.

Throughout the rest of our discussion it will be assumed that the solvability condition in Theorem 4.7 is satisfied, and we now proceed to a discussion of the numerical solution of (4-26).

4.3. Galerkin's method for a class of operator equations

Motivated by the results in 4.2 we now consider the numerical solution of the class of equations

$$TP = w \tag{4-29}$$

where $T \in [H_1, H_2]$, H_i; $i = 1,2$ are Hilbert spaces, $T = H + K$ where H is unitary and K is compact. From Theorem 4.4, (4-29) can be written in the equivalent form

$$(I + H^*K)P = H^*w. \tag{4-30}$$

(4-30) is an equation of the second kind and since there are many well understood methods for solving such equations [84] we consider the possibility of using them to find numerical algorithms for (4-30). For our purposes Galerkin's method appears to make best use of the theoretical structure of (4-30) and we now give a brief discussion of this popular technique.

Assume that $\{\psi_n\}_1^\infty$ is a complete orthonormal basis for H_1 and look for approximate solutions of (4-30) of the form

$$P_N = \sum_{n=1}^{N} a_n \psi_n, \tag{4-31}$$

where the a_n's are constants to be determined. Since in general P_N will not solve (4-30) exactly we consider the residual R_N given by

$$R_N = P_N + H^*K P_N - H^*w. \tag{4-32}$$

If P_N were the true solution of (4-30) then $R_N = 0$. However, this will not be the case in general and we try to pick P_N so as to make R_N small. Galerkin's method attempts to do this by making R_N orthogonal to ψ_n; $n = 1,2,\ldots,N$. That is we require

$$\langle R_N, \psi_n \rangle_1 = 0; \; n = 1,2,\ldots,N. \tag{4-33}$$

Substitution of (4-32) into (4-33) gives the following set of linear equations to determine the a_n's:

$$a_n + \sum_{m=1}^{N} \langle H^*K\psi_m, \psi_n \rangle_1 \, a_m = \langle H^*w, \psi_n \rangle_1; \; n = 1,2,\ldots,N, \tag{4-34}$$

where the orthogonality of the ψ_n's has been used in the derivation of (4-34). If the equations in (4-34) have a unique solution then a_n; $n = 1,2,\ldots,N$ can be determined and the approximation P_N is well defined. The following

theorems, taken from Atkinson [84] justify this procedure. First we recast Galerkin's method into a slightly more abstract form.

As in Theorem 4.5 let U_N = span $\{\psi_n\}_1^N$ and let Q_N be the operator of orthogonal projection onto U_N. The Galerkin equations (4-33) and (4-34) are equivalent to the operator equation [1976,1]

$$Q_N R_N = 0, \quad P_N \in U_N. \tag{4-35}$$

Or, written out in full

$$Q_N(I+H^*K)P_N = Q_N H^*w, \quad P_N \in U_N. \tag{4-36}$$

Assume that (4-30) has a unique solution. Then from the Fredholm alternative [84] the operator $I + H^*K$ has a bounded inverse since H^*K is compact.

Theorem 4.8. Let $K_N = Q_N H^*K$. Then $\lim_{N\to\infty} \|K-K_N\| = 0$.

Proof. See Atkinson [84].

Theorem. 4.9. Let K_N be as in Theorem 4.8 and assume that N is large enough so that $\|K-K_N\| < \frac{1}{\|(I+H^*K)^{-1}\|}$. Then the operator $(I+K_N)^{-1}$ exists, is bounded and

$$\|(I+K_N)^{-1}\| \leq \frac{\|(I+H^*K)^{-1}\|}{1-\|I+H^*K\|\,\|K-K_N\|}. \tag{4-37}$$

From this it follows that the Galerkin equations (4-36) have a unique solution and

$$\|P-P_N\|_1 \leq \|(I+K_N)^{-1}\|\;\|P-Q_N P\|_1. \tag{4-38}$$

(4-38) implies that P_N converges in norm to P the solution of (4-30).

Proof. See Atkinson pp. 51-52 for details of (4-37) and (4-38). The convergence follows from (4-38) and the fact that $\{\psi_n\}_1^\infty$ is complete in H_1 so that $\|P-Q_N P\|_1 = (\sum_{N+1}^{\infty} |\langle P,\psi_n\rangle_1|^2)^{\frac{1}{2}}$ which converges to zero.

Note that (4-37) and (4-38) constitute an error estimate for the approximate solution P_N.

Theorem 4.9 is the basic convergence result that we will use in discussing Bland's method. Note that it has the immediate consequence of showing that the application of Galerkin's method to Bland's equation (2-57) is a convergent numerical method. That this is true follows from the fact that the equivalent operator version (4-26) satisfies all of the hypotheses to prove Theorem 4.9.

As pointed out in Atkinson there exists a "dual" to Theorem 4.9. That is, if one can establish the existence of a unique solution to the Galerkin equations for some sufficiently large N, then it follows that one can prove the existence of a solution to (4-30). From a practical point of view this is important, since we have the numerical information available from the TWODI program, and thus the solvability of the numerical problem can be used to infer the existence of solutions to the original problem.

Although we have established that Galerkin's method is theoretically a reasonable procedure to use numerically, it does initially appear to have several drawbacks, the most important of which is the necessity of performing the complicated integrations needed to evaluate the inner products in (4-34). Since, practically these integrals must be done numerically it is important to examine the effect of this on the Galerkin equations. Surprisingly, due to the structure of T, particularly the unitarity of H, considerable simplification results, and as will be shown, under appropriate conditions Galerkin's method becomes equivalent to collocation.

4.4. The relation between Galerkin's method and collocation

We now proceed to examine the above mentioned relation between collocation and Galerkin's method. Recall from (4-34) that the Galerkin approximation for P is obtained by solving the linear equations

$$a_n + \sum_{m=1}^{N} \langle H^*K\psi_m, \phi_n \rangle_1 \, a_m = \langle H^*w, \phi_n \rangle_1, \quad n = 1,2,\ldots,N.$$

Using the definition of adjoint, these equations become

$$a_n + \sum_{m=1}^{N} \langle K\psi_m, H\psi_n \rangle_2 \, a_m = \langle w, H\psi_n \rangle_2, \quad n = 1,2,\ldots,N. \tag{4-39}$$

Since H is unitary $\{H\psi_n\}_1^\infty = \{\chi_n\}_1^\infty$ is a complete orthonormal basis for H_2. Using this and the fact that $\langle \chi_n, \chi_m \rangle_2 = \delta_{mn}$ (4-39) becomes

$$\sum_{m=1}^{N} \{\langle H\psi_m, \chi_n \rangle_2 + \langle K\psi_m, \chi_n \rangle_2\} \, a_m = \langle w, \chi_n \rangle_2 = \sum_{m=1}^{N} \langle (H+K)\psi_m, \chi_n \rangle_2 \, a_m$$

$$= \langle w, \chi_n \rangle_2, \quad n = 1,2,\ldots,N.$$

Or, since H+K = T,

$$\sum_{m=1}^{N} \langle T\psi_m, \chi_n \rangle_2 \, a_m = \langle w, \chi_n \rangle_2; \quad n = 1,2,\ldots,N. \tag{4-40}$$

Note that (4-40) is formulated directly in terms of the original equation of the first kind TP = w and can be regarded as a projection method in its own right. To see this, again look for an approximate solution to (4-29) in the form $P_N = \sum_{n=1}^{N} a_n\psi_n$. Using the same argument as for Galerkin's method leads us to consider the residual

$$r_N = TP_N - w. \tag{4-41}$$

In order to make r_N "small" we pick a_n; n = 1,2,...,N to satisfy the orthogonality condition[1]

$$\langle r_N, \chi_n \rangle_2 = 0; \quad n = 1,2,\ldots,N. \tag{4-42}$$

Writing (4-42) out in full gives (4-40). If one knows $\{\chi_n\}_1^N$ explicitly then numerically it is more efficient to use (4-42) than (4-40).

Since our main interest is in Bland's equation (2-57) we now specialize (4-40) to the case where H_i; i = 1,2 are taken to be Hilbert spaces of

---

[1]This is sometimes called the method of weighted residuals [85].

functions on the interval [a,b] and the operator T is an integral operator of the form

$$TP(x) = \int_b^a K(x,\xi)P(\xi)d\xi, \tag{4-43}$$

where the integral in (4-43) is generally taken in the sense of a Cauchy principal value. Let

$$L_m(x) = T\psi_m(x). \tag{4-44}$$

Then

$$\langle T\psi_m, \chi_n\rangle_2 = \langle L_m, \chi_n\rangle_2. \tag{4-45}$$

Since the inner product in (4-45) is an integral, we assume that it can be approximated by a quadrature rule Q_N having N nodes, denoted by x_k; $k = 1,2,\ldots,N$ and corresponding weights W_k; $k = 1,2,\ldots,N$. Thus (4-45) can be approximated by the finite sum

$$\sum_{k=1}^{N} W_k L_m(x_k)\chi_n(x_k).$$

A similar approximation applied to $\langle w,\chi_n\rangle_2$ gives

$$\langle w,\chi_n\rangle_2 \approx \sum_{k=1}^{N} W_k w(x_k)\chi_n(x_k).$$

Thus the numerical solution to the Galerkin equations (4-40) is obtained by solving

$$\sum_{m=1}^{N} \hat{a}_m\Big(\sum_{k=1}^{N} W_k L_m(x_k)\chi_n(x_k)\Big) = \sum_{k=1}^{N} W_k w(x_k)\chi_n(x_k);\ n = 1,2,\ldots,N. \tag{4-46}$$

Define vectors and matrices by

$$\underline{a} = (\hat{a}_n);\ \underline{w} = (w(x_k)) \tag{4-47}$$

$$\underline{\chi} = [\chi_n(x_k)],\ \underline{L} = [L_m(x_k)],\ W = \text{diag}\,[W_k];\ m,n,k = 1,2,\ldots,N. \tag{4-48}$$

Using (4-47) and (4-48), (4-46) takes the form

$$(\underline{\chi}W)\underline{La} = (\underline{\chi}W)\underline{w}. \tag{4-49}$$

If it is assumed that the matrix $\underline{\chi}$ is nonsingular then $\underline{\chi}W$ is nonsingular and (4-49) is equivalent to

$$\underline{La} = \underline{w}. \tag{4-50}$$

Referring back to Section 4.1 it is easily seen that for Bland's equation (4-50) are just the collocation equations resulting from (4-2). Thus it

is seen that if the quadrature errors are ignored in the solution of the Galerkin equations then they will give exactly the same numerical solution as collocation, provided that the matrix $\underline{Y}$ is invertible, as will be established below. Thus from a numerical standpoint it makes little difference whether one uses collocation or Galerkin's method in the solution of (2-57) -- the result will be the same numerical approximation to P. However, from a theoretical point of view Galerkin's method appears to be more desirable, since as we have seen, it gives convergence along with computable error bounds.

To complete our equivalence proof of collocation and Galerkin's method we now establish the nonsingularity of $\underline{Y}$.

Definition 4.4. Let $\{f_n(x)\}$; $n = 1,2,\ldots,N$ be N functions defined on the interval $[a,b]$. We say that $\{f_n(x)\}_1^N$ are unisolvent if the matrix $[f_n(x_k)]$; $n,k = 1,2,\ldots,N$ is nonsingular for every set of distinct points $\{x_k\}_1^N$ in $[a,b]$.

Theorem 4.10. Let $\{p_n(x)\}_1^N$ be a basis for the polynomials of degree $\leq N-1$ on $[a,b]$. Then $\{p_n(x)\}_1^N$ are unisolvent.

Proof. Let $\pi = [p_n(x_k)]$; $n,k = 1,2,\ldots,N$. Since $p(x) = \sum_{k=0}^{N-1} p_{nk}x^k$ it follows that $\pi = PV$ where $P = [p_{nk}]$ and V is the Vandemonde matrix given by

$$V(x_1,x_2,\ldots x_N) = \begin{bmatrix} 1 & 1 & \cdots & 1 \\ x_1 & x_2 & \cdots & x_N \\ x_1^2 & x_2^2 & \cdots & x_N^2 \\ x_1^{N-1} & x_2^{N-1} & \cdots & x_N^{N-1} \end{bmatrix}.$$

Thus $\det \pi = \det P \det V$. But $\det P$ is nonzero since $\{p_n(x)\}_1^N$ is a basis and

$$\det V = (-1)^N \prod_{\substack{i<j \\ i,j=1,\ldots,N}} (x_i - x_j) \neq 0,$$

since the points x_k are distinct. Thus $\det \pi \neq 0$ and π is nonsingular.

Corollary 1. Let $\{p_n(x)\}_1^N$ be polynomials of degree $\leq N-1$ orthogonal with respect to some inner product on the set of functions on $[a,b]$. Then they are unisolvent.

Proof. The orthogonality implies that $\{p_n(x)\}_1^N$ are linearly independent and thus a basis for the polynomials of degree $\leq$ N-1 on [a,b]. The corollary now follows from the theorem.

Corollary 2. Let $\{\chi_n\}_1^N$ be the first N downwash polynomials as defined in Section 3. Then $\{\chi_n\}_1^N$ are unisolvent.

Proof. Since $\{\chi_n\}_1^N$ are orthogonal on [-1,1] with respect to the inner product $\langle\ ,\ \rangle_w$ by corollary 2 they are unisolvent.

Corollary 3. Let $\{\chi_n\}_1^N$ be as above and let $\{x_k\}_1^N$ be the zeros of χ_{n+1}, then the matrix $\underline{\chi} = \{\chi_n(x_k)\}$ is nonsingular.

Proof. From (3-24) we see that χ_{N+1} has N distinct zeros on [-1,1]. Since $\{\chi_n\}_1^N$ are unisolvent the result follows.

From Theorem 4.10 and the above discussion we arrive at our main equivalence result for collocation and Galerkin's method for Bland's equation.

Theorem 4.11. Let P_N be the approximate solution to (2-57) given by using Galerkin's method based on the pressure polynomials as a complete orthonormal basis for L_p^2. Then if the inner products in (4-40) are evaluated using the Jacobi-Gaussian quadrature rule (3-29), the resulting numerical approximation to (2-57) is the same as one obtains using collocation with the same basis and collocating at the zeros of $\chi_{N+1}(x)$.

Proof. From (4-49) it suffices to prove invertibility of $\underline{\chi}$ which was done in Theorem 4.10.

The importance of Theorem 4.11 is that it enables us to regard collocation as numerically equivalent to Galerkin's method. As we have seen Galerkin's method is convergent, and since neglecting the quadrature errors in the evaluation of the inner product in (4-40) gives Bland's collocation equations, we can conclude that this method is convergent. We summarize this, our main result, as Theorem 4.12.

Theorem 4.12. Let P_N^C be the numerical approximation to the solution of (2-57) as described in Section 4.1. Let P_N^G be the Galerkin approximation to P as described in Section 4.3. Let $\hat{P}_N^G$ be the approximation to P_N^G obtained by evaluating the inner products by the Jacobi-Gaussian rule (3-29). Then $\hat{P}_N^G = P_N^C$ and thus neglecting these quadrature errors $\hat{P}_N^G$ converges in the norm of L_p^2 to P and thus so does P_N^C. The error in this approximation is given by (4-38) and so

$$\|P_N^G - P\|_p \leq C_N \|P - Q_N P\|_p = C_N \left(\sum_{n=N+1}^{\infty} |\langle P, \phi_n \rangle_p|^2 \right)^{\frac{1}{2}}. \tag{4-51}$$

Note that (4-51) shows that the rate of convergence of P_N^G to P depends on the smoothness of P and thus requires a knowledge of the behavior of the generalized Fourier coefficients of functions expanded in airfoil polynomials. In addition it requires estimates of the smoothness of the solutions P. We expect to pursue these points in future work.

As we stated at the beginning of this section Bland's starting point for the solution of (2-57) was a least squares procedure which he claimed was equivalent to collocation. His proof of this fact [12] resided in the assumption that the collocation matrix $(L_n(x_k))$ was nonsingular. As a further consequence of the Galerkin theory we establish the validity of this proposition.

Let G denote the matrix $[\langle T\psi_m, \chi_n \rangle_2]$ given in (4-40). From the properties of Jacobi-Gaussian quadrature $\langle T\psi_m, \chi_n \rangle_2 = g_{nm} + e_{nm}$ where $[g_{nm}]$ is the matrix $\underline{\chi W L}$ as defined in (4-49) and $[e_{nm}] = E$ is the matrix of quadrature errors. Thus

$$G = \underline{\chi W L} + E. \tag{4-52}$$

By Theorem 4.10

$$\underline{L} = (\chi W)^{-1}(G - E). \tag{4-53}$$

From (4-53) it is seen that $\underline{L}$ has an inverse if and only if G-E does. From Theorem 4.9 we know that for all sufficiently large N, G has an inverse. Thus $G - E = G(I - G^{-1}E)$ and it follows from Banach's lemma [B5] that $I - G^{-1}E$ has an inverse provided that $\|G^{-1}E\| < 1$ where $\| \ \|$ is any matrix norm on the set of NxN complex matrices. Since $\|G^{-1}E\| \leq \|G^{-1}\| \ \|E\|$ it suffices to show that $\|E\| < \frac{1}{\|G^{-1}\|}$. Under the assumption that the quadrature errors can be made arbitrarily small if N is large enough we can pick N so that G^{-1} exists and $\|E\| < \frac{1}{\|G^{-1}\|}$. Thus we conclude that for N large enough the collocation matrix is nonsingular and consequently Bland's observation that collocation is equivalent to least squares is valid. Theorem 4.13 states this result.

Theorem 4.13. Provided that N is sufficiently large Bland's least squares method, his collocation method and our Galerkin method all give the same numerical approximation to the solution of (2-57).

4.5. Conditioning of the collocation matrix

As a final application of the Galerkin approach to (2-57) we offer a brief discussion of the conditioning of the collocation matrix $\underline{L}$. In [12,1968] and [5,1970], Bland remarks on the fact that L is well conditioned without offering any proof. The accuracy of our own numerical results also supports this observation. It also appears to be part of the folklore of singular integral equations of the first kind that the strong Cauchy singularity leads to numerical methods which are well conditioned [86,1971] and [87,1975]. Although this is intuitively reasonable we are unaware of any mathematical proof of this fact. For equations of the second kind there exist fairly complete results on conditioning. A summary of these may be found in Atkinson [84,1976]. Since we know that (2-57) is equivalent to an equation of the second kind these results should be of use here. That this is the case is demonstrated below.

Definition 4.5. Let A be an NxN complex matrix. Let $\|\ \|$ be a matrix norm on C^N. The condition number of A relative to $\|\ \|$ is given by

$$C(A) = \|A\|\ \|A^{-1}\|. \tag{4-54}$$

A matrix is said to be well conditioned if C(A) is of order 1 and poorly conditioned if C(A) is large [84,1976]. It follows immediately from (4-54) that if A and B are matrices then

$$C(AB) \leq C(A)C(B) \tag{4-55}$$

and

$$C(A^{-1}) = C(A). \tag{4-56}$$

Since $\underline{L} = (\underline{\chi}W)^{-1}(G-E) = (\underline{\chi}W)^{-1}G^{-1}(I-G^{-1}E)$, (4-55) and (4-56) give

$$C(\underline{L}) \leq C(\underline{\chi})C(W)C(G)C(I-G^{-1}E). \tag{4-57}$$

Since W is a diagonal matrix and one can show that $C(W) \leq c\,\frac{\max|W_k|}{\min|W_k|}$ where c is a constant independent of W. Since W_k; k = 1,2,...,N are the quadrature weights $C(W) \sim cN$. Now for N large $I-G^{-1}E \sim I$ so that $C(I-G^{-1}E) \sim C(I) \sim O(1)$. Thus $C(\underline{L}) \sim c'NC(\underline{\chi})C(G)$. From Atkinson's results [1976,1] one can show that $\|G\| \leq c''$ so that $C(\underline{L}) \sim c'''NC(\underline{\chi})$, which gives a reasonable estimate of the conditioning of $\underline{L}$. It appears then, if N is not too large, that $C(\underline{L})$ is well conditioned. A more complete analysis will have to await future work.

4.6. Convergence of integrated aerodynamic forces

Although the above theory gives convergence of P_N to P in the norm of L^2_p it is important to note that this generalized convergence of P_N gives strict convergence of integrated aerodynamic forces to their true values. To see this we define

$$\Delta p_N(\xi) = \sqrt{\frac{1-\xi}{1+\xi}}\, P_N(\xi) \tag{4-58}$$

as our approximation to $\Delta p(\xi)$. Let $f(\xi)$ be a real valued weighting function as in equations (3-35), (3-36), (3-39), etc., and Let $\mathcal{F}$ represent an integrated force,

$$F = \int_{-1}^{1} \Delta p(\xi) f(\xi) d\xi. \tag{4-59}$$

We take as our approximation to F

$$F_N = \int_{-1}^{1} \Delta p_N(\xi) f(\xi) d\xi. \tag{4-60}$$

By definition of the inner product on L^2_p,

$$F_N = \pi \langle P_N, f \rangle_p. \tag{4-61}$$

Theorem 4.14. $\lim_{N\to\infty} F_N = F.$

Proof.

$$|F - F_N| = \pi\, |\langle P, f\rangle_p - \langle P_N, f\rangle_p| = \pi\, |\langle P - P_N, f\rangle_p|. \tag{4-62}$$

By the Cauchy-Schwarz inequality

$$|\langle P - P_N, f\rangle_p| \leq \|P - P_N\|_p \|f\|_p. \tag{4-63}$$

Thus the result follows from Theorem 4.9.

§5. Organization of the computer program

The computer program developed during this work is a user-oriented, working, pilot version written in extended FORTRAN IV. To accomplish this, several helpful guidelines were followed during its planning and development:

(1) Input and output quantities were established first. These were selected primarily according to the general needs of the intended user community;

(2) A hierarchial, modularized system of executive and computational subroutines together with a complete list of all working equations was established and iterated once prior to actual coding;

(3) Coding was performed with visibility as the primary criterion, facilitating changes;

(4) All computational subroutines were carefully checked against independent calculations, using exact closed form special cases whenever possible to verify accuracy as well as correctness;

(5) Due to the go-no go nature of unsteady kernel function programs, computational correctness was deemed more important than algorithmic efficiency;

(6) The organization of the computer program was structured to facilitate correctness of the pilot version and future modifications.

The calling hierarchy of the computer program is shown in Figure 5, with arrows indicating the direction of call. The main program, named TWODI for two dimensional, is strictly an executive program. TWODI directs two supervisory subroutines named PREP and SOLVE, and one interim subroutine named CHECK. If called by TWODI, CHECK systematically calls each of the major computational subroutines and checks their current computational results against the most accurately known results, which are stored within CHECK. CHECK is primarily a developmental tool, secondarily a diagnostic tool, and does not appear in released versions of TWODI.

PREP is a supervisory subroutine, whose purpose is to prepare input data in a form acceptable to the solution process which is subsequently

implemented by SOLVE. PREP reads and prints back all input data. A title, supplied as input data by the user, is centered by subroutine CENTER, and the time and date, centered title and page number are printed at the top of each page using subroutine PAGE. PREP tests all input data except the flow parameters (M,k,η_H and c_W). Data lying outside their acceptable ranges result in the problem being deleted by PREP, with an explanatory comment. The input data specifies mode shapes at discrete points that are selected by the user. PREP collocates a linear combination of airfoil polynomials through these discrete points and stores the resulting Fourier coefficients for later use by SOLVE. Values of airfoil polynomials are calculated by subroutine AFP using recursion formulas, and collocation is performed using subroutine CSIMAL to solve complex (or real) simultaneous algebraic equations. Once the input data have been read, checked, printed back and prepared for use by SOLVE, PREP returns control of the program to TWODI, and TWODI calls SOLVE.

SOLVE is a supervisory subroutine whose purpose is to solve the integral equation for each M,k,η_H and c_W case, and to compute and print the airloads for as many downwash modes as were given by input data. Each problem may have numerous cases of M,k,η_H and c_W. These are tested individually by SOLVE, and erroneous cases are deleted without affecting the others. The eigenvalues appearing in equation (2-54) are calculated by subroutine PICARD using Picard iteration. To avoid repetition, these eigenvalues are calculated at the outset and stored for later use. Subroutine WASH calculates the matrix of downwashes at the appropriate collocation points. Subroutine BMN calculates the collocation matrix using closed form integrations for the Cauchy and logarithmically singular parts of the kernel, and uses Jacobi-Gaussian quadrature for the bounded part of the kernel. The quadrature points and collocation points are interdigitated according to equation (3-26) and the continuous part of the kernel is calculated by subroutine KC. The infinite series for F and F' appearing in the kernel are calculated by subroutine SUM. If convergence of these series requires eigenvalues beyond those already stored, SUM calls PICARD as necessary. After the downwash and collocation matrices have been calculated, SOLVE calls CSIMAL and the generalized Fourier coefficients of the pressure for all downwash modes are thereby determined. SOLVE then calls LOADS which calculates and prints the particular combination of pressure, section coefficients and generalized forces as stipulated by the input data. LOADS calls AFP if pressures are

required. Output is supplied in redundant real-imaginary-magnitude-phase angle format using subroutine ATANC. After SOLVE has completed one case of M,k,η_H and c_W, the remaining cases are solved in succession. Upon completion control returns to TWODI. TWODI then calls PREP for another problem, the solution to which is computed by SOLVE, until eventually all problems are solved.

In its present form, the TWODI program works, it is believed to be free of error, and is convenient to use. Complete instructions for its use are supplied in Section 7.

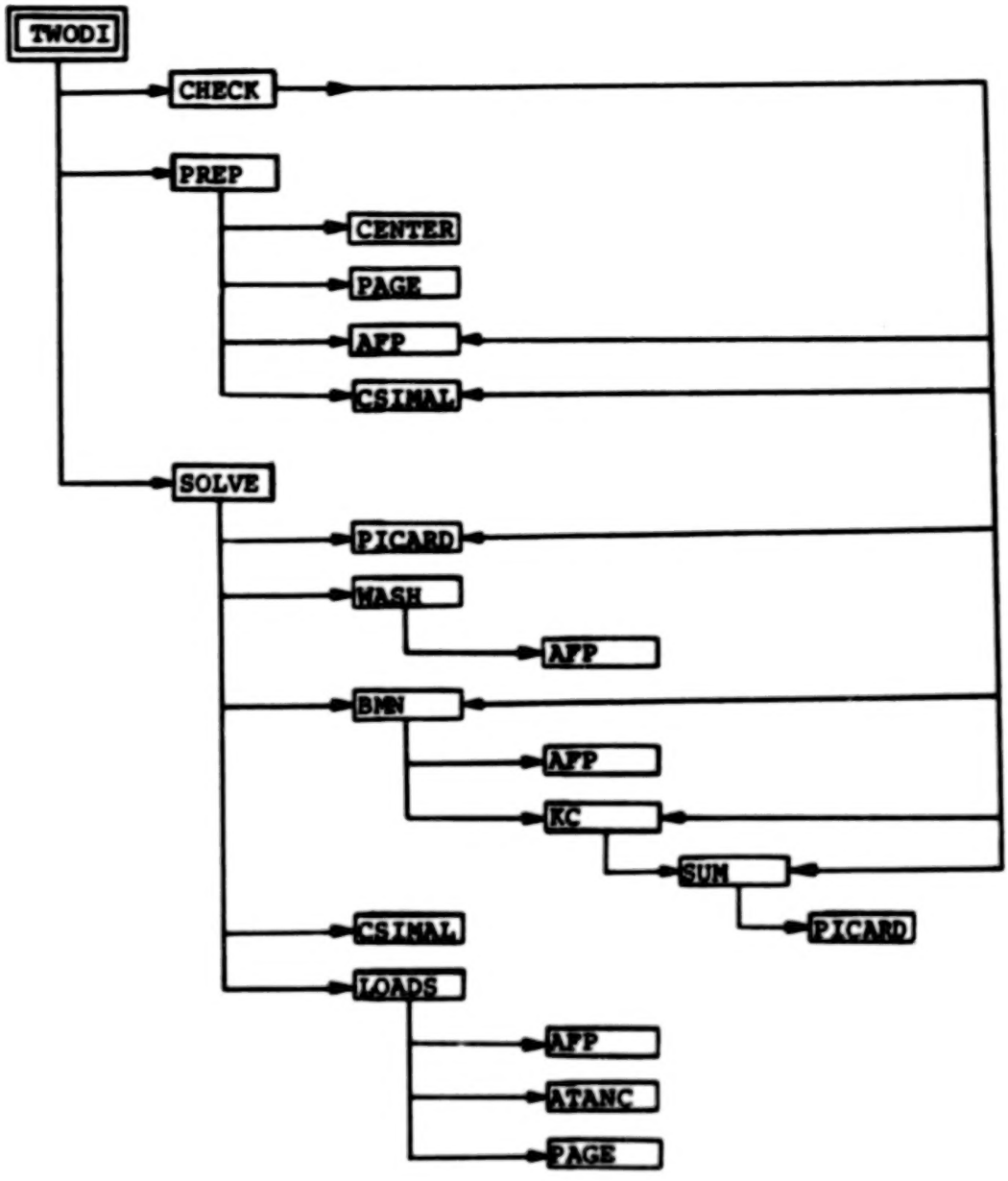

Figure 5. Calling hierarchy of the TWODI program

§6. Some numerical considerations

This Section discusses some of the numerical considerations made in computing Bland's kernel as given by equations (2-50) to (2-55). All computations involve elementary operations using standard FORTRAN functions except the determination of the eigenvalues of equation (2-54) and the summation of the infinite series of F given by equation (2-51), and its derivative F'. Since these computations, especially the latter, are the most difficult part of computing the kernel, they are discussed in detail.

The positive solutions $\{\lambda_n\}_{n=1}^{\infty}$ of the transcendental equation

$$\tan \lambda + \gamma\lambda = 0 \tag{6-1}$$

are depicted in Figure 6(a) as the projections onto the λ-axis of the intersections of a straight line with branches of the tangent function. Equation (6-1) occurs elsewhere in mechanics[1] with both positive and negative values of the parameter γ being physically meaningful. In the present study, only nonnegative values of γ are meaningful but the solution algorithm we use is equally valid for all real values of γ:

$$-\infty < \gamma < \infty. \tag{6-2}$$

The eigenvalues are well separated and satisfy the inequalities

$$\pi(n-\tfrac{1}{2}) < \lambda_n < \pi(n+\tfrac{1}{2}); \; n = 1,2,... \tag{6-3}$$

Figure 6(b) depicts a natural iteration scheme. Because of the behavior of the derivative of the inverse tangent function, if $\lambda_n^{(k)}$ is any approximation whatsoever to λ_n, then the number

$$\lambda_n^{(k+1)} = \pi n - \tan^{-1}(\gamma\lambda_n^{(k)}) \tag{6-4}$$

is a better approximation, as illustrated by Figure 6(b). The following theorem proves that this method always works.

---

[1]For example, the buckling of a beam built in at one end and clamped at the other is governed by the equation

$$\sqrt{\frac{PL^2}{EI}} = \tan\sqrt{\frac{PL^2}{EI}},$$

where P is the axial buckling load, L is the length of the beam, E is Young's modulus and I is the usual moment of inertia.

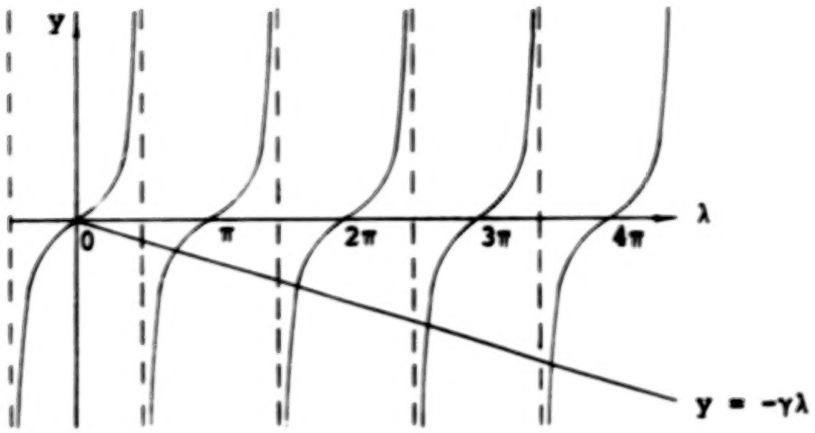

(a) Eigenvalues of $\tan \lambda + \gamma\lambda = 0$

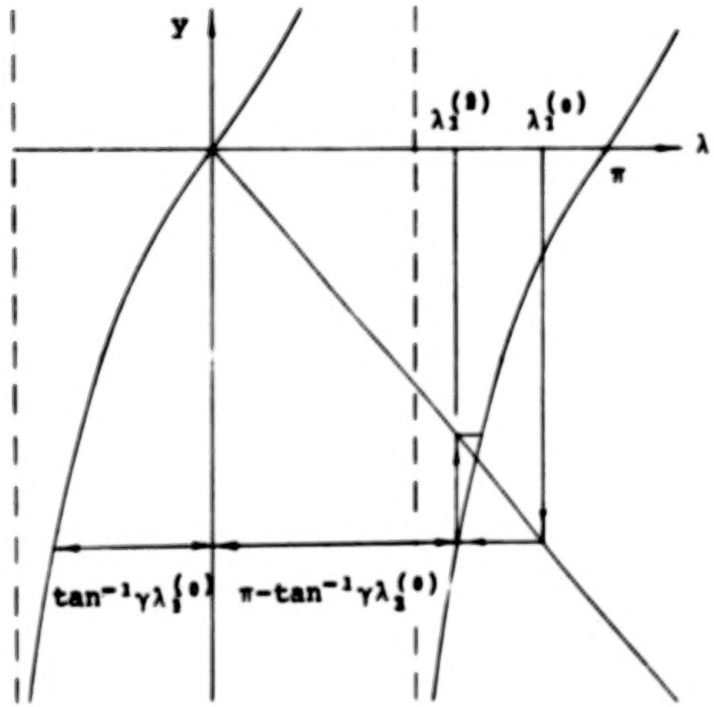

(b) Iteration by $\lambda_n^{(k+1)} = \pi n - \tan^{-1}(\gamma\lambda_n^{(k)})$

Figure 6. The eigenvalue problem $\tan \lambda + \gamma\lambda = 0$

Theorem: For arbitrary $\lambda_n^{(0)}$, the sequence $\{\lambda_n^{(k)}\}_{k=1}^{\infty}$ converges to λ_n. The convergence is geometric with rate

$$\rho_n < \min \{\frac{1}{\pi(2n-1)}, \frac{1}{\gamma\pi^2(2n-1)^2}\}. \tag{6-5}$$

Proof: For fixed γ and n, let

$$g(\lambda) = n\pi - \tan^{-1}(\gamma\lambda)$$

and let I_n denote the closed interval $[(n-\frac{1}{2})\pi, (n+\frac{1}{2})\pi]$. Then $g(\lambda_n^{(0)}) \in I_n$, regardless of the initial value $\lambda_n^{(0)}$. Hence all elements of the sequence $\{\lambda_n^{(k)}\}_{k=1}^{\infty}$ belong to I_n. It is sufficient to show that g is a contraction mapping on I_n, because the iteration defined by (6-4) is just the usual Picard approximation scheme applied to the fixed point equation

$$\lambda_n = g(\lambda_n).$$

Since g is differentiable on I_n, it suffices to show that

$$\sup_{\lambda \in I_n} \{|g'(\lambda)|\} < 1.$$

But

$$g'(\lambda) = -\frac{\gamma}{1+\gamma^2\lambda^2} = -\frac{\gamma\lambda}{1+\gamma^2\lambda^2}\frac{1}{\lambda} = -\frac{\gamma^2\lambda^2}{1+\gamma^2\lambda^2}\frac{1}{\gamma\lambda^2}.$$

Therefore

$$\sup_{\lambda \in I_n} \{|g'(\lambda)|\} \leq \frac{1}{2} \sup_{\lambda \in I_n} \{\frac{1}{|\lambda|}\} = \frac{1}{\pi(2n-1)}$$

and

$$\sup_{\lambda \in I_n} \{|g'(\lambda)|\} \leq \sup_{\lambda \in I_n} \{\frac{1}{|\gamma\lambda^2|}\} = \frac{4}{\gamma\pi^2(2n-1)^2}. \quad \text{QED}$$

The above algorithm has been coded as a function subroutine named PICARD using

$$\lambda_n^{(0)} = n\pi \tag{6-6}$$

as an initial value, and using the relative error test

$$|\lambda_n^{(k+1)} - \lambda_n^{(k)}| < \epsilon\, |\lambda_n^{(k+1)}| \tag{6-7}$$

for convergence.[2]

---

[2]The relative error test (6-7) is useful whenever the exact limit is not known in advance and whenever the limits may be extremely large or extremely small. It does not guarantee that convergence is achieved to within ϵ of the exact value, but is a reasonably general test and has worked well in the present study.

Typically, for n = 50, ten decimal convergence is achieved in 3-4 iterations. The convergence characteristics of PICARD are shown in Table 1 for several combinations of n and ϵ in terms of the numbers

$$k_{max}(n,\epsilon) = \max_{-\infty<\gamma<\infty} \{\max\{k+1: |\lambda_n^{(k+1)} - \lambda_n^{(k)}| \leq \epsilon |\lambda_n^{(k+1)}|\}\} \qquad (6\text{-}8)$$

which represent the maximum number of iterations required for all values of γ.

Table 1. Convergence of function subroutine PICARD

n = eigenvalue no., $k_{max} = \max_{\gamma}$ no. iterations required

$\epsilon = 10^{-6}$		$\epsilon = 10^{-8}$		$\epsilon = 10^{-10}$	
n	k_{max}	n	k_{max}	n	k_{max}
1	9	1	12	1	14
2-3	6	2	8	2	10
4-5	5	3	7	3	9
6-12	4	4-6	6	4	8
13-71	3	7-11	5	5-6	7
72-500000	2	12-31	4	7-10	6
500001-∞	1	32-338	3	11-21	5
		339-49999990	2	22-78	4
		49999991-∞	1	79-1566	3
				1567-5000014179	2
				5000014180-∞	1

The rapid convergence with large n is explained by the convergence rate bounds given by equation (6-5). Values of k_{max} were estimated by comparing results for 25 values of γ which, to within the single precision accuracy of a CDC 6400, were given by values of γ_ℓ such that:

$$\tan^{-1}\gamma_\ell = \frac{\ell\pi}{24}, \quad -12 \leq \ell \leq 12.$$

Only one iteration is required for $\ell = 0$ because the choice (6-6) of the initial value is then the exact eigenvalue, but the maximum number of iterations usually occurred for $\ell = 1$. This behavior can be understood from the graph of the eigenspectra vs. γ. Since γ can be any real number, the domain can be mapped onto a finite interval by employing the inverse tangent transformation. The resulting eigenspectra for all real values of γ are shown in Figure 7. A gradually steepening shoulder with increasing n is observed near $\gamma = 0$, which is where the maximum number of iterations should

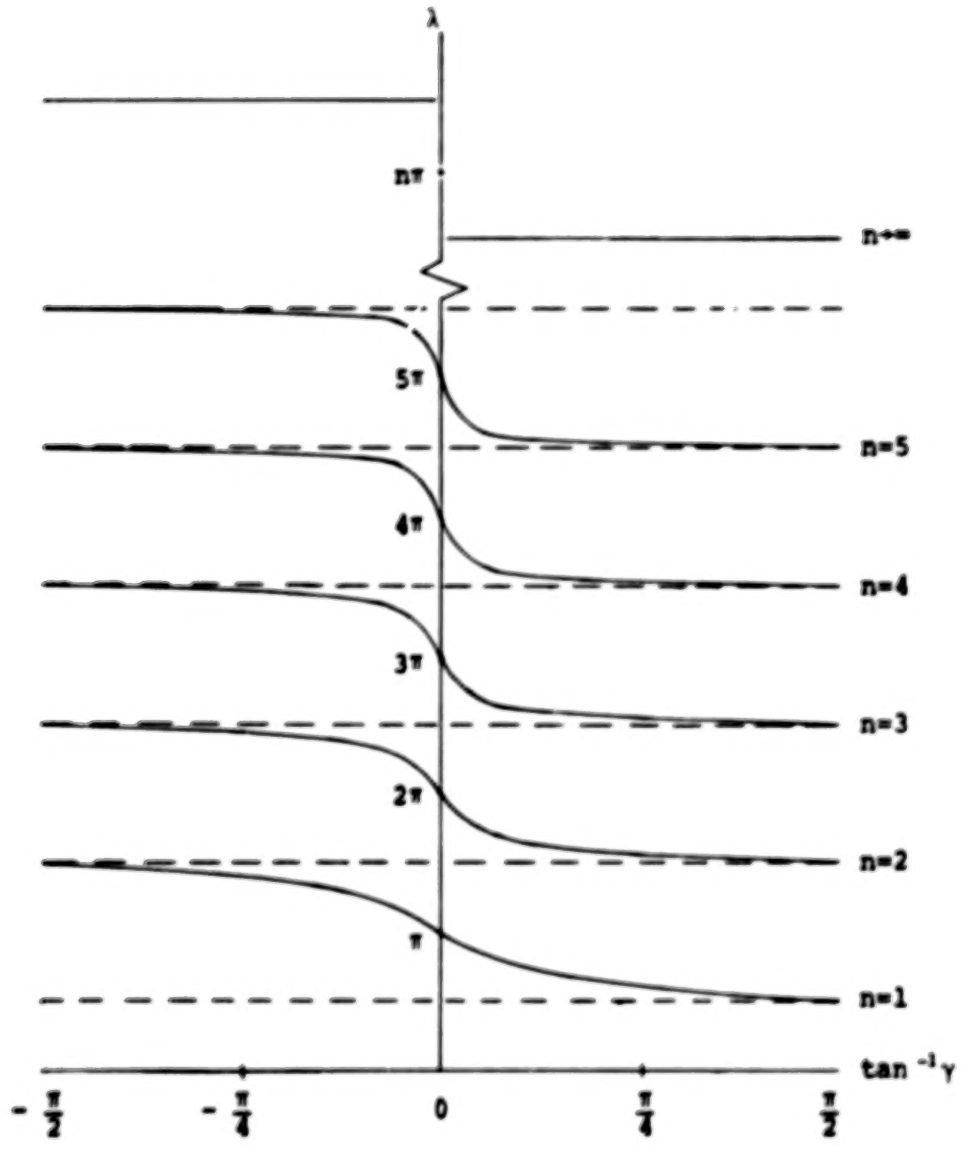

Figure 7. Spectra of tan λ + γλ = 0 vs. $\tan^{-1}\gamma$

be expected. This shoulder is merely exhibiting the fact that

$$\lim \lambda_n = \begin{cases} \pi(n+\frac{1}{2}) & \gamma < 0 \\ \pi n & \gamma = 0 \\ \pi(n-\frac{1}{2}) & \gamma > 0 \end{cases}$$

which is obvious from Figure 6(a).

The infinite series (2-51) and its derivative are the result of a uniformly but slowly convergent series which has been modified for improved convergence. Consider the infinite series

$$f(\delta) = \sum_{n=1}^{\infty} \frac{a_n}{\lambda_n} \exp(-\lambda_n \delta), \tag{6-10}$$

$$f'(\delta) = -\sum_{n=1}^{\infty} a_n \exp(-\lambda_n \delta), \tag{6-11}$$

where a_n and λ_n are given by (2-52) and (2-53). From (6-9), it follows that if $\gamma > 0$ the terms of the series (6-10) and (6-11) for large n approach the corresponding terms of the series

$$\hat{f}(\delta) = \sum_{n=1}^{\infty} \frac{1}{\pi(n-\frac{1}{2})} \exp(-\pi(n-\tfrac{1}{2})\delta), \tag{6-12}$$

$$\hat{f}'(\delta) = -\sum_{n=1}^{\infty} \exp(-\pi(n-\tfrac{1}{2})\delta), \tag{6-13}$$

respectively. The series (6-10)-(6-13) diverge if $\delta \leq 0$ and converge uniformly on any closed interval such that

$$\delta > 0. \tag{6-14}$$

The derived series for f' and $\hat{f}'$ are the more slowly convergent, converging geometrically with rate which approaches 1 as δ approaches 0. However, the minimum argument needed for the collocation method is

$$\delta_{min} = \min_{x,\xi} \frac{|x-\xi|}{\beta \eta_H}, \tag{6-15}$$

where x is a collocation point and ξ is a quadrature node. Although Hsu's interdigitation procedure tends to maximize this difference, the argument can still be quite small. Taking the number of quadrature points equal to the number of pressure basis functions,

$$NP = NQ \tag{6-16}$$

and referring to formulas (3-24) and (3-25), one finds that

$$\min_{1 \leq i,j \leq NP} \left|\cos \frac{2i\pi}{2NP+1} + \frac{\cos 2j\pi}{2NP+1}\right| = \cos \frac{\pi}{2NP+1} - \cos \frac{2\pi}{2NP+1} = \frac{3\pi^2}{8NP^2}. \tag{6-17}$$

Consequently, applying a relative convergence criterion to the series (6-10) to (6-13), it can be estimated that the number of terms NT required to achieve ND decimal convergence is given by

$$NT \approx .28\eta_H(ND)(NP)^2. \tag{6-18}$$

For example if M = 0, $\eta_H \approx 15$, ND = 10 and NP = 10, then NT ≈ 3000 terms.

The series (6-10) and (6-11) appeared in the original expression for Bland's kernel. He improved their weak convergence properties by subtracting the corresponding terms of the series (6-12) and (6-13) and adding their closed form sums

$$\hat{f}(\delta) = \frac{4}{\pi} \log \coth \frac{\pi\delta}{4}, \tag{6-19}$$

$$\hat{f}'(\delta) = -2 \operatorname{csch} \frac{\pi\delta}{2} \tag{6-20}$$

to obtain

$$f(\delta) = \sum_{n=1}^{\infty} \left[\frac{a_n}{\lambda_n} \exp(-\lambda_n\delta) - \frac{1}{\pi(n-\frac{1}{2})} \exp(-\pi(n-\tfrac{1}{2})\delta)\right] + \frac{4}{\pi} \log \coth \frac{\pi\delta}{4}, \tag{6-21}$$

$$f'(\delta) = -\sum_{n=1}^{\infty} \left[a_n \exp(-\lambda_n\delta) - \exp(-\pi(n-\tfrac{1}{2})\delta)\right] - 2 \operatorname{csch} \frac{\pi\delta}{2}. \tag{6-22}$$

The infinite series appearing in (6-21) and (6-22) equal F and F' as defined by (2-51). F and F' are nonsingular at $\delta = 0$, whereas f, f', $\hat{f}$ and $\hat{f}'$ are all singular at $\delta = 0$. The resulting smooth behavior of F and F' vs. δ is depicted in Figure 8 for k = 0 and for γ = 0,1 and ∞. In the case $\gamma = k = 0$, it is possible to sum the series for F and F' in closed form:

$$F(\delta) = -\frac{2}{\pi} \log \left(1+\exp(-\frac{\pi\delta}{2})\right) \text{ if } \gamma = k = 0, \tag{6-23}$$

$$F'(\delta) = \frac{1}{1+\exp(-\frac{\pi\delta}{2})} \text{ if } \gamma = k = 0, \tag{6-24}$$

thereby permitting an exact and independent check of numerical computations. Table 2 shows a comparison for small values of δ, including $\delta = 0$.

Table 2. Accuracy of subroutine SUM for $\gamma = k = 0$
(using a relative convergence test on F' with $\epsilon = 10^{-10}$)

δ	Decimals of accuracy F(δ)	F'(δ)	no. of terms
.000[3]	5	0	60057
.001	10	6	5496
.002	10	7	2859
.003	10	8	1485
.020	10	9	323
.200	10	10	37

Thus, while the series reformulations described above have succeeded in removing the singularity and improving the convergence somewhat, it is apparent from Figure 8 and Table 2 that additional gains in efficiency remain to be accomplished. Variations in frequency and Mach number are shown in Figures 9-11.

The prospects for improving the efficiency of subroutine SUM appear favorable for several reasons. The present version is accurate and provides a sound basis for comparison. The data presented above represent a worst case in the sense that convergence is more rapid with increasing γ ($\gamma = 0$ corresponds to an open tunnel, $\gamma = \infty$ to a closed tunnel).

---

[3]In the case $\gamma = k = 0$, the series for F(0) is an alternating harmonic series and converges slowly to

$$F(0) = \frac{2}{\pi} \log 2,$$

but the derived series is null and does not converge to

$$F'(0) = \frac{1}{2}.$$

This is due to the non uniform convergence of F(δ) at $\delta = 0$ so that interchange of summation and differentiation is not valid.

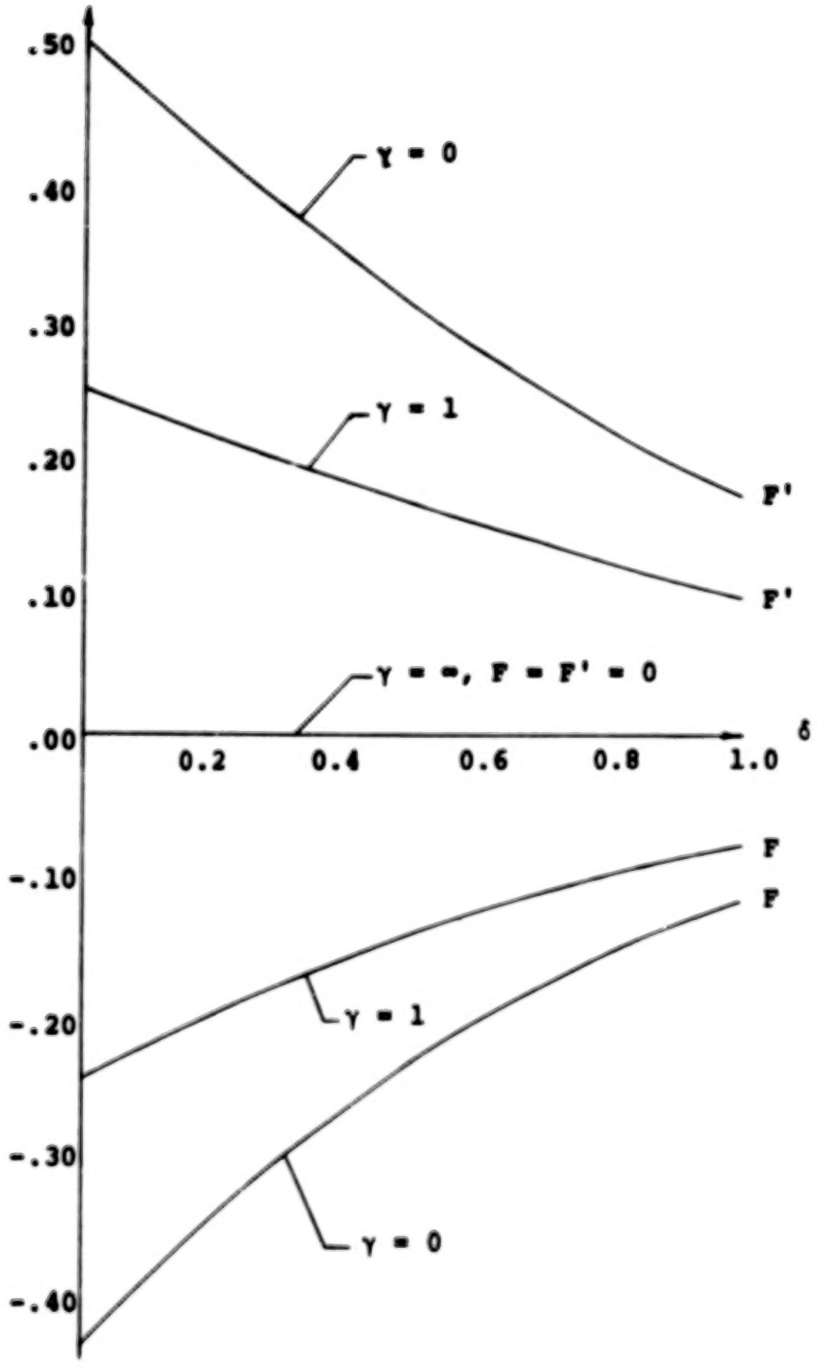

Figure 8. F(δ) and F'(δ) for k=0 and γ=0,1,∞

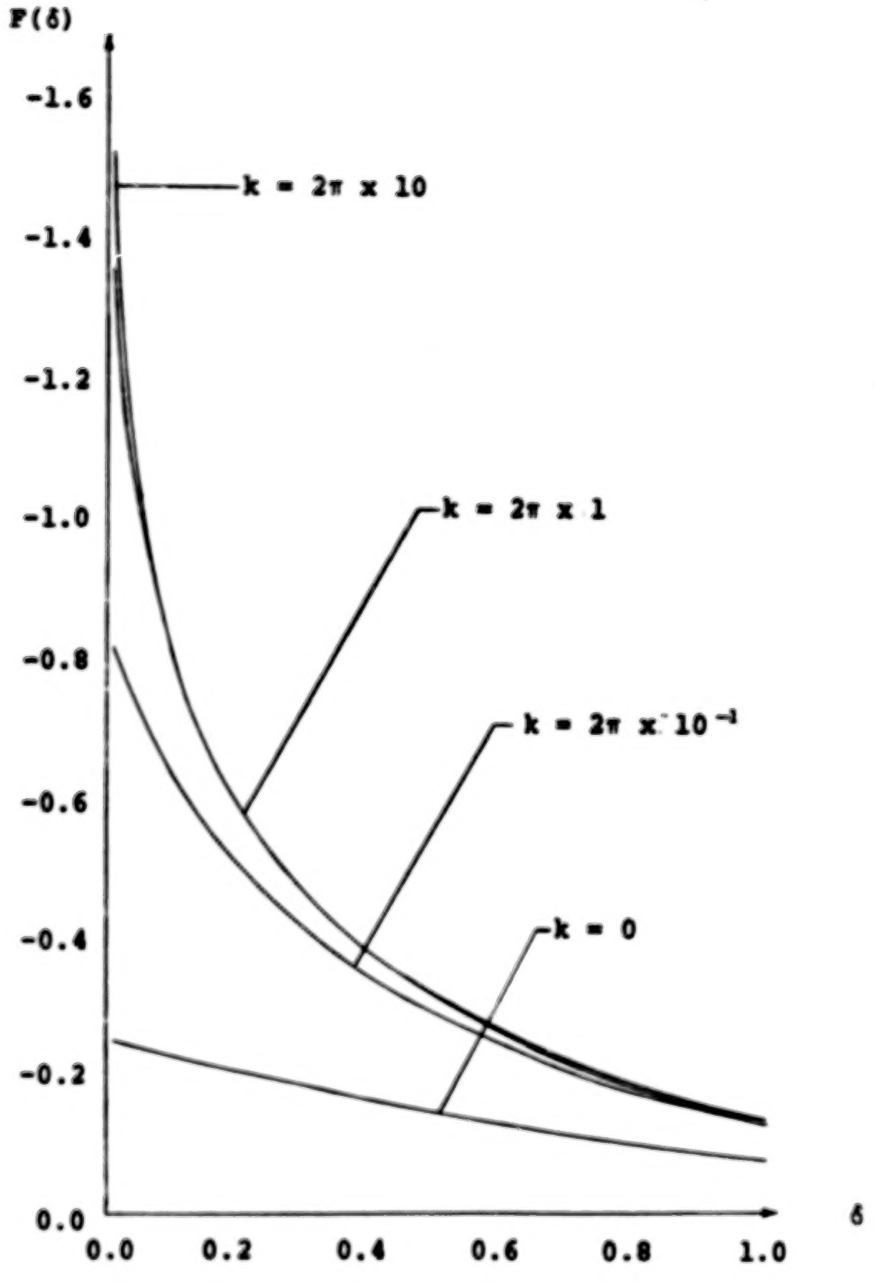

Figure 9. Parametric behavior of F(δ) vs. k for M=0, η_H=10, γ=1

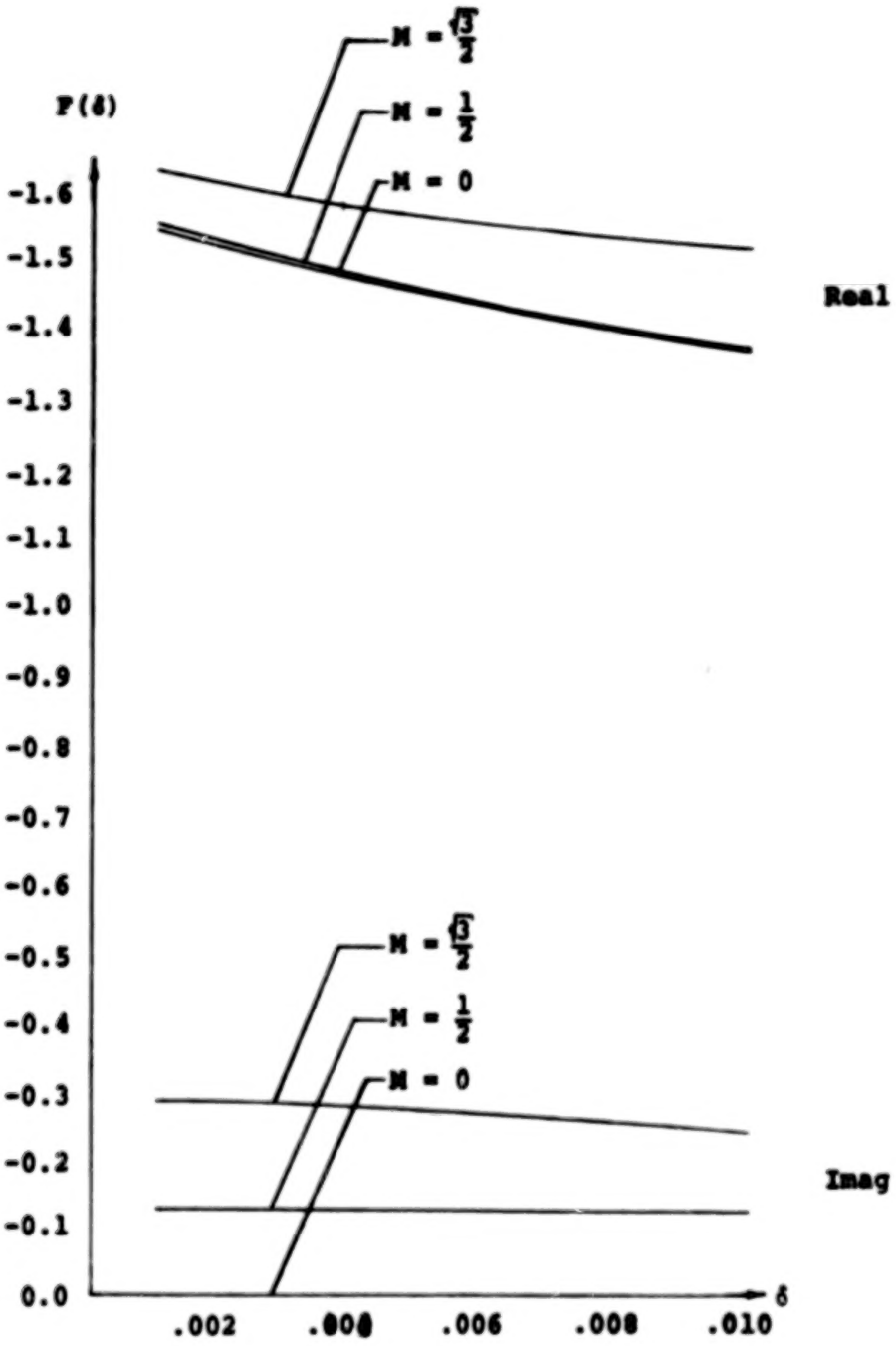

Figure 10. Parametric behavior of F(δ) vs. M for $k = 2\pi, \eta_M = 10, \gamma = 1$

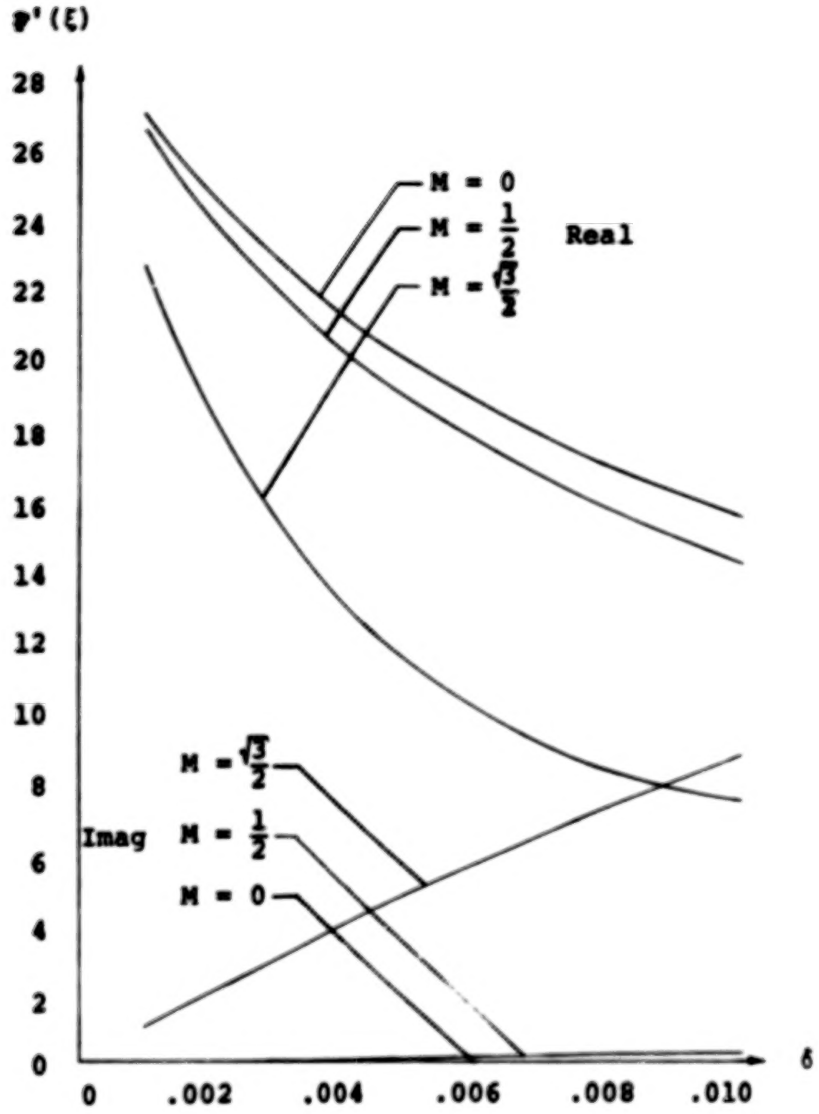

Figure 11. Parametric behavior of F'(δ) vs. M for k=2π, η_H=10, γ=1

§7. Use of the TWODI program

This section describes the preparation of input data for the pilot version of the TWODI program. It is assumed that the user knows the physical meaning of all input and output quantities, and the procedure for submitting a run at the computer facility. We reiterate that the solution is based upon the assumption of linearized inviscid subsonic potential flow about a thin airfoil located midway between two parallel walls using the boundary condition (2-49).

TWODI will predict any combination of pressure, section coefficients and generalized aerodynamic forces for the following primary parameters:

(1) mode shape,

(2) reduced frequency,

(3) Mach number,

(4) tunnel depth to airfoil chord ratio,

(5) tunnel wall ventilation coefficient.

Additional parameters are the number of pressure terms used in the solution process, the number of points at which pressure is to be calculated, etc. TWODI will operate in either BATCH (noninteractive card jobs) or TIMESHARE (interactive remote terminal) modes. Input and output are fully compatible between BATCH and TIMESHARE. A problem is defined by a set of data sufficient to cause execution of the program, and contains from 1 to 50 combinations of (M,k,η_H,c_W), called data cases. As many problems may be loaded in succession as desired. All input data and their acceptable values are precisely defined in Section 7.1 below. Input data are automatically checked for acceptability and unacceptable data cases or unacceptable problems will be selectively deleted by TWODI with an explanatory comment. The input format is defined in Section 7.2 consisting of six input data units. For BATCH runs the format may be formal on a column by column basis, or it may be free with individual data separated by a comma or blanks. Each input data unit (and certain subunits) must begin on a new card. TIMESHARE input is prompted in a self-explanatory fashion, and the interactive communication between TWODI and user is described in Section 7.3. At the present time, comprehensive estimates of computer time and the number NP of pressure modes required to achieve a certain accuracy are not available.

7.1 Definition of input data

TITLE - From 1 to 72 alphanumeric characters of user-selected title. Printed at the top of each page, with the time and date.

NC - Number of M,k,η_H,c_W data cases to follow for this problem. Each problem consists of NC cases. As many problems may be run as desired. $1 \leq NC \leq 50$

NP - Number of aerodynamic pressure modes to be used in the solution process. $1 \leq NP \leq 30$

NH - Number of airfoil deflection modes. $1 \leq NH \leq 5$

NX - Number of points at which the airfoil deflection modes are to be collocated to the input data. $1 \leq NX \leq 10$

NL - Number of loading points at which pressure is to be calculated. $0 \leq NL \leq 50$

SEC - Logical variable whose truth value is to calculate section coefficients (lift, pitching moment, center of pressure) for each deflection mode. T or F

GAF - Logical variable whose truth value is to calculate the generalized aerodynamic force coefficient matrix. T or F

TSH - Logical variable whose truth value is interactive timesharing remote terminal operation. T or F

XM(M) - Chordwise coordinate of matching point M of NX for airfoil centerline deflections. Nondimensionalized by the semichord, -1 at the leading edge, +1 at the trailing edge. $-1 \leq XM(M) \leq 1$. If $M \neq N$, $XM(M) \neq XM(N)$.

HM(NR,M) - Vertical coordinate of matching point M for airfoil centerline deflection mode NR. Nondimensionalized by the semichord, positive up.

XL(L) - Chordwise coordinate of loading point L of NL at which pressure is to be calculated. To be omitted if NL = 0. $-1 < XL(L) \leq +1$

MACH - Mach number, M. $0 \leq M < 1$

FREQ - Airfoil reduced frequency, k, referred to semichord.

CW - Tunnel wall porosity coefficient, c_W. $0 \leq c_W < \infty$. Use $c_W = 10^{100}$ for closed wall conditions.

ETAH - Tunnel semiheight nondimensionalized by the airfoil semichord. Equals the tunnel height to airfoil chord ratio η_H. Positive.

7.2. Input data format

DIGITAL COMPUTER INPUT DATA SHEETS

Programmer_____Date_____Page___of___Ident._____

DATA	SEQUENCE	DESCRIPTION - DO NOT KEYPUNCH
1 TITLE	INPUT DATA UNIT I	VARIABLE TITLE
13		
25		72 ALPHANUMERIC CHARACTERS
37		
49		
61 73 80		
1 NC NP	INPUT DATA UNIT II	CONTROL PARAMETERS
13 NH NX		
25 NL SRF		SEPARATE INDIVIDUAL DATA
37 GAF TSH		WITH A COMMA OR BLANKS
49		
61 73 80		
1 XM(1)	INPUT DATA UNIT III	MATCHING POINTS
13 XM(2)		
25 ...		SEPARATE INDIVIDUAL DATA
37 XM(NX)		WITH A COMMA OR BLANKS
49		
61 73 80		
1 HM(1,1)	INPUT DATA UNIT IV	MODE SHAPES
13 HM(2,1)		
25 ...		SEPARATE INDIVIDUAL DATA
37 HM(NX,1)		WITH A COMMA OR BLANKS. START
49		EACH MODE ON A NEW CARD
61 73 80		

DIGITAL COMPUTER INPUT DATA SHEETS

Programmer_____Date_____Page___of___Ident._____

DATA	SEQUENCE	DESCRIPTION - DO NOT KEYPUNCH
1 XL(1)	INPUT DATA UNIT V	LOADING POINTS
13 XL(2)		OMIT IF NL = 0
25 ...		SEPARATE INDIVIDUAL DATA
37 XL(NL)		WITH A COMMA OR BLANKS
49		
61	73 80	
1 MACH	INPUT DATA UNIT VI	FLOW PARAMETERS
13 FREQ		
25 ETAH		SEPARATE INDIVIDUAL DATA
37 CW		WITH A COMMA OR BLANKS. START
49		EACH CASE ON A NEW CARD
61	73 80	
1		REPEAT INPUT DATA UNITS I-VI
13		FOR AS MANY ADDITIONAL
25		PROBLEMS AS DESIRED
37		
49		
61	73 80	
1		
13		
25		
37		
49		
61	73 80	

7.3. Prompted interactive input

The following is an example of automatically prompted interactive communication between TWODI and its user. Responses by the user are underlined. The particular data are for the problem of Section 10, and the output is presented as the APPENDIX.

```
 ENTER TITLE.
?COMPARISON WITH THE KUESSNER-SCHWARZ SOLUTION USING ETAH = 300
 ENTER NC,NP,NH,NX,NL,SEC,GAF,TSH
?1,10,5,5,20,T,T,T
 ENTER MATCHING POINTS.
?-1,-.5,0,.5,1
 ENTER MODE SHAPE FOR MODE 1
?1,1,1,1,1
 ENTER MODE SHAPE FOR MODE 2
?-3,-2,-1,0,1
 ENTER MODE SHAPE FOR MODE 3
?5,1,-1,-1,1
 ENTER MODE SHAPE FOR MODE 4
?-7,1,1,-1,1
 ENTER MODE SHAPE FOR MODE 5
?9,-2,1,0,1
 ENTER LOADING POINTS
?-.9,-.8,-.7,-.6,-.5,-.4,-.3,-.2,-.1,0,.1,.2,.3,.4,.5,.6,.7,.8,.9,1
 ENTER MACH,FREQ,ETAH,CW FOR CASE 1
?0,1,300,1E100
```

§8. Convergence characteristics of TWODI

Numerical calculations with the TWODI program reflect the theoretical convergence predicted mathematically in Section 4. Tables 3 and 4 show for M = 0 and k = 0 the convergence of lift coefficient and center of pressure vs. NP with orders of magnitude variation in tunnel depth to chord ratio and for both the open and closed wall conditions. For the open wall condition, slower convergence of the infinite series for F and F' resulted in our omitting some of the calculations for the deeper tunnel cases.

Table 3. Convergence of C_{L_0} vs. NP for M = 0 and k = 0

(flat plate at unit angle of attack)

Wall	NP	η_H=1	η_H=10	η_H=100	η_H=1000	η_H=10000
Open	1	1.91357	5.39195	6.18551	6.27333	6.28220
"	2	1.91357	5.39195	6.18551	6.27333	6.28220
"	3	1.91357	5.39195	6.18551	6.27333	
"	4	1.91357	5.39195	6.18551		
"	5	1.91357	5.39195			
"	10	1.91357				
Closed	1	9.20520	6.30906	6.28344	6.28319	6.28319
"	2	8.26642	6.30894	6.28344	6.28319	6.28319
"	3	8.30090	6.30894	6.28344	6.28319	6.28319
"	4	8.29957	6.30894	6.28344	6.28319	6.28319
"	5	8.29957	6.30894	6.28344	6.28319	6.28319
"	10	8.29957	6.30894	6.28344	6.28319	6.28319

Table 4. Convergence of $\bar{x}_{CP}$ vs. NP for M = 0 and k = 0

(flat plate at unit angle of attack)

Wall	NP	η_H=1	η_H=10	η_H=100	η_H=1000	η_H=10000
Open	1	.250000	.250000	.250000	.250000	.250000
"	2	.110850	.247953	.249979	.250000	.250000
"	3	.111373	.247954	.249979	.250000	
"	4	.111440	.247954	.249979		
"	5	.111434	.247954			
"	10	.111435				
Closed	1	.250000	.250000	.250000	.250000	.250000
"	2	.307484	.251020	.250010	.250000	.250000
"	3	.306176	.251019	.250010	.250000	.250000
"	4	.306172	.251019	.250010	.250000	.250000
"	5	.306175	.251019	.250010	.250000	.250000
"	10	.306175	.251019	.250010		

Whereas section coefficients depend upon only the first two Fourier coefficients P_{ψ_1} and P_{ψ_2}, the generalized aerodynamic forces and the details of the pressure functions depend upon all the Fourier coefficients P_{ψ_n}; n = 1,...,NP. Tables 5 and 6 show, for steady and unsteady flow respectively, the convergence of these truncated sequences of Fourier coefficients with respect to the number NP of pressure basis functions employed, for both the open and closed tunnel wall conditions. The convergence for steady flow is much more rapid than for unsteady flow.

Table 5. Convergence of P_{ψ_n} vs. NP for M = 0, k = 0 and η_H = 10

(flat plate at unit angle of attack)

Wall	NP	P_{ψ_1}	P_{ψ_2}	P_{ψ_3}	P_{ψ_4}
Open	1	3.43262			
"	2	3.43262	-.014052		
"	3	3.43262	-.014047	.000023	
"	4	3.43262	-.014047	.000023	.000006
"	5	3.43262	-.014047	.000023	.000006
Closed	1	4.01647			
"	2	4.01640	.008194		
"	3	4.01640	.008188	-.000023	
"	4	4.01640	.008188	-.000023	-.000006
"	5	4.01640	.008188	-.000023	-.000006

Table 6. Convergence of P_{ψ_n} vs. NP for M = .5, k = .1 and η_H = 10

(flat plate oscillating about midchord-unit maximum angle of attack)

Wall	NP	P_{ψ_1}	P_{ψ_2}	P_{ψ_3}
Open	1	3.60308-.261310i		
"	2	3.64729-.260306i	-.007670+.522590i	
"	3	3.64763-.260345i	-.007831+.523485i	-.010920+.000024i
"	4	3.64772-.260359i	-.007871+.523535i	-.011029+.000015i
"	5	3.64776-.260365i	-.007853+.523553i	-.011068+.000013i
"	10	3.64779-.260371i	-.007898+.523572i	-.011106+.000012i
"	15	3.64780-.260372i	-.007900+.523574i	-.011111+.000012i
Closed	1	3.77355-.762277i		
"	2	3.81694-.772065i	.038394+.519791i	
"	3	3.81729-.772203i	.038279+.520718i	-.010978+.000855i
"	4	3.81739-.772245i	.038244+.520744i	-.011093+.000861i
"	5	3.81743-.772262i	.038232+.520794i	-.011134+.000865i
"	10	3.81747-.772280i	.038220+.520815i	-.011174+.000869i
"	15	3.81747-.772282i	.038219+.520817i	-.011787+.000869i

In general, we have found that the convergence of the TWODI program with respect to the number of pressure basis functions is remarkably good for steady flow and good for unsteady flow with the program being most efficient for narrow tunnels and low frequencies. The practical utility of the TWODI program would be improved by the incorporation of more efficient computer algorithms for deep tunnels and higher frequencies.

§9. Comparison with the Söhngen solution

For steady incompressible flow in an infinite atmosphere, the results of the TWODI program can be compared against the exact closed form Söhngen solution. This solution is given by the Söhngen inversion formula[1] (2-25) or, equivalently, by Bland's solution (3-24) in terms of airfoil polynomials. We shall utilize the latter because of their elegant simplicity.

Since the downwash polynomials are complete, they may be used as basis functions for deflections. In the present comparison, airloads will be calculated for airfoil deflections, or contours, spanned by the first five downwash polynomials (Fig. 3):

$$\zeta_n = \chi_n; \quad n = 1,2,3,4,5. \tag{9-1}$$

Written out, the first five downwash and pressure polynomials are

$$\chi_1(x) = 1, \tag{9-2$_1$}$$
$$\chi_2(x) = -1+2x, \tag{9-2$_2$}$$
$$\chi_3(x) = -1-2x+4x^2, \tag{9-2$_3$}$$
$$\chi_4(x) = 1-4x-4x^2+8x^3, \tag{9-2$_4$}$$
$$\chi_5(x) = 1+4x-12x^2-8x^3+16x^4, \tag{9-2$_5$}$$

$$\phi_1(\xi) = 1, \tag{9-3$_1$}$$
$$\phi_2(\xi) = 1+2\xi, \tag{9-3$_2$}$$
$$\phi_3(\xi) = -1+2\xi+4\xi^2, \tag{9-3$_3$}$$
$$\phi_4(\xi) = -1-4\xi+4\xi^2+8\xi^3, \tag{9-3$_4$}$$
$$\phi_5(\xi) = 1-4\xi-12\xi^2+8\xi^3+16\xi^4. \tag{9-3$_5$}$$

Then the downwash functions

$$w_n = \chi_n' \tag{9-4}$$

---

[1] Extensive closed form integrals based on the Söhngen and Küssner-Schwarz solutions have been tabulated by Fromme [88,1964,App. B and C] for piecewise continuous downwash functions expressed as powers.

are found to be

$$w_1 = 0, \tag{9-5$_1$}$$

$$w_2 = 2x_1, \tag{9-5$_2$}$$

$$w_3 = 2x_1+4x_2, \tag{9-5$_3$}$$

$$w_4 = 4x_1+2x_2+6x_3, \tag{9-5$_4$}$$

$$w_5 = 4x_1+6x_2+2x_3+8x_4, \tag{9-5$_5$}$$

and by equation (3-24), the corresponding pressures are

$$\Delta p_1(\xi) = 0, \tag{9-6$_1$}$$

$$\Delta p_2(\xi) = -\sqrt{\frac{1-\xi}{1+\xi}}\,[8\phi_1(\xi)], \tag{9-6$_2$}$$

$$\Delta p_3(\xi) = -\sqrt{\frac{1-\xi}{1+\xi}}\,[8\phi_1(\xi)+16\phi_2(\xi)], \tag{9-6$_3$}$$

$$\Delta p_4(\xi) = -\sqrt{\frac{1-\xi}{1+\xi}}\,[16\phi_1(\xi)+8\phi_2(\xi)+24\phi_3(\xi)], \tag{9-6$_4$}$$

$$\Delta p_5(\xi) = -\sqrt{\frac{1-\xi}{1+\xi}}\,[16\phi_1(\xi)+24\phi_2(\xi)+8\phi_3(\xi)+32\phi_4(\xi)]. \tag{9-6$_5$}$$

The results in (9-6), based on the Bland transform, have been checked independently with the formulas of Fromme, and are in agreement. Numerical values of pressure are presented in Table 7. Figure 12 depicts the deflection basis functions and the corresponding pressure functions. These results have been used to check the predictions of the TWODI code using six pressure basis functions with $\eta_H = 10^4$ and $c_W = 10^{100}$. To within the six decimal accuracy of printout,[2] the pressures predicted by TWODI are correct for all five deflections.

---

[2]In this work, we adopt a standard of six decimal accuracy as a compromise between reasonable generality and practical utility. Greater accuracy is attainable, but we note that six decimal accuracy is already orders of magnitude above experimental accuracy. However, intermediate calculations, especially those which occur many times, are performed to higher accuracies that are established internally in the computer program.

Table 7. Pressures for the Söhngen comparison

ξ	$\Delta p_1(\xi)$	$\Delta p_2(\xi)$	$\Delta p_3(\xi)$	$\Delta p_4(\xi)$	$\Delta p_5(\xi)$
-.9	0.0000	-34.8712	20.9227	-87.8754	-2.51073
-.8	0.0000	-24.0000	4.80000	-30.7200	-67.5840
-.7	0.0000	-19.0438	-3.80876	-5.33227	-84.2498
-.6	0.0000	-16.0000	-9.60000	7.68000	-81.4080
-.5	0.0000	-13.8564	-13.8564	13.8564	-69.2820
-.4	0.0000	-12.2202	-17.1083	15.6419	-53.1823
-.3	0.0000	-10.9022	-19.6239	14.3909	-36.3696
-.2	0.0000	-9.79796	-21.5555	10.9737	-21.0068
-.1	0.0000	-8.84433	-22.9953	6.01415	-8.56131
0	0.0000	-8.00000	-24.0000	.000000	.000000
.1	0.0000	-7.23627	-24.6033	-6.65737	4.11020
.2	0.0000	-6.53197	-24.8215	-13.5865	3.55339
.3	0.0000	-5.87040	-24.6557	-20.4290	-1.54978
.4	0.0000	-5.23723	-24.0913	-26.8146	-10.7258
.5	0.0000	-4.61880	-23.0940	-32.3316	-23.0940
.6	0.0000	-4.00000	-21.6000	-36.4800	-37.2480
.7	0.0000	-3.36067	-19.4919	-38.5805	-51.0016
.8	0.0000	-2.66667	-16.5333	-37.5467	-60.7573
.9	0.0000	-1.83533	-12.1132	-31.0537	-59.1324
1.0	0.0000	0.00000	0.00000	0.00000	0.00000

Values of section coefficients may be obtained by inspection of (9-6) using (3-37) and (3-38). The results are given in Table 8. Again the predictions of TWODI are correct to within the six decimals of printout.

Table 8. Section coefficients for the Söhngen comparison

Mode	C_L	C_M
1	0	0
2	-4π	0
3	-4π	-4π
4	-8π	-2π
5	-8π	-6π

To calculate the generalized aerodynamic force matrix, we expand the deflection functions given by (9-1) in terms of the pressure polynomials.

It is easy to show that

$$\chi_1 = \psi_1, \tag{9-7$_1$}$$

$$\chi_2 = -2\psi_1+\psi_2, \tag{9-7$_2$}$$

$$\chi_3 = 2\psi_1-2\psi_2+\psi_3, \tag{9-7$_3$}$$

$$\chi_4 = -2\psi_1+2\psi_2-2\psi_3+\psi_4, \tag{9-7$_4$}$$

$$\chi_5 = 2\psi_1-2\psi_2+2\psi_3-2\psi_4+\psi_5. \tag{9-7$_5$}$$

Combining equations (9-6), (9-7) and (3-42), we have our final result.

$$[A_{rs}] = \begin{bmatrix} 0 & -4\pi & -4\pi & -8\pi & -8\pi \\ 0 & 8\pi & 0 & 12\pi & 4\pi \\ 0 & -8\pi & 8\pi & -20\pi & 4\pi \\ 0 & 8\pi & -8\pi & 32\pi & -16\pi \\ 0 & -8\pi & 8\pi & -32\pi & 32\pi \end{bmatrix} \tag{9-8}$$

Again, the TWODI program is correct to within the accuracy of printout.

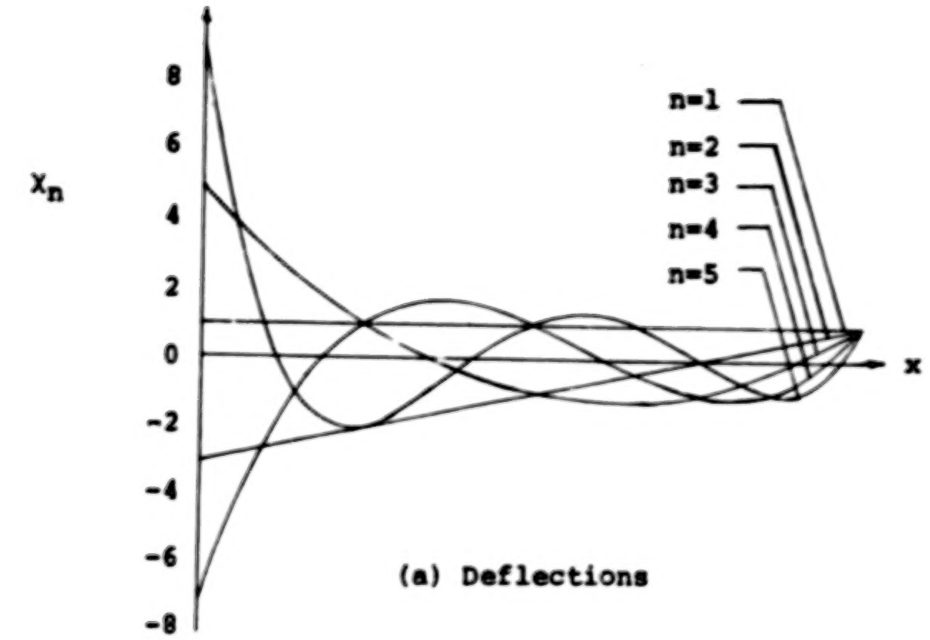

(a) Deflections

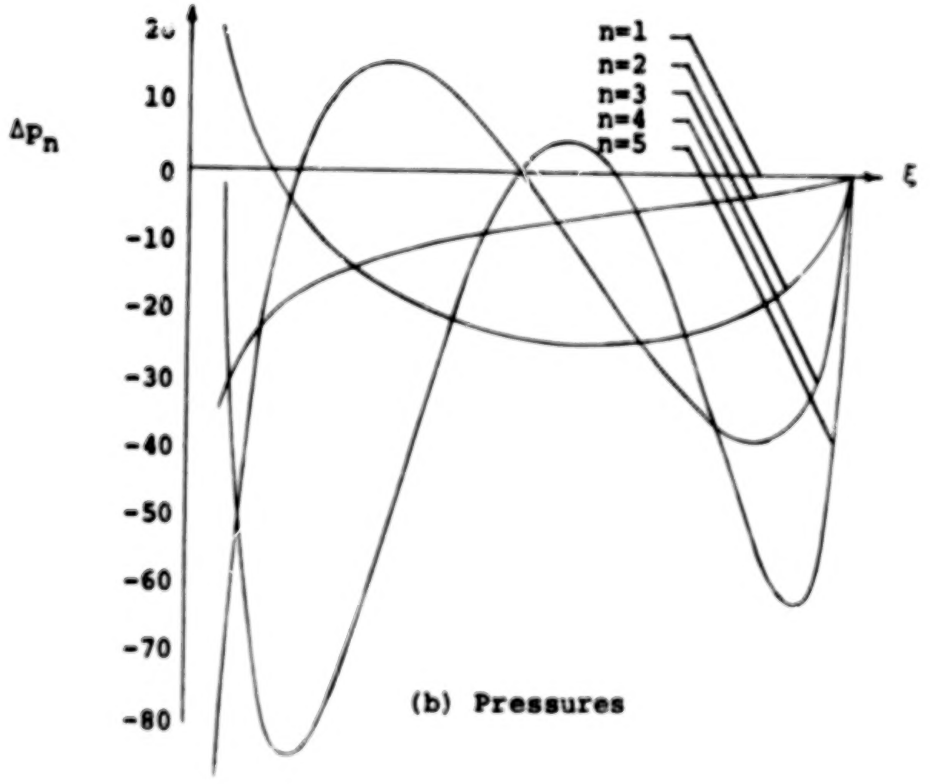

(b) Pressures

Figure 12. Deflections and pressures for the Söhngen comparison

§10. Comparison with the Küssner-Schwarz solution

This section compares the exact closed form Küssner-Schwarz solution for unsteady incompressible flow in an infinite atmosphere against the results of the TWODI program. Also, this section presents new and simplified expressions using airfoil polynomials for unsteady airloads based on the Küssner-Schwarz solution.

For airfoil deflections spanned by the first five downwash polynomials, the downwashes are

$$w_n = \left(\frac{d}{dx} + ik\right) \chi_n; \quad n = 1,2,3,4,5 \tag{10-1}$$

and it follows that

$$w_1 = ik\chi_1, \tag{10-2$_1$}$$

$$w_2 = 2\chi_1 + ik\chi_2, \tag{10-2$_2$}$$

$$w_3 = 2\chi_1 + 4\chi_2 + ik\chi_3, \tag{10-2$_3$}$$

$$w_4 = 4\chi_1 + 2\chi_2 + 6\chi_3 + ik\chi_4, \tag{10-2$_4$}$$

$$w_5 = 4\chi_1 + 6\chi_2 + 2\chi_3 + 8\chi_4 + ik\chi_5. \tag{10-2$_5$}$$

To organize the calculations, we make use of the inverse of the Bland transform, the Lambda transform and the Theodorsen functional, defined as follows:

$$H^{-1}w(\xi) \equiv \frac{1}{\pi} \int_{-1}^{1} \sqrt{\frac{1+x}{1-x}}\ \frac{w(x)}{x-\xi}\, dx \tag{10-3}$$

$$\Lambda w(\xi) \equiv \frac{1}{\pi} \sqrt{\frac{1+\xi}{1-\xi}} \int_{-1}^{1} \Lambda(x,\xi) w(x) dx \tag{10-4}$$

$$\mathcal{H} w \equiv \frac{1}{\pi} \int_{-1}^{1} \sqrt{\frac{1+x}{1-x}}\, w(x) dx \tag{10-5}$$

Thus,

$$\Delta p(\xi) = 4 \sqrt{\frac{1-\xi}{1+\xi}} \left(-H^{-1} - ik\Lambda + [1-C(k)]\mathcal{H}\right) w(\xi). \tag{10-6}$$

(a) The inverse Bland transform. Since

$$H^{-1}\chi_n = \psi_n, \tag{10-7}$$

then

$$H^{-1}w_1 = ik\psi_1, \tag{10-8$_1$}$$

$$H^{-1}w_2 = 2\psi_1+ik\psi_1, \tag{10-8$_2$}$$

$$H^{-1}w_3 = 2\psi_1+4\psi_2+ik\psi_3, \tag{10-8$_3$}$$

$$H^{-1}w_4 = 4\psi_1+2\psi_2+6\psi_3 ik\psi_4, \tag{10-8$_4$}$$

$$H^{-1}w_5 = 4\psi_1+6\psi_2+2\psi_3+8\psi_4+ik\psi_5. \tag{10-8$_5$}$$

(b) The Lambda transform. Fromme[1] has shown that

$$\Lambda[1] = 1 + \xi, \tag{10-9$_1$}$$

$$\Lambda[x] = \frac{1}{2}\xi + \frac{1}{2}\xi^2, \tag{10-9$_2$}$$

$$\Lambda[x^2] = \frac{1}{6} + \frac{1}{6}\xi + \frac{1}{3}\xi^2 + \frac{1}{3}\xi^3, \tag{10-9$_3$}$$

$$\Lambda[x^3] = \frac{1}{8}\xi + \frac{1}{8}\xi^2 + \frac{1}{4}\xi^3 + \frac{1}{4}\xi^4, \tag{10-9$_4$}$$

$$\Lambda[x^4] = \frac{3}{40} + \frac{3}{40}\xi + \frac{1}{10}\xi^2 + \frac{1}{10}\xi^3 + \frac{1}{5}\xi^4 + \frac{1}{5}\xi^5. \tag{10-9$_5$}$$

Hence,

$$\Lambda x_1 = \frac{1}{2}\psi_1 + \frac{1}{2}\psi_2, \tag{10-10$_1$}$$

$$\Lambda x_2 = \frac{1}{2}\psi_1 - \frac{1}{4}\psi_2 + \frac{1}{4}\psi_3, \tag{10-10$_2$}$$

$$\Lambda x_3 = - \frac{1}{4}\psi_2 - \frac{1}{12}\psi_3 + \frac{1}{6}\psi_4, \tag{10-10$_3$}$$

$$\Lambda x_4 = - \frac{1}{6}\psi_3 - \frac{1}{24}\psi_4 + \frac{1}{8}\psi_5, \tag{10-10$_4$}$$

$$\Lambda x_5 = - \frac{1}{8}\psi_4 - \frac{1}{40}\psi_5 + \frac{1}{10}\psi_6. \tag{10-10$_5$}$$

---

[1] [88,1964,Appendix C, formulas (C-45) to (C-49)].

Combining equations (10-2), (10-3) and (10-10), we get

$$Aw_1 = \tfrac{1}{2}ik\psi_1 + \tfrac{1}{2}ik\psi_2, \tag{10-11$_1$}$$

$$Aw_2 = (1-\tfrac{1}{2}ik)\psi_1 + (1-\tfrac{1}{4}ik)\psi_2 + \tfrac{1}{4}ik\psi_3, \tag{10-11$_2$}$$

$$Aw_3 = -\psi_1 - \tfrac{1}{4}ik\psi_2 + (1-\tfrac{1}{12}ik)\psi_3 + \tfrac{1}{6}\psi_4, \tag{10-11$_3$}$$

$$Aw_4 = \psi_1 - \tfrac{1}{6}ik\psi_3 + (1-\tfrac{1}{24}ik)\psi_4 + \tfrac{1}{8}ik\psi_5, \tag{10-11$_4$}$$

$$Aw_5 = -\psi_1 - \tfrac{1}{8}ik\psi_4 + (1-\tfrac{1}{40}ik)\psi_5 + \tfrac{1}{10}ik\psi_6. \tag{10-11$_5$}$$

(c) <u>The Theodorsen functional</u>. Since

$$\frac{1}{\pi}\int_{-1}^{1}\sqrt{\frac{1+x}{1-x}}\,\chi_m(x)\chi_n(x)\,dx = \delta_{mn}$$

and since $\chi_1(x) = 1$, it follows from (10-2) and (10-5) that

$$Hw_1 = ik, \tag{10-12$_1$}$$

$$Hw_2 = 2, \tag{10-12$_2$}$$

$$Hw_3 = 2, \tag{10-12$_3$}$$

$$Hw_4 = 4, \tag{10-12$_4$}$$

$$Hw_5 = 4. \tag{10-12$_5$}$$

The Fourier solution for pressure now follows.

$$\Delta p_1(\xi) = \sqrt{\frac{1-\xi}{1+\xi}}\,\{[-4ikC(k)+2k^2]\psi_1(\xi)+2k^2\psi_2(\xi)\}, \tag{10-13$_1$}$$

$$\Delta p_2(\xi) = \sqrt{\frac{1-\xi}{1+\xi}}\,\{[-8C(k)-4ik-2k^2]\psi_1(\xi)-(k^2+8ik)\psi_2(\xi)+k^2\psi_3(\xi)\}, \tag{10-13$_2$}$$

$$\Delta p_3(\xi) = \sqrt{\frac{1-\xi}{1+\xi}}\,\{[-8C(k)+4ik]\psi_1(\xi)-(16+k^2)\psi_2(\xi) - (8ik+\tfrac{1}{3}k^2)\psi_3(\xi)+\tfrac{2}{3}k^2\psi_4(\xi)\}, \tag{10-13$_3$}$$

$$\Delta p_4(\xi) = \sqrt{\frac{1-\xi}{1+\xi}}\,\{[-16C(k)-4ik]\psi_1(\xi)-8\psi_2(\xi)-(24+\tfrac{2}{3}k^2)\psi_3(\xi) - (8ik+\tfrac{1}{6}k^2)\psi_4(\xi)+\tfrac{1}{2}k^2\psi_5(\xi), \tag{10-13$_4$}$$

$$\Delta p_5(\xi) = \sqrt{\frac{1-\xi}{1+\xi}}\,\{[-16C(k)+4ik]\psi_1(\xi)-24\psi_2(\xi)-8\psi_3(\xi) - (32+\tfrac{1}{2}k^2)\psi_4(\xi)-(8ik+\tfrac{1}{10}k^2)\psi_5(\xi)+\tfrac{2}{5}k^2\psi_6(\xi)\}. \tag{10-13$_5$}$$

The section coefficients follow by inspection of (10-13)

$$C_{L_1} = \pi[-2ikC(k)+k^2], \tag{10-14$_1$}$$

$$C_{L_2} = \pi[-4C(k)-2ik-k^2], \tag{10-14$_2$}$$

$$C_{L_3} = \pi[-4C(k)+2ik], \tag{10-14$_3$}$$

$$C_{L_4} = \pi[-8C(k)-2ik], \tag{10-14$_4$}$$

$$C_{L_5} = \pi[-8C(k)+2ik], \tag{10-14$_5$}$$

$$C_{M_1} = \pi(\tfrac{1}{2}k^2), \tag{10-15$_1$}$$

$$C_{M_2} = \pi(\tfrac{1}{4}k^2-2ik), \tag{10-15$_2$}$$

$$C_{M_3} = \pi(-4-\tfrac{1}{4}k^2), \tag{10-15$_3$}$$

$$C_{M_4} = \pi(-2), \tag{10-15$_4$}$$

$$C_{M_5} = \pi(-6), \tag{10-15$_5$}$$

and the generalized aerodynamic forces follow from (3-42) using (9-7) and (10-11).

$$A_{11} = \pi[-2ikC(k)+k^2], \qquad (10\text{-}16_1)$$

$$A_{12} = \pi[-4C(k)-2ik-k^2], \qquad (10\text{-}16_2)$$

$$A_{13} = \pi[-4C(k)+2ik], \qquad (10\text{-}16_3)$$

$$A_{14} = \pi[-8C(k)-2ik], \qquad (10\text{-}16_4)$$

$$A_{15} = \pi[-8C(k)+2ik], \qquad (10\text{-}16_5)$$

$$A_{21} = \pi[4ikC(k)-k^2], \qquad (10\text{-}16_6)$$

$$A_{22} = \pi[8C(k)+\tfrac{3}{2}k^2], \qquad (10\text{-}16_7)$$

$$A_{23} = \pi[8C(k)-8-4ik-\tfrac{1}{2}k^2], \qquad (10\text{-}16_8)$$

$$A_{24} = \pi[16C(k)-4+4ik], \qquad (10\text{-}16_9)$$

$$A_{25} = \pi[16C(k)-12-4ik], \qquad (10\text{-}16_{10})$$

$$A_{31} = \pi[-4ikC(k)], \qquad (10\text{-}16_{11})$$

$$A_{32} = \pi[-8C(k)+4ik-\tfrac{1}{2}k^2], \qquad (10\text{-}16_{12})$$

$$A_{33} = \pi[-8C(k)+16+\tfrac{5}{6}k^2], \qquad (10\text{-}16_{13})$$

$$A_{34} = \pi[-16C(k)-4-4ik-\tfrac{1}{3}k^2], \qquad (10\text{-}16_{14})$$

$$A_{35} = \pi[-16C(k)+20+4ik], \qquad (10\text{-}16_{15})$$

$$A_{41} = \pi[4ikC(k)], \qquad (10\text{-}16_{16})$$

$$A_{42} = \pi[8C(k)-4ik], \qquad (10\text{-}16_{17})$$

$$A_{43} = \pi[8C(k)-16+4ik-\tfrac{1}{3}k^2], \qquad (10\text{-}16_{18})$$

$$A_{44} = \pi[16C(k)+16+\tfrac{7}{12}k^2], \qquad (10\text{-}16_{19})$$

$$A_{45} = \pi[16C(k)-32-4ik-\tfrac{1}{4}k^2], \qquad (10\text{-}16_{20})$$

$$A_{51} = \pi[-4ikC(k)], \qquad (10\text{-}16_{21})$$

$$A_{52} = \pi[-8C(k)+4ik], \qquad (10\text{-}16_{22})$$

$$A_{53} = \pi[-8C(k)+16-4ik], \qquad (10\text{-}16_{23})$$

$$A_{54} = \pi[-16C(k)-16-4ik-\tfrac{1}{4}k^2], \qquad (10\text{-}16_{24})$$

$$A_{55} = \pi[-16C(k)+48+\tfrac{9}{20}k^2]. \qquad (10\text{-}16_{25})$$

Numerical values of airloads based on the exact values given by (10-13) to (10-16) are presented in Tables 9 to 11 and Figure 13. The pilot version of TWODI will not accept $\eta_H = \infty$, and in its present form is most efficient for small values of η_H and k. Thus, the Küssner-Schwarz comparison represents a worthy test. Numerical values predicted by TWODI for $\eta_H = 300$, $k = 1$ and $NP = 8$, presented as the APPENDIX, are seen to be in close agreement. The aeroelastic effect is bounded by the relative error supremum norm of the generalized aerodynamic force matrix:

$$\epsilon_{[A]} \equiv \frac{\| A_{rs}^{EXACT}(\eta_H=\infty) - A_{rs}^{TWODI}(\eta_H=300) \|_{sup}}{\| A_{rs}^{EXACT}(\eta_H=\infty) \|_{sup}} = .0859\% \qquad (10\text{-}17)$$

This error norm represents the maximum difference between the exact solution in an infinite atmosphere and the numerical solution by TWODI, considering the combined effects of numerical inaccuracies, finite tunnel depth, and of using only eight pressure basis functions.

Table 9. Pressures for the Küssner-Schwarz comparison with k = 1

ξ	Re(Δp_1)	Re(Δp_2)	Re(Δp_3)	Re(Δp_4)	Re(Δp_5)
-.9	-0.00476	-22.1235	39.8542	-58.0293	31.2030
-.8	1.19673	-17.2664	19.0216	-10.3985	-45.0000
-.7	1.90178	-15.1291	7.87586	11.3355	-67.3412
-.6	2.39782	-13.7510	0.15838	22.4864	-68.0052
-.5	2.76939	-12.6708	-5.74258	27.4860	-58.0773
-.4	3.05338	-11.7245	-10.4536	28.3354	-43.2973
-.3	3.26916	-10.8415	-14.2720	26.1859	-27.2281
-.2	3.42795	-9.98838	-17.3565	21.8174	-12.2751
-.1	3.53653	-9.14889	-19.7975	15.8246	-0.10282
0	3.59891	-8.31548	-21.6488	8.70238	8.16904
.1	3.61715	-7.48545	-22.9421	0.89173	11.8675
.2	3.59169	-6.65892	-23.6943	-7.19346	10.7190
.3	3.52144	-5.83773	-23.9107	-15.1462	4.83414
.4	3.40348	-5.02478	-23.5855	-22.5477	-5.27874
.5	3.23253	-4.22359	-22.6988	-28.9431	-18.6663
.6	2.99945	-3.43774	-21.2084	-33.8024	-33.8236
.7	2.68808	-2.66984	-19.0296	-36.4390	-48.4592
.8	2.26630	-1.91849	-15.9772	-35.8007	-58.8993
.9	1.65154	-1.16439	-11.5352	-29.6921	-57.9349
1.0	0.00000	0.00000	0.00000	0.00000	0.00000

ξ	Im(Δp_1)	Im(Δp_2)	Im(Δp_3)	Im(Δp_4)	Im(Δp_5)
-.9	-9.40537	13.9580	5.56891	-10.7213	40.2743
-.8	-6.47322	4.80655	15.3666	-23.1229	41.3507
-.7	-5.13645	0.00520	19.8108	-25.0513	32.0497
-.6	-4.31548	-3.19563	21.7644	-22.5833	20.3991
-.5	-3.73731	-5.53878	22.1740	-18.0058	9.70705
-.4	-3.29600	-7.32879	21.5109	-12.5557	1.50242
-.3	-2.94050	-8.71875	20.0630	-7.01504	-3.63101
-.2	-2.64268	-9.79529	18.0309	-1.91505	-5.69315
-.1	-2.38547	-10.6108	15.5684	2.37511	-5.06828
0	-2.15774	-11.1978	12.8022	5.60437	-2.39563
.1	-1.95175	-11.5761	9.84331	7.61651	1.52646
.2	-1.76179	-11.7558	6.79503	8.33836	5.81963
.3	-1.58335	-11.7392	3.75865	7.77561	9.59778
.4	-1.41257	-11.5205	0.83939	6.01520	12.0401
.5	-1.24577	-11.0839	-1.84626	3.23568	12.4733
.6	-1.07887	-10.3989	-4.15891	-0.26982	10.4758
.7	-0.90643	-9.40897	-5.91387	-4.04442	6.03222
.8	-0.71925	-7.99927	-6.82594	-7.34788	-0.18414
.9	-0.49502	-5.87254	-6.31302	-8.75717	-6.07319
1.0	0.00000	0.00000	0.00000	0.00000	0.00000

Table 10. Section coefficients for the Küssner-Schwarz comparison with k = 1

Mode	C_L	C_M
1	2.51156 - 3.38937i	1.57080
2	-9.92033 - 5.02312i	-.785398 - 6.28319i
3	-6.77874 + 7.54325i	-13.3518
4	-13.5575 - 3.76305i	-6.28319
5	-13.5575 + 8.80332i	-18.8496

Table 11. Generalized aerodynamic forces for the Küssner-Schwarz comparison with k = 1

s	r = 1	r = 2	r = 3	r = 4	r = 5
1	2.51156 -3.38937i	-9.92033 -5.02312i	-6.77874 +7.54325i	-13.5575 -3.76305i	-13.5575 +8.80332i
2	-1.88153 +6.77874i	18.2699 -2.52013i	-13.1461 -15.0865i	14.5486 +7.52611i	-10.5842 -17.6066i
3	-1.26007 -6.77874i	-15.1283 +15.0865i	39.3260 +2.52013i	-40.7285 -7.52611i	35.7169 +17.6066i
4	1.26007 +6.77874i	13.5575 -15.0865i	-37.7520 +10.0462i	79.2130 -5.04027i	-74.2014 -17.6066i
5	-1.26007 -6.77874i	-13.5575 +15.0865i	36.7080 -10.0462i	-78.1658 +17.6066i	125.095 +5.04027i

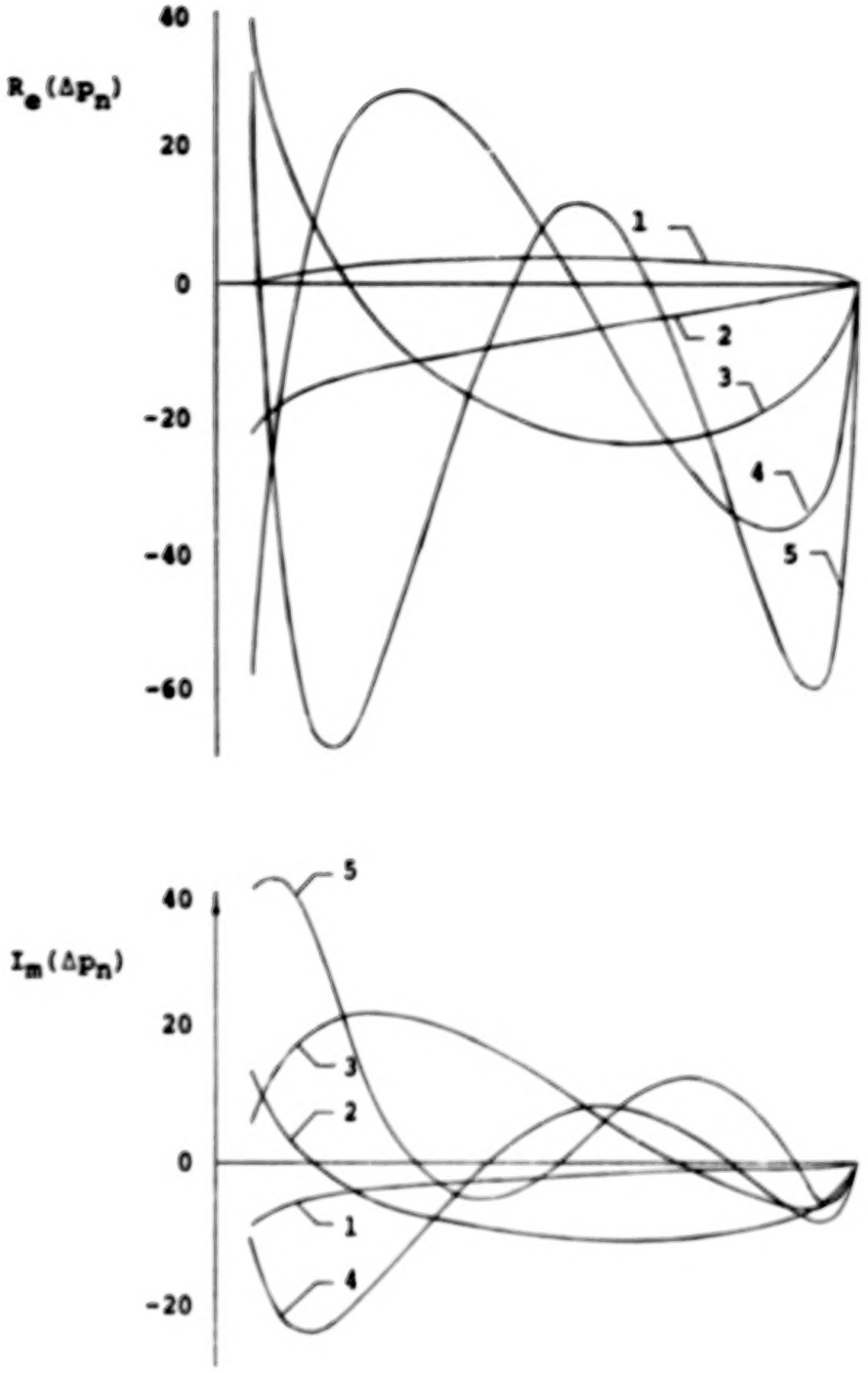

Figure 13. Pressures for Küssner-Schwarz comparison with k = 1

§11. Verification and extension of Bland's results

Bland [5,1970] presented numerical results for a flat plate oscillating about the 42.5% chord at M = .85 in a closed wind tunnel with $\eta_H = 7.5$. His published values of lift coefficient magnitude for various frequencies

$$|C_L| = 12.2351 \qquad k = 0$$
$$|C_L| = 7.99420 \qquad k = .1$$
$$|C_L| = 5.43569 \qquad k = .2$$

have been verified with the TWODI program, as have his values for generalized forces, etc.

Bland's results were based on a computer program written only for the closed tunnel condition $c_W = \infty$. We have extended these results to include the effect of ventilating the wind tunnel walls. Table 12 shows the effect on $C_{L_{\alpha}}$ of variations in the parameters η_H and c_W and indicates continuous behavior with respect to both parameters. Values of $c_W \geq 10^6$ reproduce Bland's closed wall results for $\eta_H = 7.5$ and the lift coefficient for M = .85, $\eta_H = 1000$ and $c_W = 10^6$ agrees to six decimals with the well known infinite atmosphere solution $C_{L_{\alpha}} = 2\pi/\beta$. We have since observed that the numerics are not adversely sensitive to large values of c_W and that the convergence rate of the infinite series in the kernel improves somewhat with large values of c_W/η_H. Consequently we now use $c_W = 10^{100}$ to represent a closed wall condition.

Table 12 also indicates that the effect of ventilation is considerably more pronounced for narrow tunnels than deep tunnels. Furthermore, for each value of η_H shown, the lift coefficient for an open jet tunnel is lower than the infinite atmosphere value and increases monotonically with increasing ventilation coefficient until the lift coefficient exceeds the infinite atmosphere value. These calculation therefore indicate that for every finite value of tunnel depth to chord ratio, there exists a unique ventilation coefficient such that the lift coefficient equals the value of the lift coefficient in an infinite atmosphere. In the case of an infinite atmosphere, the lift coefficient is the same for all values of ventilation coefficient as is to be expected.

Table 12. Lift coefficient C_{L_α} vs. η_H and c_W for M = .85 and k = 0

c_W	η_H = 1	η_H = 7.5	η_H = 10	η_H = 100	η_H = 1000
0	1.99486(5)[1]	8.22740(5,10)	8.98389(5)	11.5788(5)	11.8920(3)
10^{-4}	1.99506(5)	8.22744(5)	8.98391(5)	11.5788(4)	11.8920(3)
10^{-2}	2.01449(5)	8.23118(5)	8.98630(5)	11.5788(4)	11.8920(3)
1	3.83187(5)	8.57219(5)	9.20734(5)	11.5822(4)	11.8920(3)
10^4	20.1757(5)	11.8449(5)	11.7403(5)	11.7513(3)	11.8952(3)
10^6	21.8952(5)	12.2308(5)	12.0980(5)	11.9257(3)	11.9243(3)
10^{100}		12.2351(5)	12.0121(5)	11.9292(3)	11.9275(3)[3]
∞		12.2442(1)[2]			
∞		12.2351(2-20)[2]			

[1]Numbers in parenthesis indicate the number of pressure basis functions used in the calculations.

[2]These results are those of Bland's, which were programmed only for $c_W = \infty$.

[3]Compare with $\eta_H = \infty$, $C_{L_\alpha} = 2\pi/\beta = 11.9275$.

Table 12 indicates that section coefficients are continuous with respect to ventilation coefficient for all values of ventilation coefficient. Since c_W can be any nonnegative real number, it is convenient for graphing purposes to map the domain of c_W onto a finite interval. This can be accomplished by the transformation

$$\theta_W = \cot^{-1} c_W \tag{11-1}$$

which is equivalent to restating the boundary condition (2-49) as

$$p \sin \theta_W + \frac{\partial P}{\partial y} \cos \theta_W = 0. \tag{11-2}$$

Then $\theta_W = 0$ corresponds to a closed tunnel and $\theta_W = \frac{\pi}{2}$ corresponds to an open jet tunnel. Thus, we may call θ_W the ventilation angle. Graphs of section coefficients vs. ventilation angle are presented in Figures 14 to 16. Lift and moment are seen to be monotonically decreasing functions of ventilation angle. The ventilation angle at which the lift coefficient equals the corresponding infinite atmosphere value differs from the ventilation angle at which the moment coefficient equals the corresponding infinite atmosphere value (alas). The center of pressure, shown in Figure 16, is aft of the quarter chord for zero ventilation angle and is forward of the quarter chord for an open jet.

TABLE OF CONTENTS

SUMMARY	ii	1/A12
TABLE OF CONTENTS	iii	1/A1
LIST OF FIGURES	iv	1/A2
LIST OF TABLES	vi	1/A4
LIST OF SYMBOLS	vii	1/A5
§ 1. Introduction	1	1/A13
§ 2. History of the two dimensional problem	3	1/B1
§ 3. Theory of airfoil polynomials	21	1/C5
§ 4. Analytical and numerical properties of Bland's equation	28	1/C12
§ 5. Organization of the computer program	47	1/E3
§ 6. Some numerical considerations	51	1/E7
§ 7. Use of the TWODI program	63	1/F5
§ 8. Convergence characteristics of TWODI	68	1/F10
§ 9. Comparison with the Söhngen solution	71	1/F13
§10. Comparison with the Küssner-Schwarz solution	76	1/G4
§11. Verification and extension of Bland's results	85	1/G13
§12. Combined effects of depth to chord ratio and wall ventilation	90	2/A13
§13. Effect of wall ventilation of airfoil - tunnel acoustic resonance	107	2/C2
§14. Concluding remarks	111	2/C6
REFERENCES	113	2/C8
APPENDIX	119	2/C14

LIST OF FIGURES

1.	Coordinate system and airfoil contour.	4	1/B2
2.	Airfoil in a wind tunnel	15	1/B13
3.	Airfoil polynomials.	22	1/C6
4.	Interdigitation of zeros	25	1/C9
5.	Calling hierarchy of the TWODI program	50	1/E6
6.	The eigenvalue problem $\tan\lambda+\gamma\lambda=0$.	52	1/E8
7.	Spectra of $\tan\lambda+\gamma\lambda=0$ vs. $\tan^{-1}\gamma$	55	1/E11
8.	$F(\delta)$ and $F'(\delta)$ for $k=0$ and $\gamma=0,1,\infty$	59	1/F1
9.	Parametric behavior of $F(\delta)$ vs. k for $M=0,\eta_H=10,\gamma=1$.	60	1/F2
10.	Parametric behavior of $F(\delta)$ vs. M for $k=2\pi,\eta_H=10,\gamma=1$	61	1/F3
11.	Parametric behavior of $F'(\delta)$ vs. M for $k=2\pi,\eta_H=10,\gamma=1$.	62	1/F4
12.	Deflections and pressures for the Söhngen comparison	75	1/G3
13.	Pressures for the Küssner-Schwarz comparison with k=1.	84	1/G12
14.	Lift coefficient vs. ventilation angle for M=.85,k=0 and η_H=7.5.	87	2/A10
15.	Moment coefficient vs. ventilation angle for M=.85,k=0 and η_H=7.5.	88	2/A11
16.	Center of pressure vs. ventilation angle for M=.85,k=0 and η_H=7.5.	89	2/A12
17.	Wind tunnel depth angle.	90	2/A13
18.	Lift coefficient C_{L_α} vs. depth and ventilation for M=0 and k=0	93	2/B2
19.	Lift coefficient C_{L_α} vs. depth and ventilation for $M=\frac{1}{\sqrt{2}}$ and k=0.	94	2/B3
20.	Moment coefficient C_{M_α} vs. depth and ventilation for M=0 and k=0	95	2/B4
21.	Moment coefficient C_{M_α} vs. depth and ventilation for $M=\frac{1}{\sqrt{2}}$ and k=0.	96	2/B5
22.	Center of pressure $\bar{x}_{CP}$ vs. depth and ventilation for M=0 and k=0	97	2/B6
23.	Center of pressure $\bar{x}_{CP}$ vs. depth and ventilation for $M=\frac{1}{\sqrt{2}}$ and k=0.	98	2/B7
24.	Lift coefficient magnitude $\lvert C_{L_h}\rvert$ vs. depth and ventilation for M=0 and k=.1	99	2/B8
25.	Lift coefficient magnitude $\lvert C_{L_\alpha}\rvert$ vs. depth and ventilation for M=0 and k=.1	100	2/B9
26.	Moment coefficient magnitude $\lvert C_{M_h}\rvert$ vs. depth and ventilation for M=0 and k=.1	101	2/B10
27.	Moment coefficient magnitude $\lvert C_{M_\alpha}\rvert$ vs. depth and ventilation for M=0 and k=.1	102	2/B11

28. Lift phase angle ϕ_{L_h} vs. depth and ventilation for M=0 and k=.1. . . . 103 **2/B12**

29. Lift phase angle ϕ_{L_α} vs. depth and ventilation for M=0 and k=.1. . . . 104 **2/B13**

30. Moment phase angle ϕ_{M_h} vs. depth and ventilation for M=0 and k=.1. . . 105 **2/B14**

31. Moment phase angle ϕ_{M_α} vs. depth and ventilation for M=0 and k=.1. . . 106 **2/C1**

32. Effect of ventilation on $|C_{L_\alpha}|$ vs. k with acoustic resonance effects . 109 **2/C4**

33. Effect of ventilation on ϕ_{L_α} vs. k with acoustic resonance effects . . 110 **2/C5**

LIST OF TABLES

1.	Convergence of function subroutine PICARD.	54	1/E10
2.	Accuracy of subroutine SUM for γ=k=0	58	1/E14
3.	Convergence of C_{L_α} vs. NP for M=0 and k=0.	68	1/F10
4.	Convergence of $\bar{x}_{CP}$ vs. NP for M=0 and k=0.	68	1/F10
5.	Convergence of P_{ψ_n} vs. NP for M=0, k=0 and η_H=10	69	1/F11
6.	Convergence of P_{ψ_n} vs. NP for M=.5, k=.1 and η_H=10	69	1/F11
7.	Pressures for the Söhngen comparison	73	1/G1
8.	Section coefficients for the Söhngen comparison.	73	1/G1
9.	Pressures for the Küssner-Schwarz comparison with k=1.	82	1/G10
10.	Section coefficients for the Küssner-Schwarz comparison with k=1 . .	83	1/G11
11.	Generalized aerodynamic forces for the Küssner-Schwarz comparison with k=1	83	1/G11
12.	Lift coefficient C_{L_α} vs. η_H and c_W for M=.85, and k=0.	86	1/G14
13.	Resonant frequencies vs. ventilation coefficient for M=$\frac{\sqrt{3}}{2}$ and η_H=10.	108	2/C3

LIST OF SYMBOLS

This section provides a partial list of frequently occurring symbols and their names. Places of first occurrence or definition are given by section number denoted with §, by equation number enclosed in parentheses, etc. In a few instances the same symbol is used for different meanings but it will be clear from the context which is correct. Any consistent system of physical units may be employed, although most quantities are nondimensional.

Symbol	Name	Place
$A, C(A)$	Complex matrix, condition number.	§4.5
A_{rs}	Components of generalized aerodynamic force matrix.	(3-39)
$\underline{a} = \{\hat{a}_n\}$	Matrix of unknowns with quadrature approximation.	(4-46),(4-47)
a_n	Coefficients of pressure basis functions.	(2-5)
b	Airfoil semichord.	(2-8)
b_n	Coefficients of downwash basis functions.	(2-6)
$C(k)$	Theodorsen's circulation function.	(2-17)
Ci	Cosine integral function.	(2-12)
$C_L, \lvert C_L \rvert$	Lift coefficient and magnitude.	(3-35)
$C_M, \lvert C_M \rvert$	Moment coefficient and magnitude.	(3-36)
C_{L_h}, C_{L_α}	Lift coefficients due to unit plunging and pitching motions.	§§8,12
C_{M_h}, C_{M_α}	Moment coefficients due to unit plunging and pitching motions.	§§11,12
C_{L_i}, C_{M_i}	Lift and moment coefficients due to ith deflection function.	§10
c_∞	Speed of sound.	(2-43)
c_W	Wall ventilation coefficient.	(2-49)
$E = [\epsilon_{mn}]$	Matrix of quadrature errors.	§4.4

Symbol	Name	Place
F,F'	Function defined by infinite series, and its derivative.	(2-51)
f,f'	Function defined by infinite series, and its derivative.	(6-10),(6-11)
$\hat{f},\hat{f}'$	Closed form sums for infinite series and its derivative.	(6-12),(6-13)
G	Infinite series of Mathieu functions.	(2-40)
G	Matrix of inner products $<\psi_m,\chi_n>_2$	§4.4
$[g_{mn}]$	Quadrature of $G = [<\psi_m,\chi_n>_2]$.	§4.4
H_1,H_2	Hilbert spaces.	§4.2
$[H_1,H_2]$	Bounded linear operators from H_1 to H_2.	§4.2
H,H^{-1},H^*	Element of $[H_1,H_2]$, its inverse and adjoint.	§4.2
H,H^{-1}	Bland transforms.	(3-25),(3-26)
$H_n^{(2)}$	Hankel function of the second kind.	(2-18)
h	Airfoil profile function.	Figure 1
h_r	rth structural basis function.	(3-39)
h_{nr}	nth generalized Fourier coefficient of h_r.	(3-40)
I	Identity operator in a Hilbert space.	§4
Im	Imaginary part.	Table 9
I_n	Interval.	§6
i	Imaginary unit, $i^2 = -1$.	(2-9)
J_n	Bessel function of the first kind.	(2-18)
$K,\tilde{K}$	Kernel functions.	(2-1),(4-4)
K_C,K_{SC}	Continuous parts of kernel functions.	(4-3),(4-5)
K,K_i	Compact operators.	Definition 4.2
k	Reduced frequency. Also integer parameter.	(2-8)
$\hat{k}$	Reduced frequency under Küssner transformation.	(2-33)
k_n	Resonant reduced frequencies.	(2-44)
k_{max}	Maximum number of iterations.	(6-8)
L	Compact operator.	(4-28)

Symbol	Name	Place
$\underline{L} = [L_m(x_k)]$	Collocation matrix.	(4-48)
L_w^2, L_p^2	Spaces of Lebesgue square integrable functions for downwash and pressure.	(3-11),(3-12)
M	Mach number, v_∞/c_∞. Also integer parameter.	(2-30)
ND	Number of decimals of accuracy.	(6-18)
Ne_n	Mathieu function of the third kind.	(2-40)
NP	Number of pressure basis functions.	(2-5)
NQ	Number of quadrature points.	(2-24)
NT	Number of terms in an infinite series calculation.	(6-18)
n,N	Integer.	
P	Nonsingular factor of pressure. Also a matrix of polynomial values in §4.	(2-56),Theorem 4.10
P_{ψ_n}	Generalized Fourier coefficient of P.	(3-24)
P_{ns}	Generalized Fourier coefficient of P due to h_s.	(3-41)
P_N	Approximation to pressure function P.	(4-1)
P_N^C, P_N^G	Collocation and Galerkin approximation to pressure function P.	Theorem 4.12
$\hat{P}_N^C$	Quadrature approximation to P_N^G.	Theorem 4.12
p_n	Polynomials.	Theorem 4.10
Q_n	Orthogonal projection operator.	(4-12)
Re	Real part.	(2-9)
R_n, r_n	Residual errors.	(4-2),(4-32)
Si	Sine integral function.	(2-12)
se_n	Mathieu function of the first kind.	(2-40)
T, T_n	Compact operators.	§4
$T(k), T(\kappa,\hat{k})$	Functions used by Küssner that are related to Theodorsen's function.	(2-27),(2-41)
t	Time.	(2-9)
U_n	Span $\{\psi_k\}_1^n$.	Theorem 4.5
V	Vandermonde matrix.	Theorem 4.10
v_∞	Free stream velocity.	(2-8)

Symbol	Name	Place
$W, [\ W_n\ ]$	Diagonal matrices of quadrature weights.	(4-48),(2-24)
$\underline{W}, \{w(x_m)\}$	Column matrices of downwashes.	(4-47),(2-24)
$[w_n(x_m)]$	Rectangular matrix of induced downwashes.	(2-23),(2-24)
$w(x), w_n(x)$	Downwash functions.	(2-4),(2-22)
$\tilde{w}$	Downwash multiplied by $\frac{4}{\beta}$.	§4.2
$x, y, \hat{x}, \hat{y}$	Body coordinates.	Figure 1,(2-33)
x, y	Vectors in a Hilbert space.	Definition 4.3
$\bar{x}_{CP}$	Center of pressure as a fraction of chord, aft of leading edge.	Table 4
x_m	Quadrature nodes. Also collocation points.	(2-24)
x_i^n	Zero of χ_n.	(3-24)
Y_n	Bessel function of the second kind.	(2-18)
β	Co Mach number, $\sqrt{1-M^2}$.	(2-21)
γ	Wind tunnel parameter.	(2-55)
$\Delta p, \Delta p_s$	Pressure jump.	(2-1)
δ	Difference variable.	(2-51)
δ_{mn}	Kronecker delta: $\delta_{mn} = 1$ if $m = n$, $\delta_{mn} = 0$ if $m \neq n$.	(3-5)
δ_{min}	Smallest argument of F.	(6-15)
ε	Error tolerance.	§6
$\varepsilon_{[A]}$	Supremum error norm of generalized aerodynamic force matrix.	(10-17)
ε_{mn}	Quadrature errors.	§4.4
ζ_n	Frequency ratio.	(2-53)
η	Dummy variable. Also elliptic coord.	(2-26),(2-38)
η_H	Wind tunnel depth to airfoil chord ratio.	Figure 2
$\eta_x(\xi)$	$K_C(x-\xi)$.	§4.2
θ	Angular streamwise coordinate.	(2-14)
θ_H, θ_W	Tunnel depth angle and ventilation angle.	(12-1),(11-1)
κ	Compressibility frequency parameter.	(2-33)
$\Lambda(x,\xi)$	Symmetric logarithmic function in inverse kernel.	(2-29)

Symbol	Name	Place
$\lambda, \lambda_n, \lambda_n^{(k)}$	Eigenvalues and iterate.	(2-54),(6-1),(6-4)
$\bar{\lambda}_n$	Eigenvalue modified by frequency ratio.	(2-53)
ξ	Streamwise coordinate, also elliptic coordinate.	(2-3),(2-38)
ξ_i^n	Zero of ψ_n.	(3-25)
Π	Product symbol.	Theorem 4.10
π	Collocation matrix for polynomials. Also 3.14159...	Theorem 4.10
ρ_n	Convergence rate.	(6-5)
$\phi_{L_\eta}, \phi_{L_\alpha}$	Lift phase angles in plunging and pitching motions.	Figures 28,29
$\phi_{M_h}, \phi_{M_\alpha}$	Moment phase angles in plunging and pitching motions.	Figures 30,31
$\underline{\chi}$	Matrix of downwash polynomials.	(4-48)
χ_n	Downwash polynomial.	(3-1)
ψ_n	Pressure polynomial.	(3-2)
ω	Frequency of oscillation (rad/sec).	(2-8)
f_{w_n}, g_{p_n}	Generalized Fourier coefficients with respect to downwash and pressure polynomials.	(3-15),(3-16)
$\langle f,g\rangle_1, \langle f,g\rangle_2$	Inner products on Hilbert spaces.	§4.2
$\langle f,g\rangle_w, \langle f,g\rangle_p$	Weighted inner products on function spaces.	(3-7),(3-8)
$\|f\|_1, \|f\|_2$	Hilbert space norms.	§4.2
$\|f\|_p, \|f\|_w$	Inner product norms.	(3-9),(3-10)
$\|\ \|$	Operator norm.	Theorem 4.2
$\|\ \|_{sup}$	Supremum norm.	(10-7)
$\rightarrow$	Implies, also limit.	§2
$\leftrightarrow$	Is equivalent to.	§3

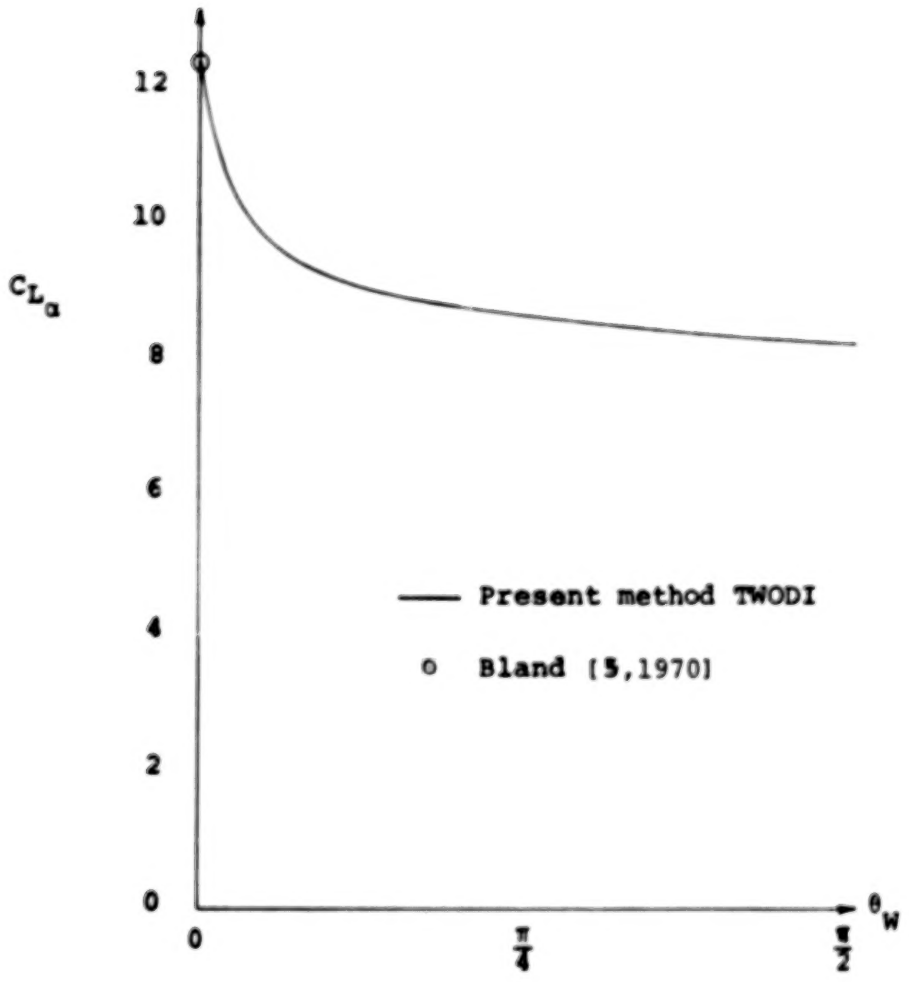

Figure 14. Lift coefficient vs. ventilation angle for M = .85, k = 0 and η_H = 7.5

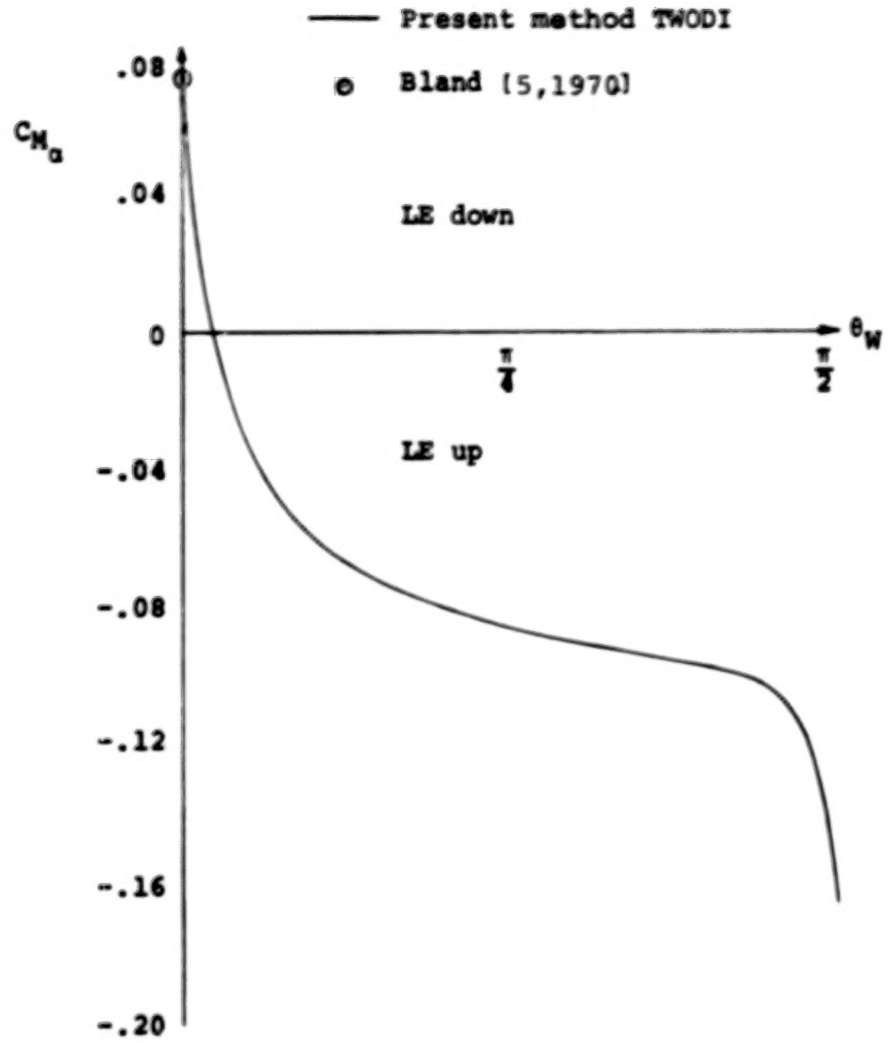

Figure 15. Moment coefficient vs. ventilation angle for B = .85, k = 0 and η_H = 7.5

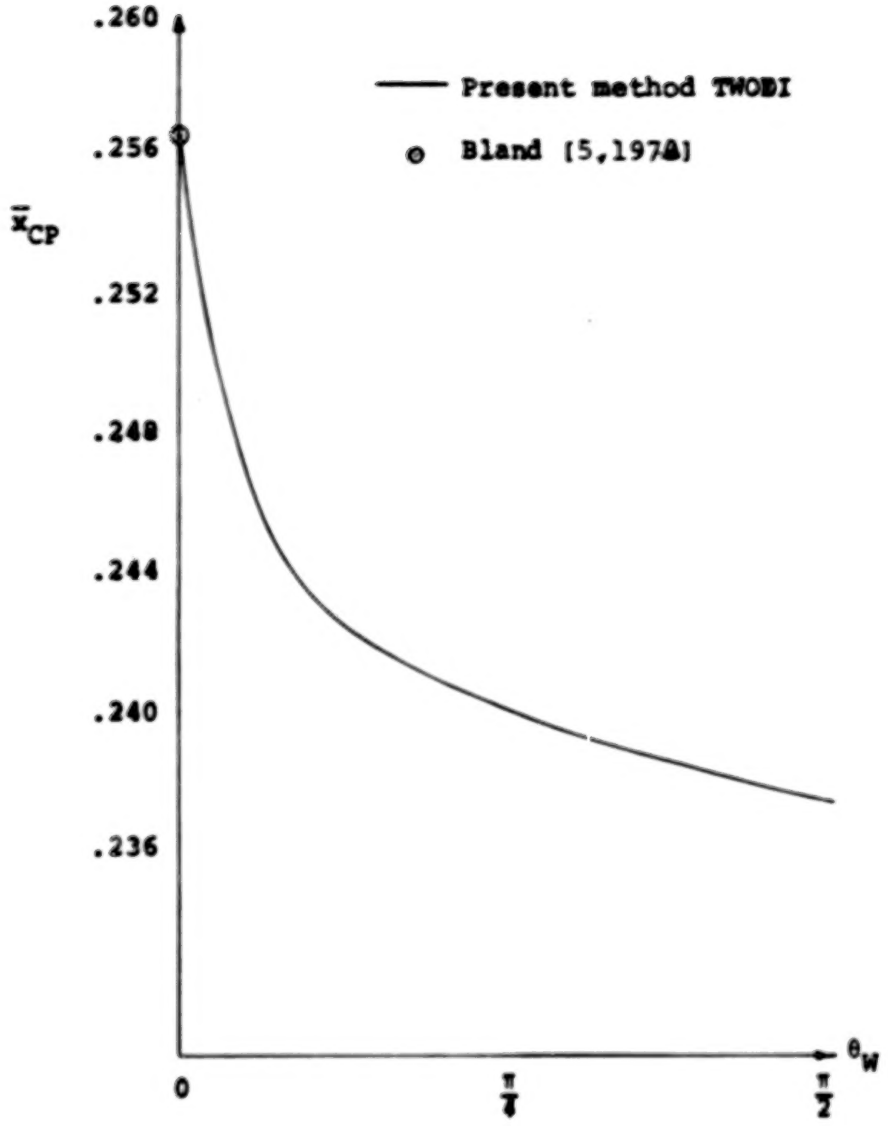

Figure 16. Center of pressure vs. ventilation angle for M = .85, k = 0 and η_H = 7.5

§12. Combined effects of depth to chord ratio and wall ventilation

This section presents predictions of the combined effects of tunnel depth to chord ratio η_H and wall ventilation coefficient c_W. Since the number of possible combinations of parameters can be quite large, we shall restrict the discussion to section coefficients defined for a limited domain of Mach number, frequency and mode shape;

(1) $M = 0,\ 1/\sqrt{2}$,

(2) $k = 0,\ .1$,

(3) vertical translation (h), pitch rotation (α),

and to the doubly infinite domain of tunnel depth and wall porosity;

(4) $1 \leq \eta_H < \infty$,

(5) $0 \leq c_W < \infty$.

The resulting section coefficients can then be graphed as surfaces defined over a two dimensional region of tunnel depth and wall ventilation. It is convenient for graphing purposes to transform the supporting domain onto one of finite extent. This has already been partially accomplished in Section 11 by introducing the ventilation angle θ_W as defined by equation (11-1). Similarly we define a tunnel depth angle θ_H by

$$\theta_H = \cot^{-1}\eta_H \tag{12-1}$$

which varies from 0 for infinite depth to $\frac{\pi}{2}$ for zero depth. The depth angle is shown in Figure 17 as the angle between the line perpendicular to the airfoil passing through the midchord and the line from the midchord to the point of intersection with the tunnel wall of a line perpendicular to the airfoil passing through the trailing edge.

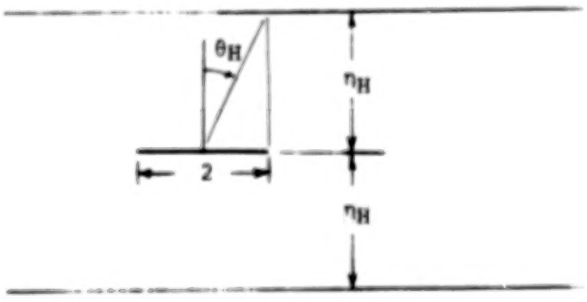

Figure 17. Wind tunnel depth angle

For present purposes, however, we shall consider only tunnels with depth greater than or equal to the airfoil chord. Thus,

$$0 \leq \theta_H \leq \frac{\pi}{4}. \tag{12-2}$$

We can now represent the section coefficients for all possible values of ventilation coefficient and tunnel depth to chord ratio as surfaces with bounded support.

$$C_{L_\alpha} = C_{L_\alpha}(\theta_H, \theta_W),\ C_{L_h} = C_{L_h}(\theta_H, \theta_W),\ \text{etc.} \tag{12-3}$$

Figure 18 presents in compact form the complete range of values of lift coefficients C_{L_α} at $M = 0$ and $k = 0$ for all tunnel depths greater than or equal to the airfoil chord and for all possible values of wall ventilation coefficient. Several features of this C_{L_α} surface may be observed. The line $\theta_H = 0$ corresponds to a tunnel of infinite depth and indicates a constant value of $C_{L_\alpha} = 2\pi$ for all values of ventilation coefficient as it should, and is in keeping with the condition that the airfoil pressure not be affected by walls if they are infinitely far away. The line $\theta_W = 0$ corresponds to a completely closed wall and indicates that C_{L_α} increases as the walls are brought closer together. The amount of increase in C_{L_α} with depth decreases with increasing ventilation so that beyond a certain value of θ_W, C_{L_α} decreases as the walls are brought closer together. At the present time, we have not investigated if the trend reversal is reflected by experiment but this question is fundamental and bears on the validity of the boundary condition (2-49).

Figure 19 shows the C_{L_α} surface for $M = 1/\sqrt{2}$ and $k = 0$, and displays the same trends as Figure 18 for $M = 0$. Along the line $\theta_H = 0$ ($\eta_H = \infty$), the value of C_{L_α} equals the expected value of $\frac{2\pi}{\beta}$ for all values of θ_W. This magnification with respect to Mach number is observed throughout the entire C_{L_α} surface, but the magnification factor is given by the well known value $\frac{1}{\beta}$ only for the infinite depth condition $\theta_H = 0$.

Figures 20 and 21 show the C_{M_α} surfaces for $M = 0$, $k = 0$ and $M = 1/\sqrt{2}$, $k = 0$ respectively. Since the pitching moment is computed about the quarter chord, $C_{M_\alpha} = 0$ along the lines $\theta_H = 0$ which correspond to the infinite depth case $\eta_H = \infty$. For closed tunnel walls, the moment coefficients increase

as the walls are brought closer together, the rate of increase being greater at the higher Mach number. For intermediate values of θ_W the increase with depth angle decreases until the moment coefficients decrease with increasing θ_H, similar to the behavior of the lift coefficient surfaces. Reversal occurs sooner at the higher Mach number.

Figures 22 and 23 show the center of pressure surfaces for the two Mach numbers. In both figures the center of pressure is at the quarter chord for infinite depth ($\theta_H = 0$), as is to be expected. For closed walls, the center of pressure moves aft as the walls are brought closer together, more so at the higher Mach number. Again, this trend reverses for ventilated walls, more pronounced at the higher Mach number.

Figures 24 to 27 show the surfaces representing magnitudes of lift and moment coefficients for vertical translation and pitch rotation about midchord at M = 0 and reduced frequency k = .1. Surfaces representing phase angles are shown in Figures 28 to 31.

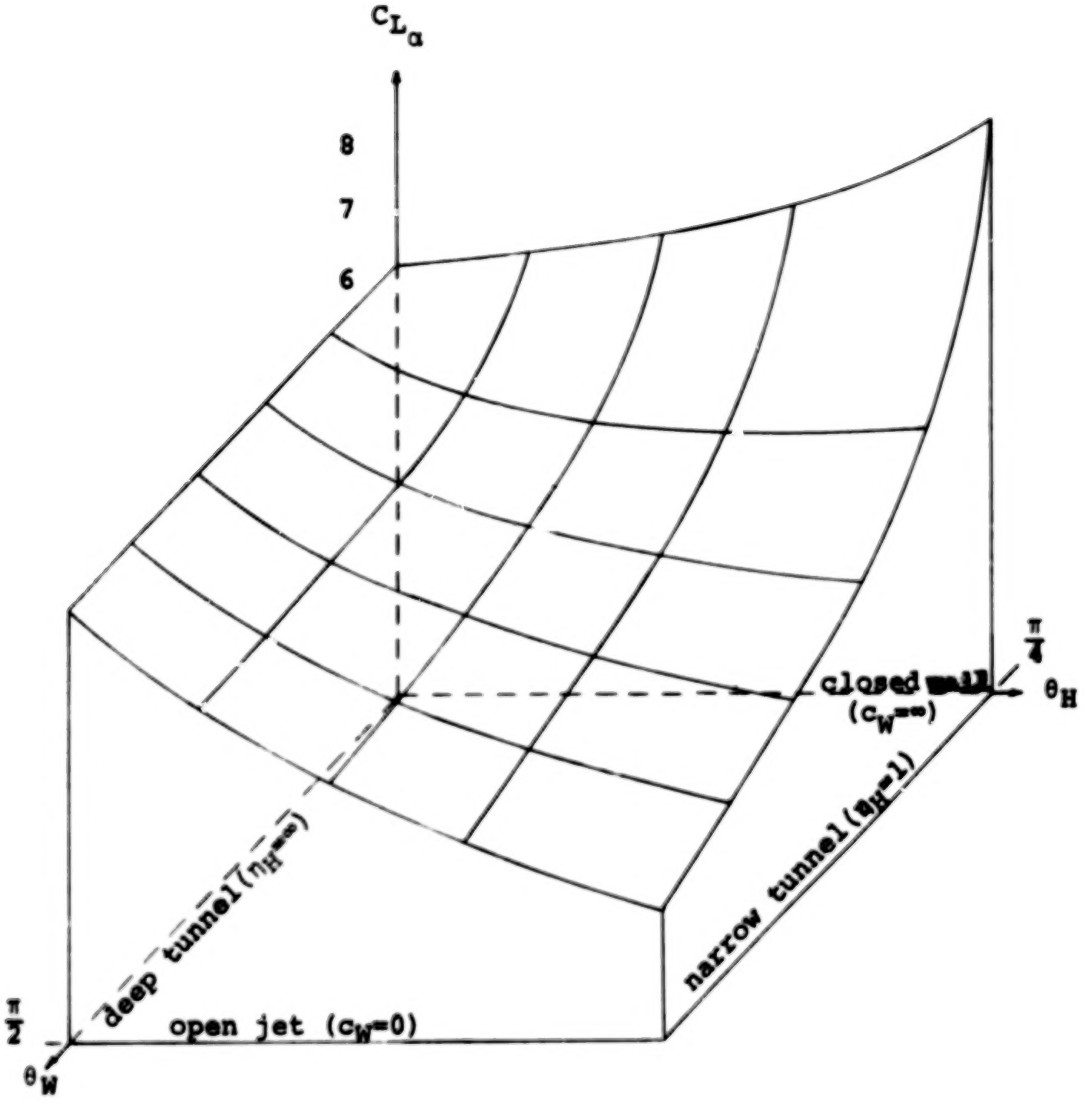

Figure 18. Lift coefficient C_{L_α} vs. depth and ventilation for M = 0 and k = 0

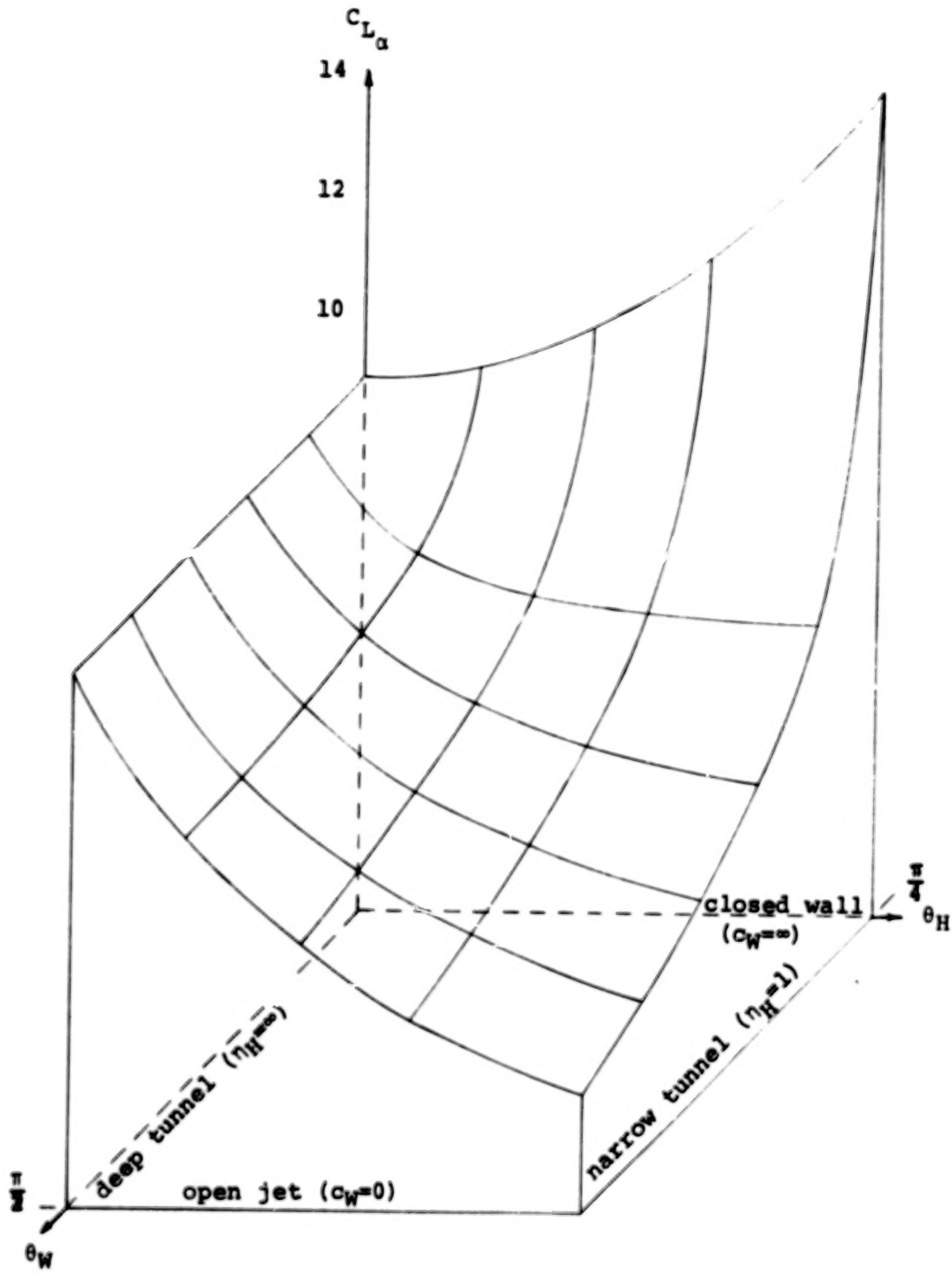

Figure 19. Lift coefficient C_{L_α} vs. depth and ventilation for $M = 1/\sqrt{2}$ and $k = 0$

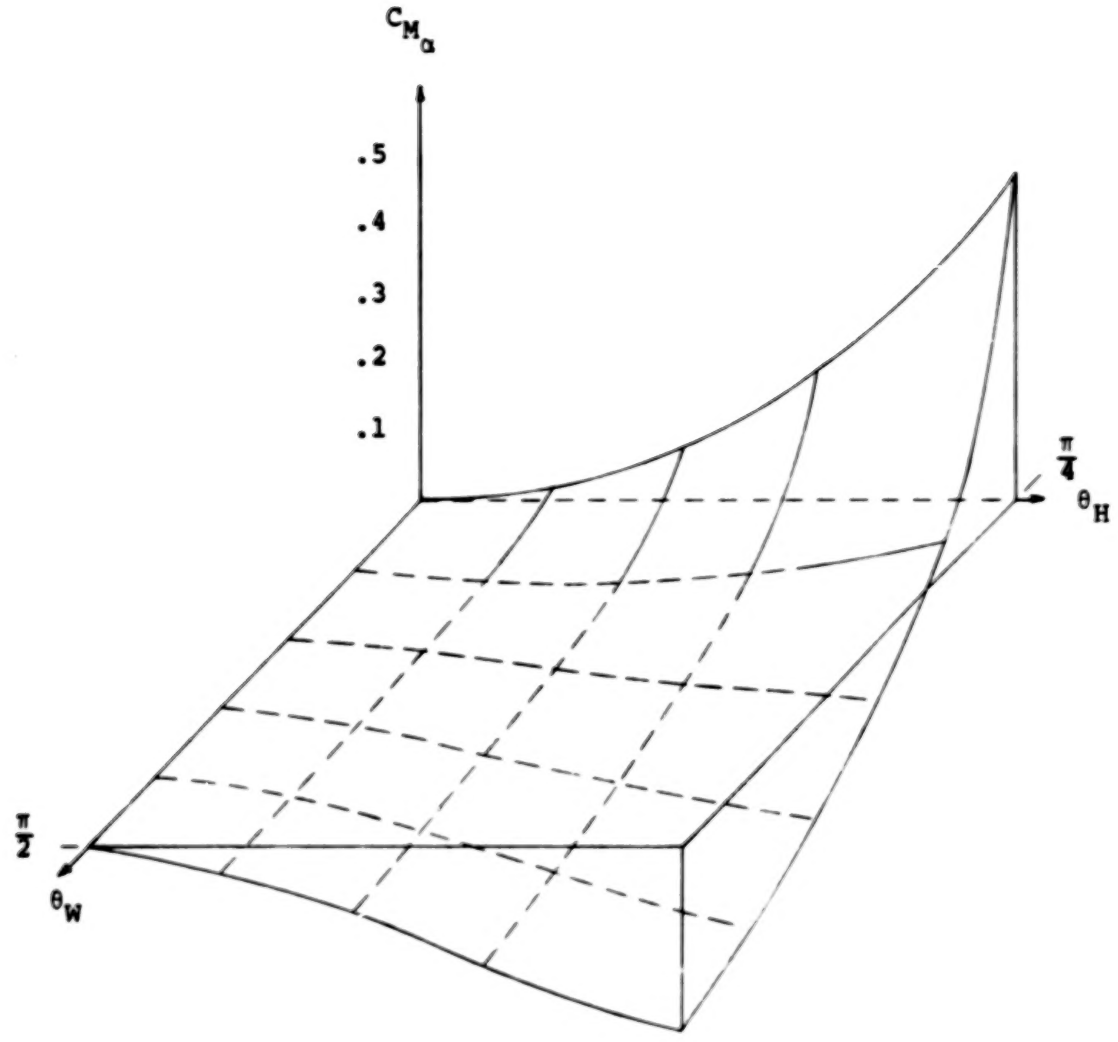

Figure 20. Moment coefficient C_{M_α} vs. depth and ventilation for M = 0 and k = 0

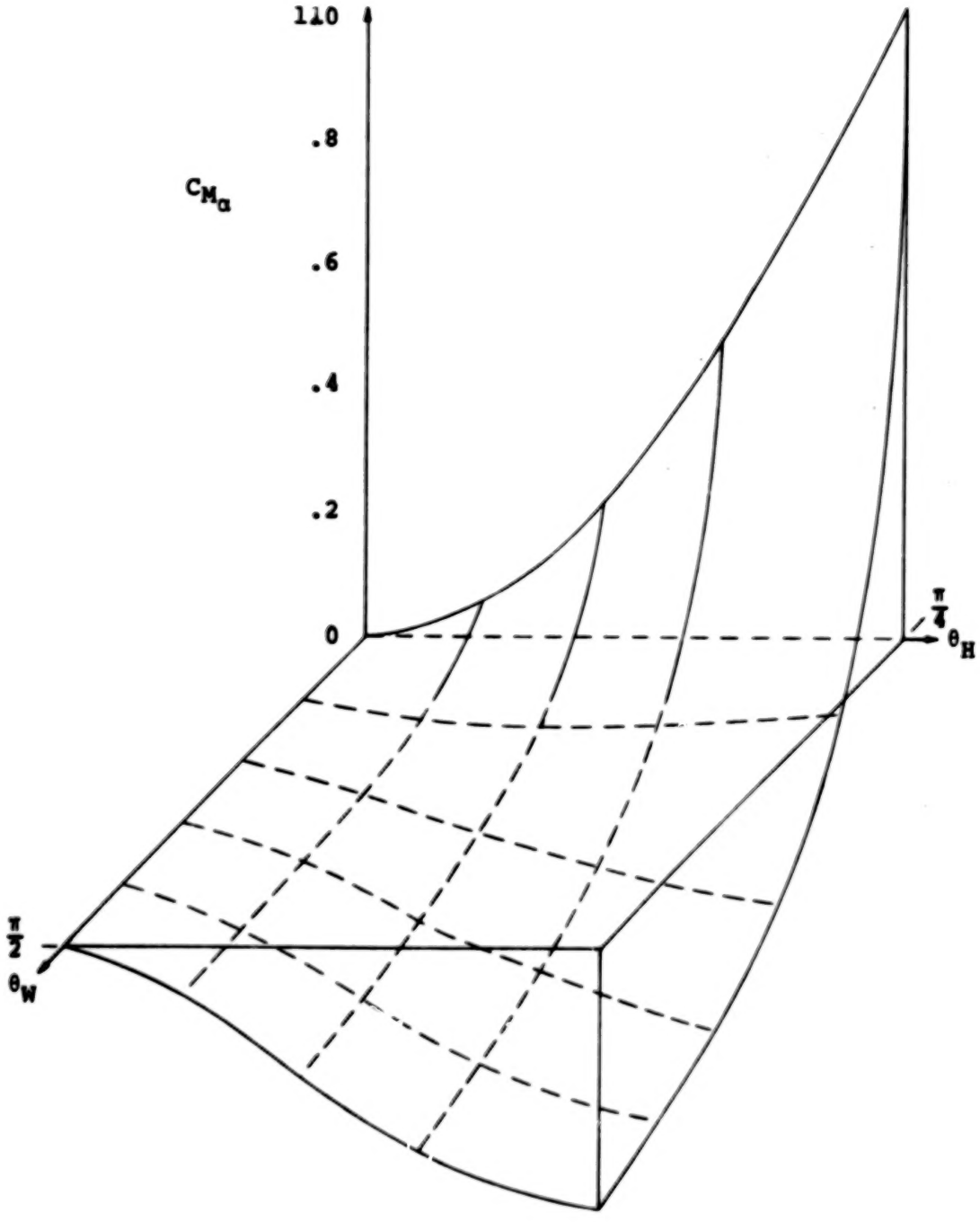

Figure 21. Moment coefficient C_{M_α} vs. depth and ventilation for $M=\frac{1}{\sqrt{2}}$ and k=0

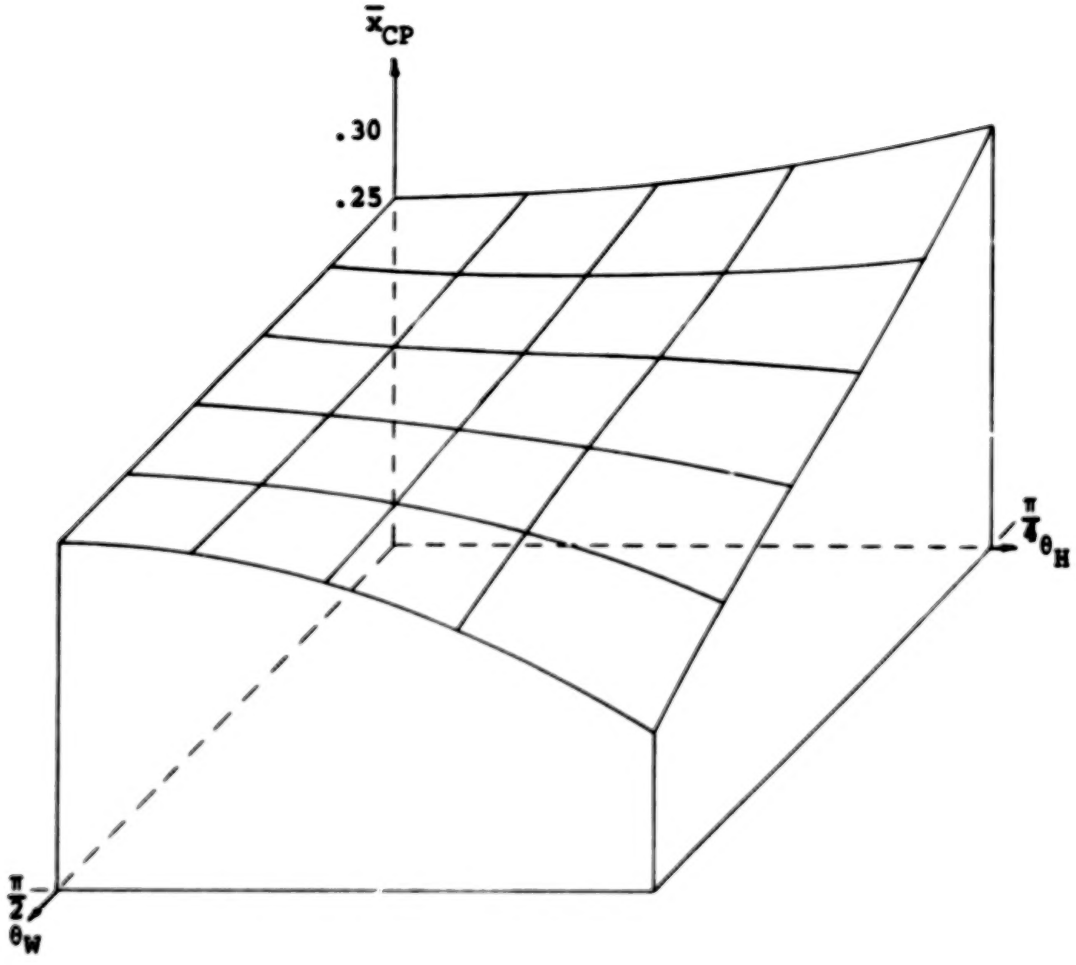

Figure 22. Center of pressure $\bar{x}_{CP}$ vs. depth and ventilation for M=0 and k=0

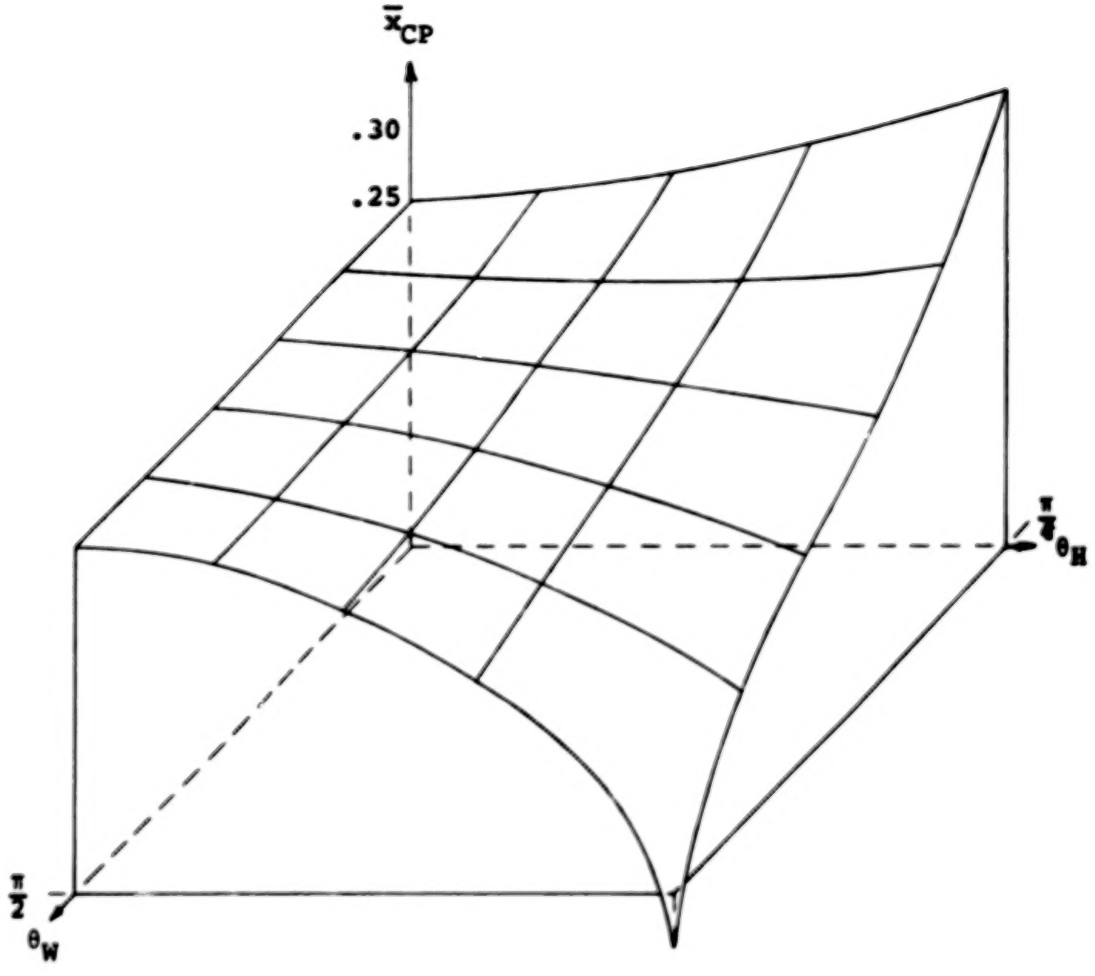

Figure 23. Center of pressure $\bar{x}_{CP}$ vs. depth and ventilation for $M=\frac{1}{\sqrt{2}}$ and k=0

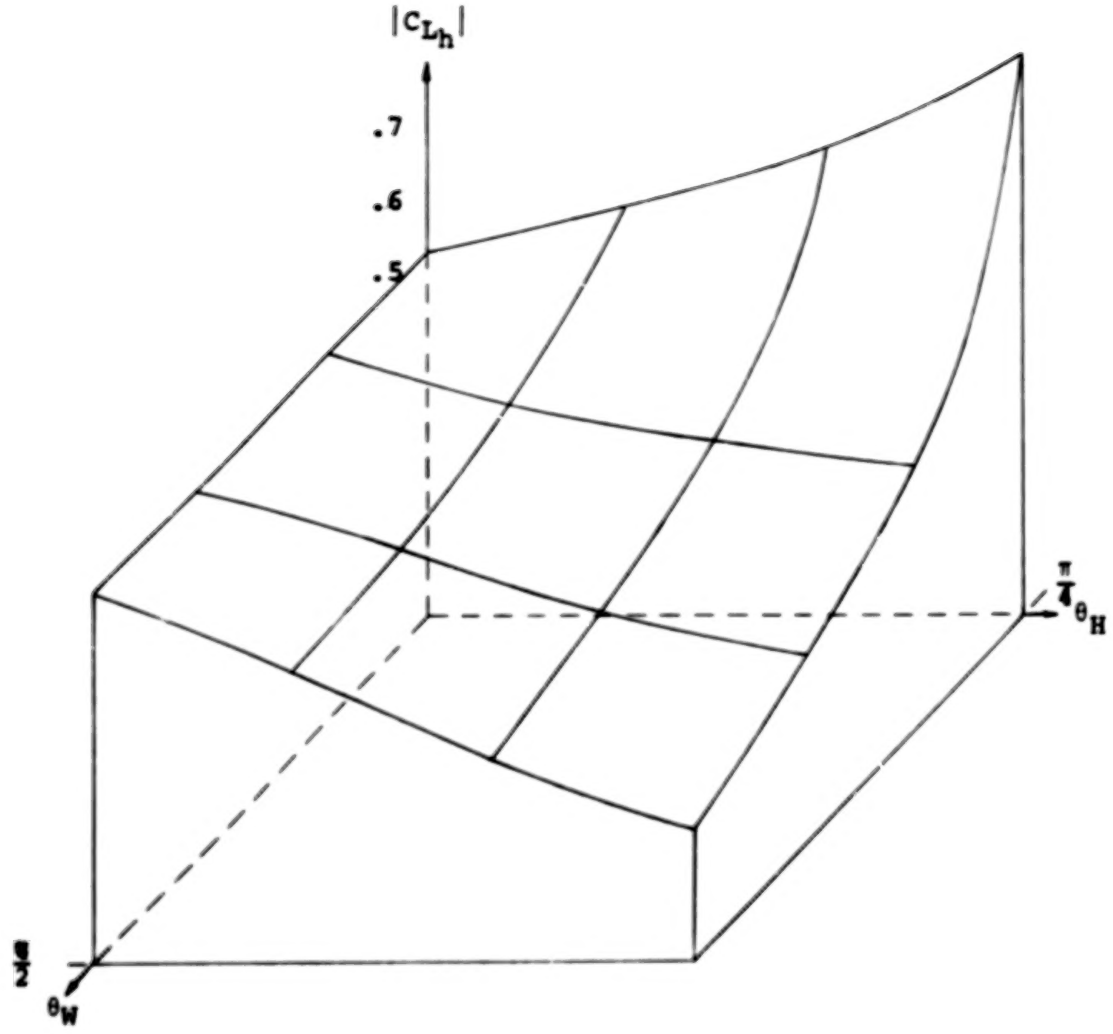

Figure 24. Lift coefficient magnitude $|C_{L_h}|$ vs. depth and ventilation for M=0 and k=.1

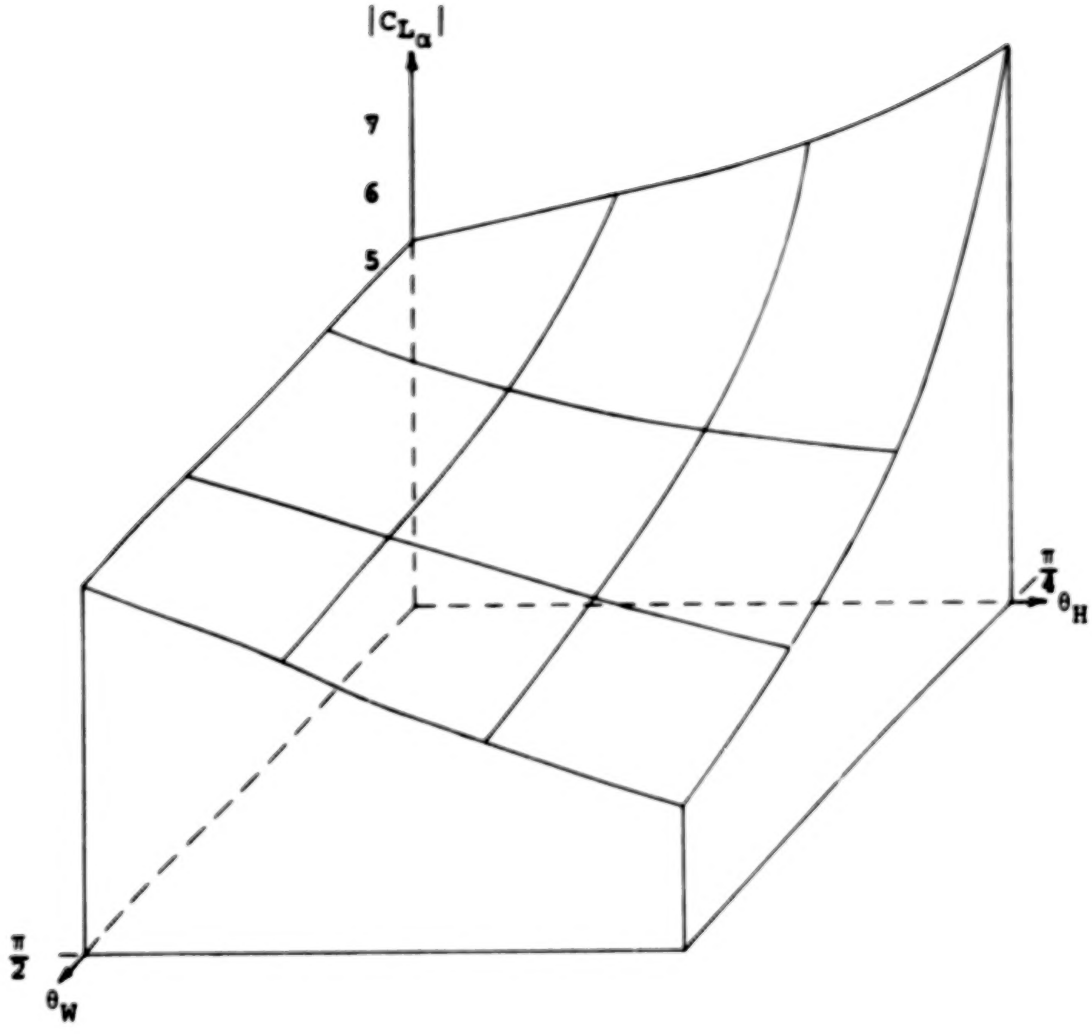

Figure 25. Lift coefficient magnitude $|C_{L_\alpha}|$ vs. depth and ventilation for M=0 and k=.1

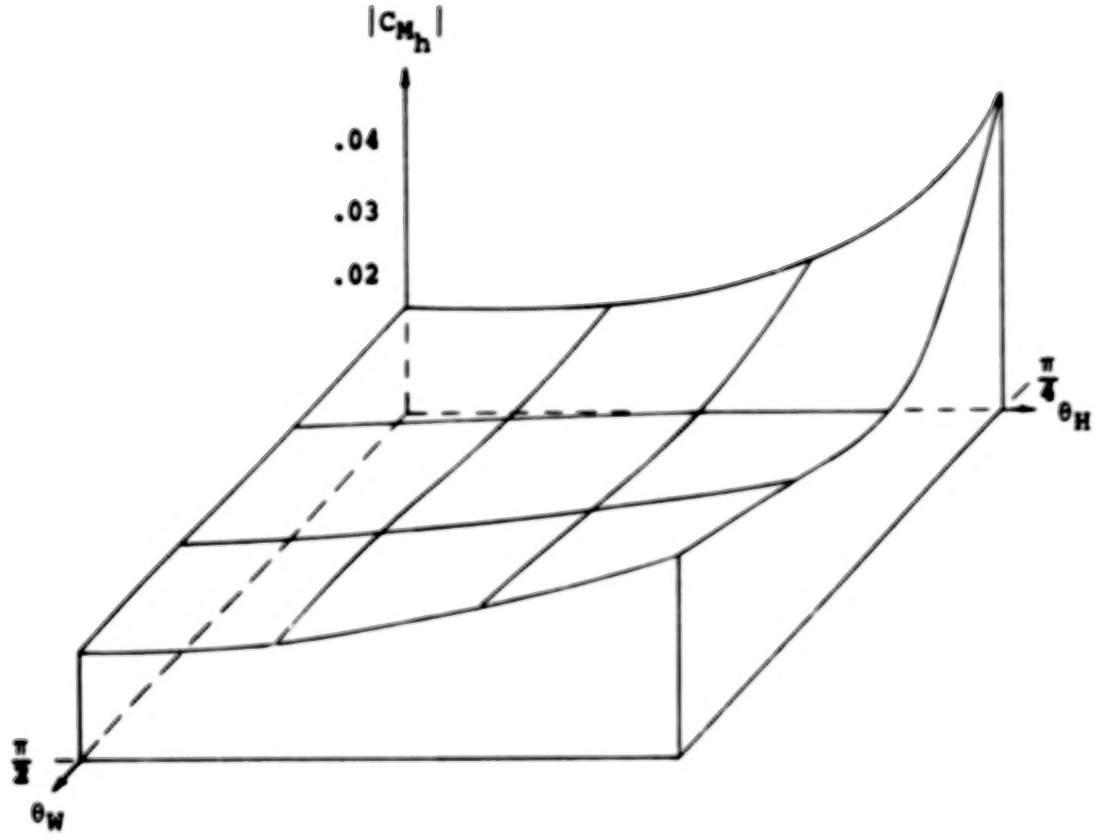

Figure 26. Moment coefficient magnitude $|C_{M_h}|$ vs. depth and ventilation for M=0 and k=.1

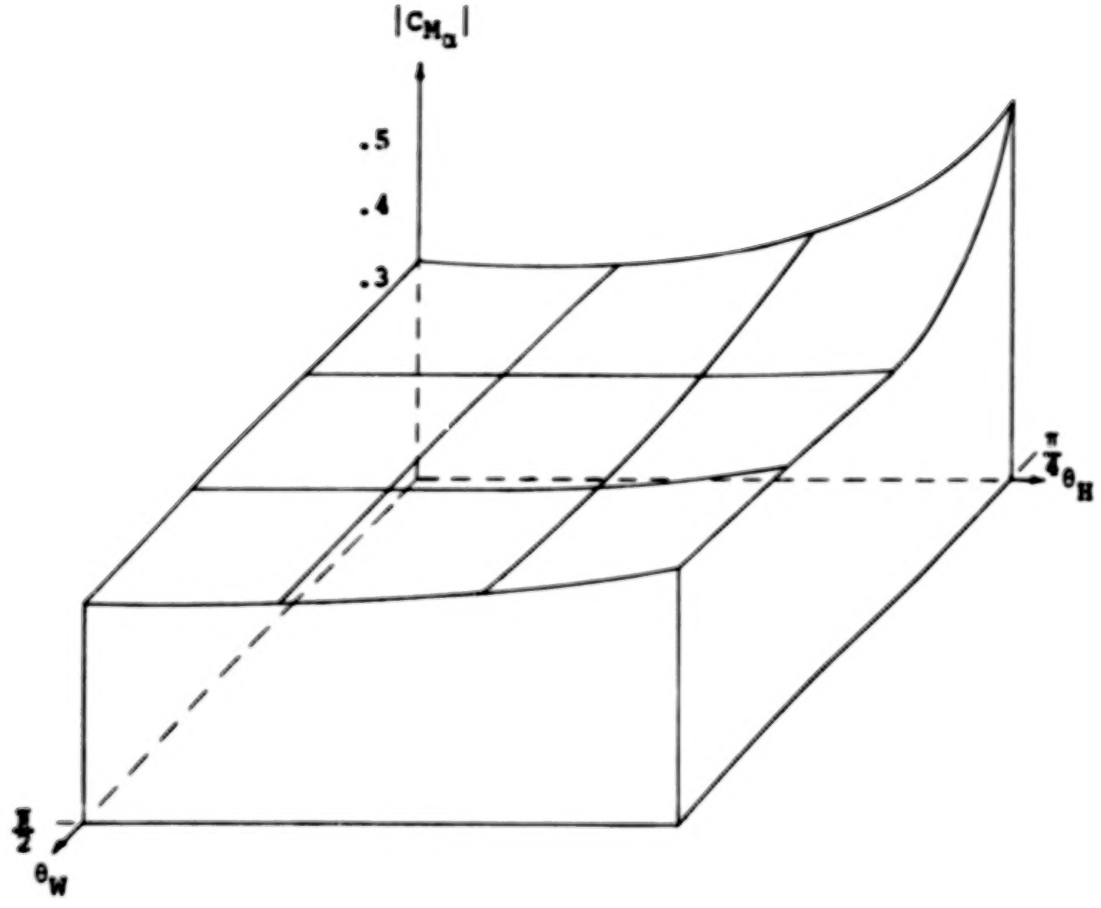

Figure 27. Moment coefficient magnitude $|C_{M_\alpha}|$ vs. depth and ventilation for M=0 and k=.1

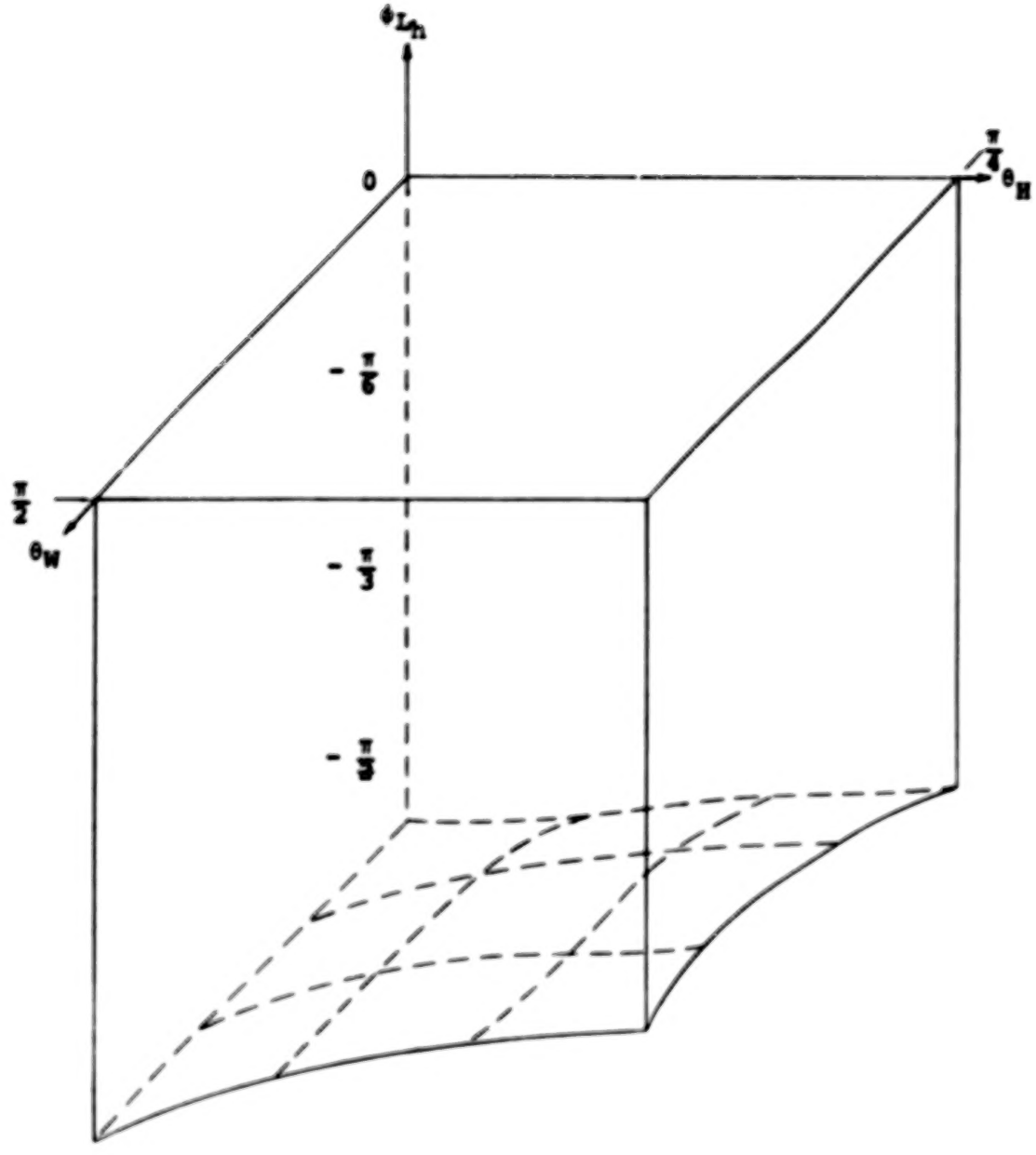

Figure 28. Lift phase angle ϕ_{L_h} vs. depth and ventilation for M=0 and k=.1

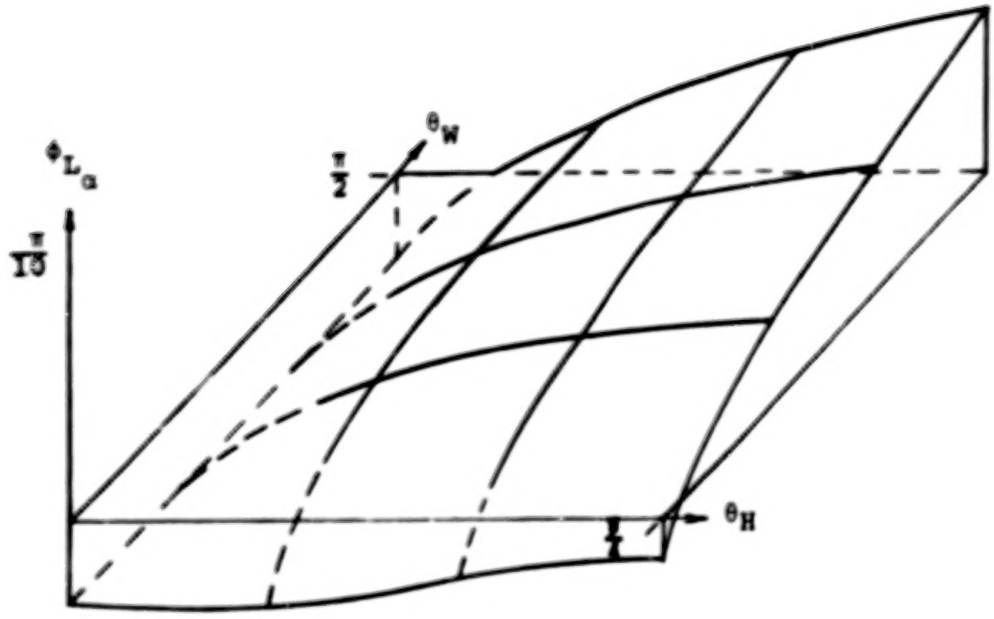

Figure 29. Lift phase angle ϕ_{L_a} vs. depth and ventilation for M=0 and k=.1

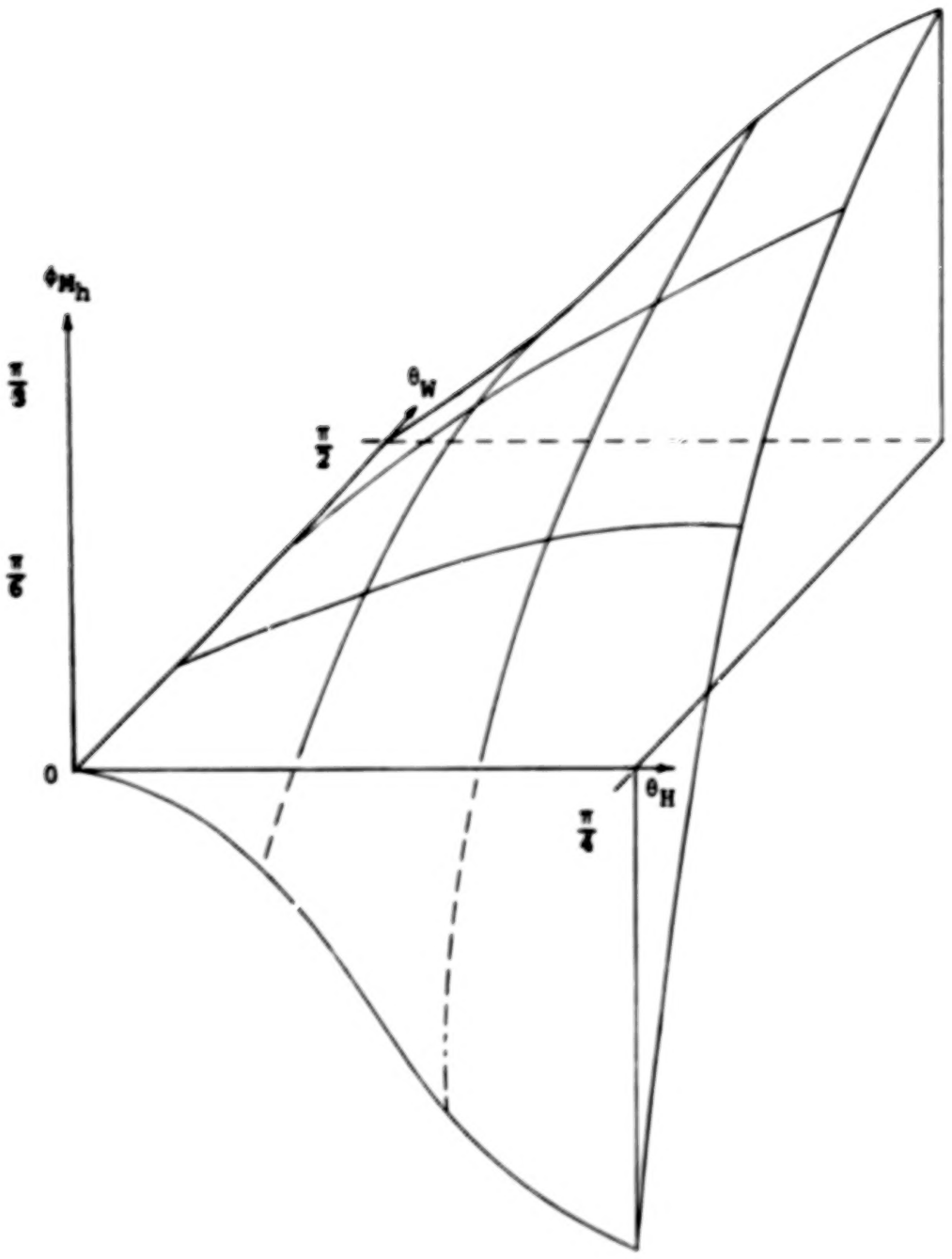

Figure 30. Moment phase angle ϕ_{M_h} vs. depth and ventilation for M=0 and k=.1

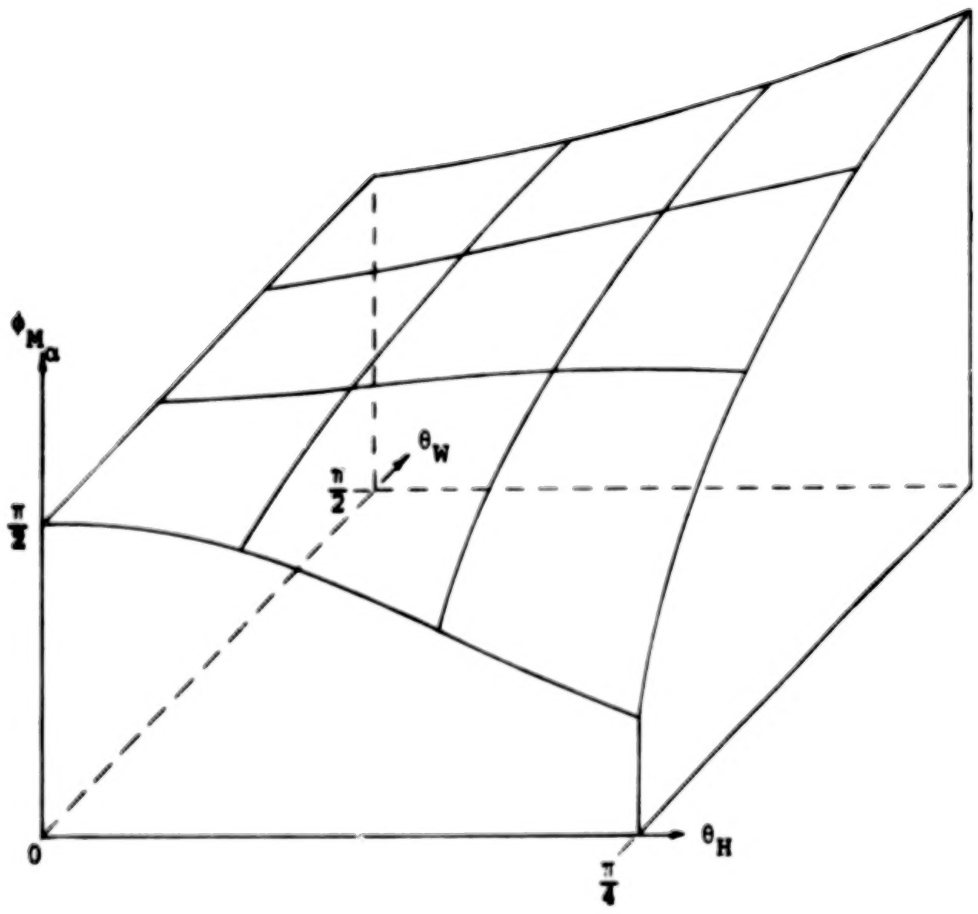

Figure 31. Moment phase angle ϕ_{M_α} vs. depth and ventilation for M=0 and k=.1

§13. Effect of ventilation on airfoil-tunnel acoustic resonance

Acoustic resonance between an airfoil and a ventilated wind tunnel will occur according to the frequency spectrum which is given by

$$k_n = \frac{\beta\lambda_n}{M\eta_H};\ n = 1,2,... \tag{13-1}$$

based on equation (2-53). The values of reduced frequency at which resonance will occur depend upon Mach number, tunnel depth to chord ratio and the ventilation coefficient. The effect of Mach number on the resonant frequencies consists in the factor

$$\frac{\beta}{M},$$

which indicates that resonance can occur only for compressible flow and that the resonant frequencies approach zero as the Mach number approaches one.

The effect of depth to chord ratio on the spectrum is most pronounced in the factor

$$\frac{1}{\eta_H},$$

indicating that narrow tunnels have higher resonant frequencies whereas deeper tunnels have lower resonant frequencies, as is to be expected. Reversing the argument, it may be noted that for a given Mach number and reduced frequency, there exist infinitely many values of depth to chord ratio at which acoustic resonance will occur:

$$\eta_H(n) = \frac{\beta\lambda_n}{Mk},\ n = 1,2,... \tag{13-2}$$

The effect of ventilation coefficient c_W on the frequency spectrum is combined with the depth to chord ratio η_H through the relation

$$\lambda_n = \lambda_n\left(\frac{c_W}{\eta_H}\right). \tag{13-3}$$

Referring to Figure 7, the effect of ventilation is to shift the spectrum within the bounds

$$\text{closed} \cdot \pi\left(n-\frac{1}{2}\right) \leq \lambda_n \leq \pi n \cdot \text{open}$$

so that increasing the amount of ventilation increases the resonant frequencies. The maximum fractional change in frequency that can be brought about by

ventilation alone is to double the fundamental frequency in going from a closed wall to an open jet. This is illustrated by Table 13.

Table 13. Resonant frequencies vs. ventilation coefficient for $M = \frac{\sqrt{3}}{2}$ and $\eta_H = 10$

	$c_W = \infty$ (closed)	$c_W = 1$ (ventilated)	$c_W = 0$ (open)
k_1	.090690	.165282	.181380
k_2	.181380	.332586	.362760
k_3	.272070	.460648	.544140

The effect of acoustic resonance is to cause the pressure to vanish at the resonant frequency. This is illustrated by Figure 32 for a flat plate oscillating about the midchord at $M = \frac{\sqrt{3}}{2}$, with three values of ventilation coefficient corresponding to a closed wall ($c_W = \infty$), a ventilated wall ($c_W = 1$), and an open jet ($c_W = 0$). For comparison, the value of $|C_{L_\alpha}|$ at $M = 0$ is shown also since resonance cannot occur in incompressible flow. The comparison is striking. Whereas the behavior of $|C_{L_\alpha}|$ vs. reduced frequency is smooth for $M = 0$ with the three curves for $c_W = 0,1$, and ∞ merging as the frequency increases, the behavior of $|C_{L_\alpha}|$ for $M = \frac{\sqrt{3}}{2}$ is quite different. The closed wall condition begins with a relatively large value of C_{L_α} at $k = 0$ and drops to 0 at resonance very abruptly, increasing for values of reduced frequency beyond resonance to a maximum value of approximately 60% of its zero frequency value, then dropping to 0 again at the second resonant frequency, and so on. Similar behavior is evidenced by the ventilated wall conditions, beginning with a lower value of C_{L_α} at $k = 0$ and displaying higher resonant frequencies. In all cases the drop to $C_{L_\alpha} = 0$ at resonance is more abrupt below resonance than above, and the abruptness appears to decrease slightly at the higher resonant frequencies. The phase angle is shown in Figure 33 with and without resonance. No resonance occurs for incompressible flow. In all cases a 90 degree phase lag is predicted at resonance, dropping very abruptly above resonance until the next resonant frequency, at which point a 90 degree phase lag occurs again, and so on.

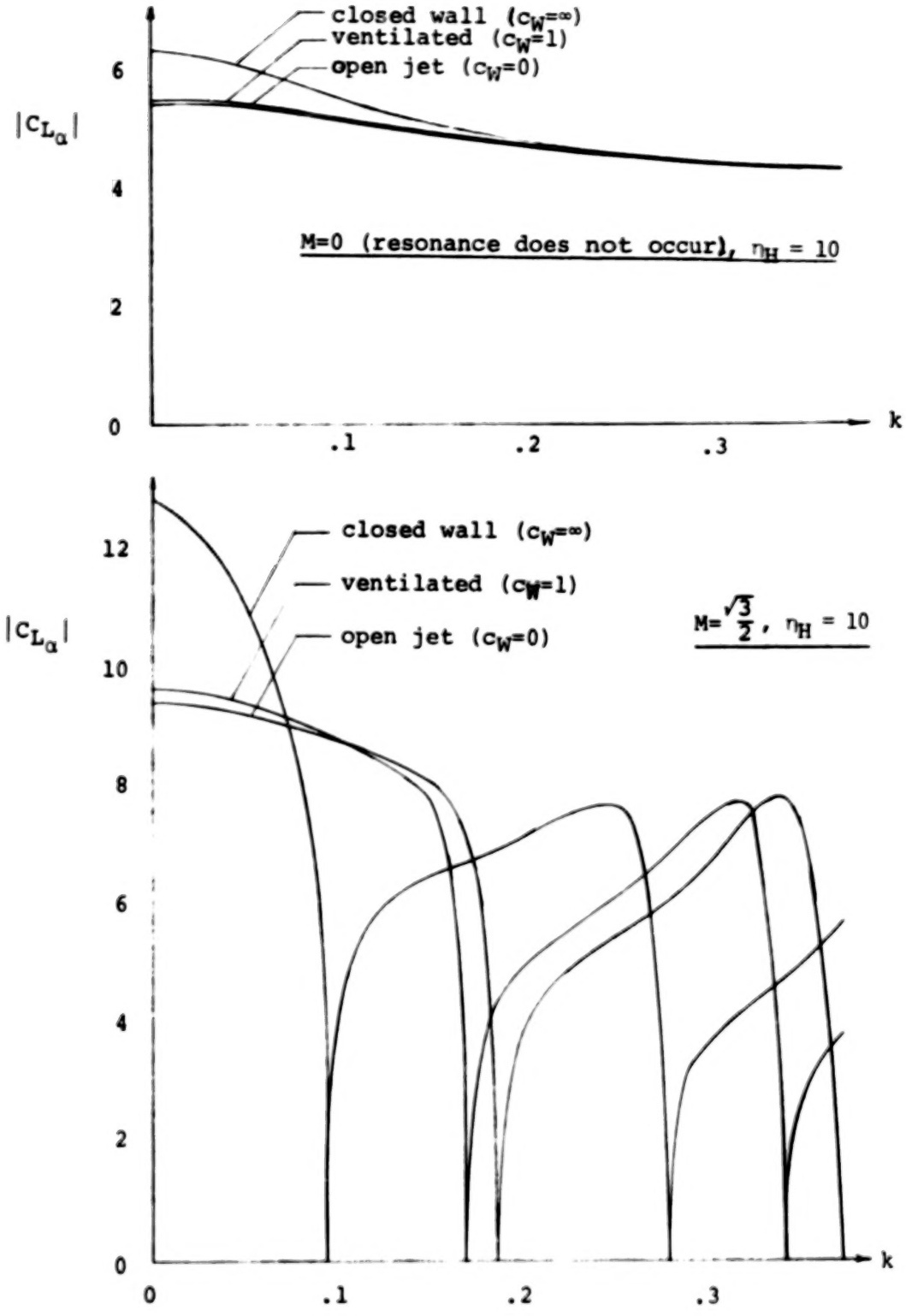

Figure 32. Effect of ventilation on $|C_{L_\alpha}|$ vs. k with acoustic resonance effects

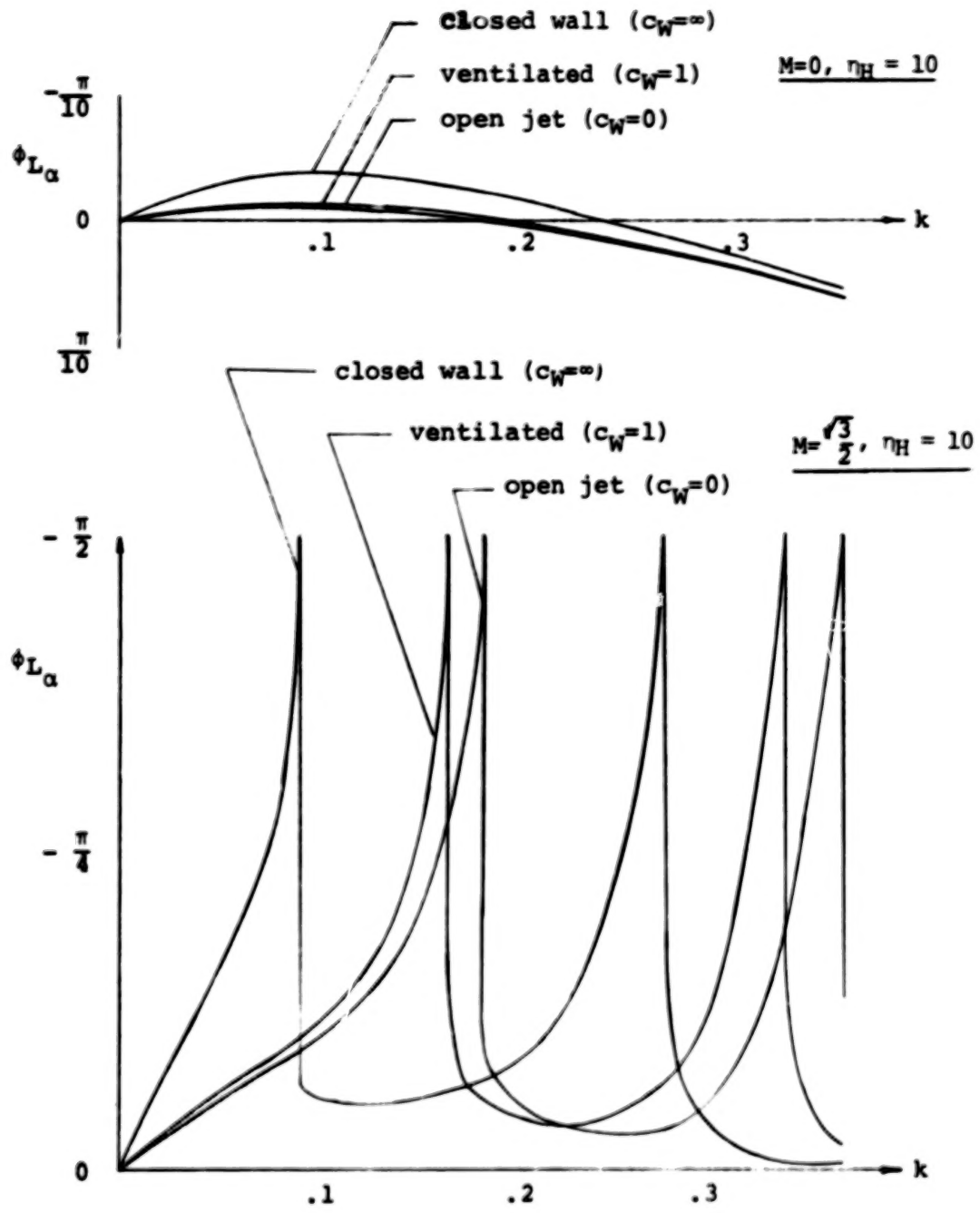

Figure 33. Effect of ventilation on ϕ_{L_α} vs. k with acoustic resonance effects

§14. Concluding remarks

The numerical calculation of unsteady airloads on thin airfoils in subsonic ventilated wind tunnels has been accomplished using Bland's kernel (2-50). Additionally, we have rigorously proved that the collocation method of solving Bland's integral equation (2-57) converges to the mathematically exact solution, and have established a new three-way equivalence between collocation, least squares and Galerkin's method whenever the collocation points are chosen as the nodes of the quadrature rule used for Galerkin's method. This convergence behavior has been demonstrated with the TWODI program. We point out that the convergence proof, given for the first time by this work, applies to an arbitrary kernel whose dominant singularity is of Cauchy type, and is thereby of a general nature. Furthermore the method of proof, based on converting the integral equation to one of the second kind, opens up the way to methods of solution and error estimates not otherwise available for equations of the first kind.

Results from the computer program have been compared with exact closed form solutions in special cases. Using $NP \leq 10$, six decimal accuracy is obtained for steady flow and three decimal accuracy or better is attained for unsteady flow. New results are presented showing the effect of wall ventilation and depth to chord ratio on section coefficients, and on acoustic resonance between the airfoil and the tunnel walls. While these results should improve the confidence and precision of wind tunnel testing, it would be desirable to compare the predictions of the TWODI program with known experimental data, and with future experimental data for unsteady flow in ventilated tunnels as they become available.

Although the TWODI program is already sufficiently accurate for most engineering purposes, large amounts of computer time are required with the pilot version for very deep tunnels, particularly in unsteady flow. This time is largely expended in subroutine SUM, and more efficient numerical algorithms would probably alleviate this difficulty. At higher frequencies, we have observed a deterioration of the rate of solution convergence with respect to the number of pressure basis functions. Preliminary indications

are that the kernel is evaluated accurately but may not be integrated accurately for high frequencies. Since Hsu's interdigitation procedure restricts the number of quadrature points to equal the number of pressure basis functions, it is obvious that for a fixed value of NP, there is a frequency k at which the factor

$$e^{-ikx}$$

in the continuous part of the kernel will render the Jacobi-Gaussian quadrature inaccurate. (This provides additional incentive for improving the efficiency of computing the infinite series in subroutine SUM.) While the physical justification of linearization fails at sufficiently high frequency [89,1948], a high frequency capability enables the complete frequency spectra to be calculated, from which point the response to arbitrary time dependent excitation can follow. It is therefore potentially valuable to study the problem of numerically computing

$$\int_{-1}^{1} e^{-ik(x-\xi)} f(x-\xi)\,d\xi$$

accurately for large k and continuous functions f, using a small number of function evaluations.

Although the convergence proof applies to discontinuous downwash functions as well, the rate of convergence for airfoils with flaps may be expected to be weaker owing to a form of Gibb's phenomenon for generalized Fourier series. Therefore, as a practical matter, it would be desirable to extend the solution method to permit the efficient analysis of multi-control airfoil configurations.

Bland's kernel is based upon a boundary condition which is phenomenologically approximate whenever the tunnel walls are other than fully closed or an open jet. Removal of this restriction awaits a more rational theory for ventilated wind tunnel walls.

REFERENCES

[1] H. Garner, E.W.E. Rogers, W.E.A. Acum and E.C. Maskell: *Subsonic wind tunnel wall corrections*, NATO Advisory Group for Aerospace Research and Development. AGARDograph 109, 1966.

[2] B. Goethert: *Transonic wind tunnel testing*, Pergamon Press, 1961.

[3] H. Glauert: *Wind tunnel interference on wings, bodies and airscrews*, British Aeronautical Research Council R.&M. 1566, 1933.

[4] A. Pope and J.J. Harper: *Low speed wind tunnel testing*, John Wiley and Sons, 1966, New York.

[5] S.R. Bland: *The two dimensional oscillating airfoil in a wind tunnel in subsonic flow*, SIAM J. Appl, Math. 18 (4), 830-848, 1970.

[6] W. Birnbaum: *Die tragende Wirbelfläche als Hilfsmittel zur Behandlung des ebenen Problems der Tragflügeltheorie*, Ztschr. f. angew. Math. und Mech. 3 (4), 277-292, 1923.

[7] M. Munk: *General theory of thin wing sections*, NACA Report 142, 1922.

[8] M. Munk: *Elemen[illegible] of the wing sections theory and of the wing theory*, NACA Report 191, 1924.

[9] V.V. Ivanov: *The theory of approximate methods and their application to the numerical solution of singular integral equations*, translated from the Russian by A. Ideh, ed. by R.S. Anderssen and D. Elliott, Noordhoff International Publishing Co, 1976.

[10] W. Birnbaum: *Das ebene Problem des schlagenden Flügels*, Ph.D. Dissertation, 1922, Universität an Göttingen.

[11] W. Birnbaum: *Das ebene Problem des schlagenden Flügels*, Hauptaufsätze, Ztschr. f. angew. Math. und Mech. 4 (4), 277-292, 1924.

[12] S.R. Bland: *The two dimensional oscillating airfoil in a wind tunnel in subsonic compressible flow*, Doctoral Thesis, North Carolina State University, 1968, Raleigh, N.C.

[13] M. Abramowitz and I.A. Stegun: *Handbook of mathematical functions, National Bureau of Standards A.M.S. 55*, U.S. Government Printing Office, 1964.

[14] C. Possio: *L'azione aerodinamica sul profilo oscillante in un fluido compressibile a velocita iposonora*, L'Aerotechnica, 18 (4), 421-458, 1938.

[15] F. Dietze: *The air forces of the harmonically vibrating wing in a compressible medium at subsonic velocity (plane problem)*, AAF Report No. F-TS-506-RE, 1946. English translation of [49,1944].

[16] C.E. Watkins, H.L. Runyan and D.S. Woolston: *On the kernel function of the integral equation relating the lift and downwash distributions of oscillating finite wings at subsonic speeds*, NACA Report 1234, 1955.

[17] R.L. Bisplinghoff, H. Ashley and R.A. Halfman: *Aeroelasticity*, Addison-Wesley Publishing Co., 1955, Cambridge, Mass.

[18] I.E. Garrick: *Nonsteady wing characteristics, Section F of Aerodynamic components of aircraft at high speeds, Vol. VII of high speed aerodynamics and jet propulsion*, A.F. Donovan and H.R. Lawrence, eds., Princeton University Press, 1957.

[19] Y.C. Fung: *An introduction to the theory of aeroelasticity*, Dover Publications, 1969, New York.

[20] H. Wagner: *Dynamischer Auftrieb von Tragflügeln*, Ztschr. f. angew. Math. und Mech. 5 (1), 17-35, 1925.

[21] H. Glauert: *The force and moment on an oscillating airfoil*, British Aeronautical Research Council R.&M. 1242, 1929.

[22] H.G. Küssner: *Schwingungen von Flugzeugflügeln*, Luftfahrtforschung, 4, 41-62, 1929.

[23] H.G. Küssner: *A review of the two dimensional problem of unsteady lifting surface theory during the last thirty years*, Lecture series 23, Max Planck Institute für Stromungsforschung, Göttingen, 1953.

[24] T. Theodorsen: *General theory of aerodynamic instability and the mechanism of flutter*, NACA Report 496, 1935.

[25] L. Schwarz: *Berechung der Druckverteilung einer harmonisch sich verformenden Tragfläche in ebener Strömung*, Luftfahrtforschung 17 (11/12), 379-386, 1940.

[26] P. Cicala: *Le azioni aerodinamiche sui profili di ala oscillante in presenza di corrente uniforme*, Mem. d. Roy. Acc. d. Sci. d. Torino 2 (68, part 1), 73-98, 1935.

[27] H.G. Küssner: *Zusammenfassender Bericht über den instationären Auftrieb von Flügeln*, Luftfahrtforschung 13, 410-424, 1936.

[28] M.J. Turner, R.W. Clough, H.C. Martin and L.J. Topp: *Stiffness and deflection analysis of complex structures*, J. Aero. Sci. 23 (9), 805-823, 854, 1956.

[29] T. von Kármán and W.R. Sears: *Airfoil theory for nonuniform motion*, J. Aero. Sci. 5 (10), 379-390, 1938.

[30] H.G. Küssner: *Allgemeine Tragflächentheorie*, Luftfahrtforschung 17 (11/12), 370-378, 1940.

[31] J.A. Fromme: *Least squares approach to unsteady kernel function aerodynamics*, J. AIAA 2 (7), 1349-1350, 1964.

[32] H. Söhngen: *Die Lösungen der Integralgleichung*

$$g(x) = \frac{1}{2\pi} \int_{-a}^{a} \frac{f(\xi)}{x-\xi}\, d\xi$$

und deren Anwendung in der Tragflügeltheorie, Mathematische Zeitschrift 45, 245-264, 1939.

[33] N.I. Mushkelishvili: *Singular integral equations*, Wolters-Noordhoff Publishing Co., 1953, Groningen.

[34] H. Söhngen: *Zur Theorie der endlichen Hilbert-Transformation*, Mathematische Zeitschrift 60, 31-51, 1954.

[35] F.G. Tricomi: *On the finite Hilbert transformation*, Quart. J. Math., 2 (2), 199-211, 1951.

[36] F.G. Tricomi: *Integral equations*, Interscience Publishers, 1957, New York.

[37] I.N. Sneddon: *The use of integral transforms*, McGraw-Hill, 1971.

[38] H.G. Küssner: *General airfoil theory*, NACA TM 979, 1940. English translation of [30,1940].

[39] H.G. Küssner and L. Schwarz: *Der schwingende Flügel mit aerodynamisch ausgeglichenem Ruder*, Luftfahrtforschung 17 (11/12), 337-354, 1940.

[40] H.G. Küssner and L. Schwarz: *The oscillating wing with aerodynamically balanced elevator*, NACA TM 991, 1941. English translation of [39,1940].

[41] H.G. Küssner: *Das zweidimensionale Problem der beliebig bewegten Tragfläche unter Berücksichtigung von Partialbewegung der Flussigkeit*, Luftfahrtforschung 17 (11/12), 355-361, 1940.

[42] H. Söhngen: *Bestimmung der Auftriebsverteilung für beliebige instationäre Bewegungen (Ebenes Problem)*, Luftfahrtforschung 17 (11/12), 401-420, 1940.

[43] B. Smilg and L.S. Wasserman: *Application of three-dimensional flutter theory to aircraft structures*, U.S. Army Air Force Technical Report 4798, 1942.

[44] L. Schwarz: *Zahlentafeln zur Luftkraftberechnung der Schwingenden Tragfläche im kompressibler ebener Unterschallströmung*, Forsch. Ber. 1838, 1943.

[45] R.A. Fraser: *Possio's derivative theory for an infinite aerofoil moving at subsonic speeds*, British Aeronautical Research Council R.&M. 2553, 1941.

[46] R.A. Fraser and S.W. Skan: *Influence of compressibility on the flexural-torsional flutter of tapered cantilever wings*, British Aeronautical Research Council R.&M. 5916, 1942.

[47] T. Schade: *Numerische Lösung des Possioschen Integralgleichung der schwingenden Tragfläche in ebener Unterschallströmung*, Deutschen Versuchanstalt für Luftfahrt, Institut für Aerodynamik, ZWB/UM/3209, 3210,3211, 1944.

[48] T. Schade: *Numerical solution of Possio's integral equation for oscillating airfoils in plane subsonic flow*, British Aeronautical Research Council R.&M. 9506, 10108, 1946. English translation of [47,1944].

[49] F. Dietze: *Die Luftkräfte des harmonisch schwingenden Flügels in kompressiblen medium bei Unterschallgeschwindigkeit (Ebenes Problem)*, Deutschen Versuchanstalt für Luftfahrt, Institut für Aerodynamik, ZWB/FB/1733, 1943.

[50] F. Dietze: *Die Luftkräfte des harmonisch schwingenden Flügels in kompressiblen medium bei Unterschallgeschwindigkeit (Ebenes Problem), Teil II, Zahlen-und Curventafeln*, Deutschen Versuchanstalt für Luftfahrt, Institut für Aerodynamik, ZWB/FB/1733-2, 1944.

[51] F. Dietze: *The air forces of the harmonically vibrating wing in a compressible medium at subsonic velocity (planar problem), Part II, Numerical tables and curves*, AAF Report No. F-TS-948-RE, 1947. English translation of [50,1944].

[52] S.N. Karp, S.S. Shu and H. Weil: *Aerodynamics of the oscillating airfoil in compressible flow*, Technical Report No. F-TR-1167-ND, Brown University, 1947.

[53] S.N. Karp and H. Weil: *The oscillating airfoil in compressible flow, Part II. A review of graphical and numerical data*, Technical Report No. F-TR-1195-ND, Brown University, 1948.

[54] M.J. Turner and S. Rabinowitz: *Aerodynamic coefficients for an oscillating airfoil with hinged flap, with tables for a Mach number of 0.7*, NACA TN 2213, 1950.

[55] Y.L. Luke: *Tables of coefficients for compressible flutter calculations*, U.S. Air Force Technical Report 6200, 1950.

[56] H.E. Fettis: *An approximate method for the calculation of non-stationary air forces at subsonic speeds*, USAF WADC TR 52-56, 1952.

[57] J.W. Miles: *Potential theory of unsteady supersonic flow*, Cambridge University Press, 1959.

[58] N.W. McLachlan: *Theory and application of Mathieu functions*, Oxford University Press, 1947.

[59] E. Reissner and S. Sherman: *Compressibility effects in flutter*, Curtis-Wright Corp. Airplane Div. (Buffalo) Report No. SB 240-S-1, 1944.

[60] M.A. Biot: *The oscillating deformable airfoil of infinite span in compressible flow*, Proc. 6th Int. Cong. Appl. Mech., 1946, Paris.

[61] R. Timman: *Beschouwingen over de luchtkrachten op Trillende Vliegtuigvleugels*, Diss. Tech. Hogeschool, 1946, Delft.

[62] M.D. Haskind: *Oscillations of a wing in a subsonic gas flow*, Prikl. Mat. i. Mekh. 11, 129-146, 1947, (in Russian).

[63] M.D. Haskind: *Oscillations of a wing in a subsonic gas flow*, Report No. A9-T-22, Brown University, 1947. English translation of [62,1947].

[64] A.F. Billington: *Harmonic oscillations of an aerofoil in subsonic flow*, ACA Report No. A65, 1949, Melbourne.

[65] R. Timman and I.A. van de Vooren: *Theory of oscillating wing with aerodynamically balanced control surface in a two dimensional compressible flow*, NLL Report F-54, 1949, Amsterdam.

[66] E. Reissner: *On the application of Mathieu functions in the theory of subsonic incompressible flow past oscillating airfoils*, NACA TN 236, 1951.

[67] E. Reissner: *On the application of Mathieu functions in the theory of subsonic compressible flow past oscillating airfoils*, NACA TN 2363, 1951.

[68] R. Timman, A.I. van de Vooren and J.H. Greidenaus: *Aerodynamic coefficients of an oscillating airfoil in two dimensional subsonic flow*, J. Aero. Sci. 18 (12), 797-802, 834, 1951.

[69] E. van Spiegel and A.I. van de Vooren: *On the theory of the oscillating wing in two dimensional subsonic flow*, National Luchtvaartlaboratorium, Report F-142, 1953, Amsterdam.

[70] E.M. de Jager: *Tables of the aerodynamic aileron coefficients for an oscillating wing-aileron system in a subsonic compressible flow*, National Luchtvaartlaboratorium, Report F-155, 1954, Amsterdam.

[71] D.E. Williams: *On the integral equations of two dimensional flutter derivative theory*, British Aeronautical Research Council R.&M. 3057, 1955.

[72] R. Timman: *The aerodynamic forces on an oscillating airfoil between two parallel walls*, Appl. Sci. Res. A3, 31-57, 1951.

[73] H.L. Runyan and C.E. Watkins: *Considerations on the effect of wind tunnel walls on oscillating air forces for two dimensional subsonic compressible flow*, NACA Report 1150, 1953.

[74] H.L. Runyan, D.S. Woolston and A.G. Rainey: *Theoretical and experimental investigation of the effect of tunnel walls on the forces on an oscillating airfoil in two dimensional subsonic compressible flow*, NACA Report 1262, 1956.

[75] S.R. Bland, R.H. Rhyne and H.B. Pierce: *Study of flow-induced vibrations of a plate in narrow channels*. Trans. ASME, Ser. B, 89,824-830, 1967.

[76] R. White and M. Landahl: *Effects of gaps on the loading distributions of planar lifting surfaces*, J. AIAA 6 (4), 626-631, 1968.

[77] M. Landahl: *Pressure loading functions for oscillating wings with control surfaces*, J. AIAA 6 (2), 345-348, 1968.

[78] W. Rowe, J. Sebastian and M. Redman: *Some recent developments in predicting unsteady airloads caused by control surface motions*, J. Aircraft 13 (12), 955-961, 1976.

[79] P.T. Hsu: *Some recent developments in the flutter analysis of low aspect ratio wings*, Proc. National Specialists Meeting on Dynamics and Aeroelasticity, 7-26, 1958, Fort Worth, Texas.

[80] D.D. Davis and D. Moore: *Analytical study of blockage and lift interference corrections for slotted tunnels obtained by the substitution of an equivalent homogeneous boundary for the discrete slots*, NACA RML53E07b, 1953.

[81] N. Dunford and J. Schwarz: *Linear operators - Part I*, Wiley-Interscience, 1967.

[82] S. Agmon: *Lectures on elliptic boundary value problems*, Van Nostrand, 1965.

[83] W.V. Lovitt: *Linear integral equations*, Dover Publications, 1950.

[84] K. Atkinson: *A survey of numerical methods for the solution of Fredholm integral equations of the second kind*, Society for Industrial and Applied Mathematics, 1976.

[85] B.A. Finlayson: *The method of weighted residuals*, Academic Press, 1972.

[86] B. Noble: *Some applications of the numerical solution of integral equations to boundary value problems*, *Conference on the Applications of Numerical Analysis*, Lecture Notes in Mathematics Series, Springer-Verlag, 1971.

[87] R.D. Milne: *Applications of integral equations to fluid flows in unbounded regions*, *Vol. 2 of Finite elements in fluids*, R.H. Gallagher, J.T. Oden, C. Taylor and O.C. Zienkiewicz, eds., John Wiley and Sons, 1975, New York.

[88] J.A. Fromme: *Extension of the subsonic kernel function analysis to incorporate partial span trailing edge control surfaces*, North American Aviation Technical Report NA 64H-209, 1964.

[89] C.C. Lin, E. Reissner and H.S. Tsien: *On two dimensional nonsteady motion of a slender body in a compressible fluid*, J. Math. Phys. 27, 220-231, 1948.

APPENDIX

COMPARISON WITH THE KUSSNER-SCHWARZ SOLUTION USING ETAH = 300
77/05/14. 09.15.51. PAGE 1

```
**********************************************************
*                                                        *
*    CALCULATION OF TWO-DIMENSIONAL UNSTEADY AIRLOADS    *
*                                                        *
*          ACTING ON A THIN FLEXIBLE AIRFOIL             *
*                                                        *
*     OSCILLATING ABOUT ZERO INITIAL ANGLE OF ATTACK     *
*                                                        *
*         MOUNTED AT THE CENTER OF A VENTILATED          *
*                                                        *
*         SUBSONIC COMPRESSIBLE FLOW WIND TUNNEL         *
*                                                        *
**********************************************************
```

NC = 1 NP = 8 NH = 5 NX = 5 NL= 20
SEC = T GAF = T TSH = T

X	H(MODE 1)	H(MODE 2)	H(MODE 3)	H(MODE 4)	H(MODE 5)
-1.000000	1.000000	-3.000000	5.000000	-7.000000	9.000000
-.500000	1.000000	-2.000000	1.000000	1.000000	-2.000000
0.000000	1.000000	-1.000000	-1.000000	1.000000	1.000000
.500000	1.000000	0.000000	-1.000000	-1.000000	0.000000
1.000000	1.000000	1.000000	1.000000	1.000000	1.000000

CASE	MACH NO.	FREQUENCY	ETA-SUB-H	C-SUB-N
1	0.000000	1.000000	300.000	.100000+101

COMPARISON WITH THE KUESSNER-SCHWARZ SOLUTION USING ETAH = 300
77/06/14. 10.35.18. PAGE 2

CASE 1 OF 1

MACH NO.	FREQUENCY	ETA-SUB-H	C-SUB-W
0.	1.00000	300.000	.100000+101

GENERALIZED FOURIER COEFFICIENTS FOR PRESSURES

DOWNWASH MODE 1

1	1.5978504	-2.1566016
2	1.9976928	-.66196353E-03
3	.82992166E-03	-.15446593E-02
4	.12593886E-02	.17347925E-03
5	-.10109623E-04	.24822167E-03
6	-.13093818E-04	.44172770E-07
7	-.44183632E-07	.89937096E-07
8	-.58979141E-07	-.39962815E-08

DOWNWASH MODE 2

1	-6.3108959	-3.1950388
2	-1.0007948	-7.9912048
3	.99346975	-.20178656E-02
4	.10936592E-03	-.52279708E-02
5	.17141097E-02	-.78836227E-04
6	.66934121E-05	.13816818E-03
7	-.62903152E-05	.15822039E-06
8	.55058372E-08	.31627731E-06

DOWNWASH MODE 3

1	-4.3097254	4.7935256
2	-16.981160	.28559312E-02
3	-.23793307	-7.9829999
4	.65289557	-.23505390E-02
5	.10493603E-03	-.82426206E-02
6	.18637804E-02	-.29696394E-04
7	.25951169E-05	.15841547E-03
8	-.35431376E-05	.15061130E-06

COMPARISON WITH THE KUESSNER-SCHWARZ SOLUTION USING ETAH = 300
77/06/14. 10.35.18. PAGE 3

DOWNWASH MODE 4

1	-8.6356097	-2.4011690
2	-7.9923758	-.15184122E-01
3	-24.640903	.48142616E-02
4	-.17623204	-7.3784145
5	.47700769	-.34203605E-02
6	.23241239E-03	-.11615341E-01
7	.20938584E-02	-.89905086E-05
8	.20343227E-05	.14845867E-03

DOWNWASH MODE 5

1	-8.6269218	5.6034186
2	-23.999738	.11720318E-02
3	-7.9922726	-.12659853E-01
4	-32.462010	.51326261E-02
5	-.11459079	-7.9713482
6	.36228735	-.43475968E-02
7	.34180281E-03	-.15953551E-01
8	.24154714E-02	.13114161E-05

COMPARISON WITH THE KUESSNER-SCHWARZ SOLUTION USING ETAH = 300
77/06/14. 10.35.18. PAGE 4

PRESSURES

MODE	X	X/C	REAL	IMAGINARY	MAGNITUDE	PHASE ANGLE
1	-.900000	.050000	.284959E-03	-9.40155	9.40155	-89.998
1	-.800000	.100000	1.20811	-6.46884	6.57922	-79.490
1	-.700000	.150000	1.90365	-5.13165	5.47337	-69.647
1	-.600000	.200000	2.39819	-4.31049	4.93271	-60.910
1	-.500000	.250000	2.76832	-3.73237	4.64695	-53.435
1	-.400000	.300000	3.05101	-3.29132	4.48792	-47.170
1	-.300000	.350000	3.26565	-2.93627	4.39160	-41.960
1	-.200000	.400000	3.42353	-2.63906	4.32264	-37.627
1	-.100000	.450000	3.53144	-2.38258	4.26002	-34.007
1	0.000000	.500000	3.59343	-2.15564	4.19041	-30.959
1	.100000	.550000	3.61156	-1.95048	4.10459	-28.372
1	.200000	.600000	3.58626	-1.76132	3.99544	-26.157
1	.300000	.650000	3.51642	-1.58362	3.85656	-24.244
1	.400000	.700000	3.39913	-1.41348	3.68130	-22.579
1	.500000	.750000	3.22903	-1.24716	3.46151	-21.118
1	.600000	.800000	2.99694	-1.08055	3.18579	-19.827
1	.700000	.850000	2.68663	-.908201	2.83598	-18.678
1	.800000	.900000	2.26586	-.720862	2.37776	-17.648
1	.900000	.950000	1.65186	-.496209	1.72478	-16.720
1	1.000000	1.000000	0.	0.	0.	0.000
2	-.900000	.050000	-22.1166	13.9362	26.1412	147.784
2	-.800000	.100000	-17.2555	4.78967	17.9079	164.487
2	-.700000	.150000	-15.1143	-.675056E-02	15.1143	-179.974
2	-.600000	.200000	-13.7333	-3.20222	14.1017	-166.875
2	-.500000	.250000	-12.6514	-5.53986	13.8111	-156.352
2	-.400000	.300000	-11.7045	-7.32451	13.8074	-147.962
2	-.300000	.350000	-10.8222	-8.70957	13.8916	-141.173
2	-.200000	.400000	-9.97075	-9.78191	13.9679	-135.548
2	-.100000	.450000	-9.13379	-10.5941	13.9879	-130.767
2	0.000000	.500000	-8.30354	-11.1789	13.9254	-126.605
2	.100000	.550000	-7.47705	-11.5560	13.7640	-122.904
2	.200000	.600000	-6.65414	-11.7358	13.4909	-119.553
2	.300000	.650000	-5.83641	-11.7203	13.0931	-116.472

COMPARISON WITH THE KUESSNER-SCHWARZ SOLUTION USING ETAH = 300
77/06/14. 10.38.08. PAGE 5

2	.400000	.700000	-5.02650	-11.5038	12.5540	-113.603
2	.500000	.750000	-4.22769	-11.0703	11.8501	-110.902
2	.600000	.800000	-3.44334	-10.3890	10.9443	-108.337
2	.700000	.850000	-2.67593	-9.40307	9.77642	-105.885
2	.800000	.900000	-1.92400	-7.99723	8.22541	-103.527
2	.900000	.950000	-1.16821	-5.87344	5.98849	-101.249
2	1.000000	1.000000	0.	0.	0.	0.000
3	-.900000	.050000	39.8107	5.58926	40.2011	7.992
3	-.800000	.100000	18.9831	15.3537	24.4150	38.966
3	-.700000	.150000	7.84448	19.7834	21.2819	68.371
3	-.600000	.200000	.137027	21.7247	21.7251	89.639
3	-.500000	.250000	-5.75172	22.1258	22.8612	104.572
3	-.400000	.300000	-10.4495	21.4587	23.8677	115.964
3	-.300000	.350000	-14.2549	20.0112	24.5693	125.464
3	-.200000	.400000	-17.3276	17.9838	24.9732	133.935
3	-.100000	.450000	-19.7591	15.5292	25.1312	141.835
3	0.000000	.500000	-21.6039	12.7733	25.0975	149.406
3	.100000	.550000	-22.8940	9.82604	24.9136	156.771
3	.200000	.600000	-23.6464	6.78949	24.6018	163.980
3	.300000	.650000	-23.8664	3.76377	24.1614	171.038
3	.400000	.700000	-23.5477	.853010	23.5632	177.925
3	.500000	.750000	-22.6696	-1.82716	22.7431	-175.392
3	.600000	.800000	-21.1890	-4.13799	21.5893	-168.950
3	.700000	.850000	-19.0199	-5.89500	19.9125	-162.780
3	.800000	.900000	-15.9758	-6.81261	17.3677	-156.905
3	.900000	.950000	-11.5389	-6.30739	13.1503	-151.338
3	1.000000	1.000000	0.	0.	0.	0.000
4	-.900000	.050000	-57.9898	-10.7160	58.9716	-169.530
4	-.800000	.100000	-10.3804	-23.0932	25.3189	-114.204
4	-.700000	.150000	11.3234	-25.0051	27.4495	-65.637
4	-.600000	.200000	22.4443	-22.5341	31.8046	-45.114
4	-.500000	.250000	27.4200	-17.9662	32.7817	-33.234
4	-.400000	.300000	28.2548	-12.5359	30.9105	-23.924
4	-.300000	.350000	26.1017	-7.01818	27.0287	-15.050
4	-.200000	.400000	21.7403	-1.94244	21.8269	-5.106
4	-.100000	.450000	15.7637	2.32700	15.9346	8.397

COMPARISON WITH THE KUESSNER-SCHWARZ SOLUTION USING ETAH = 300
77/06/14. 10.38.08. PAGE 6

4	0.000000	.500000	8.66429	5.54207	10.2852	32.605
4	.100000	.550000	.879524	7.54837	7.59943	83.354
4	.200000	.600000	-7.13029	8.27314	10.9545	130.955
4	.300000	.650000	-15.1117	7.72111	16.9699	152.936
4	.400000	.700000	-22.4988	5.97701	23.2792	165.123
4	.500000	.750000	-28.8899	3.21609	29.0674	173.648
4	.600000	.800000	-33.7529	-.272434	33.7540	-179.538
4	.700000	.850000	-36.4031	-4.03566	36.6261	-173.674
4	.800000	.900000	-35.7843	-7.33642	36.5286	-168.414
4	.900000	.950000	-29.6948	-8.75209	30.9577	-163.578
4	1.000000	1.000000	0.	0.	0.	0.000
5	-.900000	.050000	31.1405	40.2407	50.8827	52.265
5	-.800000	.100000	-44.9802	41.2824	61.0528	137.455
5	-.700000	.150000	-67.2518	31.9825	74.4693	154.566
5	-.600000	.200000	-67.8793	20.3629	70.8679	163.301
5	-.500000	.250000	-58.9520	9.71526	58.7607	170.483
5	-.400000	.300000	-43.2034	1.55265	43.2312	177.942
5	-.300000	.350000	-27.1849	-3.55274	27.4160	-172.554
5	-.200000	.400000	-12.2385	-5.60663	13.5071	-155.475
5	-.100000	.450000	-.166128	-4.99352	4.99628	-91.905
5	0.000000	.500000	8.07256	-2.34813	8.40714	-16.219
5	.100000	.550000	11.7605	1.53882	11.8607	7.455
5	.200000	.600000	10.6249	5.79789	12.1039	28.621
5	.300000	.650000	4.77267	9.55125	10.6773	63.449
5	.400000	.700000	-5.29617	11.9839	13.1021	113.843
5	.500000	.750000	-18.6395	12.4243	22.4008	146.314
5	.600000	.800000	-33.7547	10.4476	35.3441	162.807
5	.700000	.850000	-48.3910	6.02970	48.7652	172.897
5	.800000	.900000	-58.8496	-.168415	58.8499	-179.836
5	.900000	.950000	-57.9853	-6.05846	58.3010	-174.035
5	1.000000	1.000000	0.	0.	0.	0.000

COMPARISON WITH THE KUESSNER-SCHWARZ SOLUTION USING ETAH = 300
77/06/14. 10.41.12. PAGE 7

SECTION COEFFICIENTS

MODE	COEFF	REAL	IMAGINARY	MAGNITUDE	PHASE ANGLE
1	LIFT	2.50990	-3.38758	4.21608	-53.465
1	MOMENT	1.56898	-.519905E-03	1.56898	-.019
1	X-CP	.471642	.298941	.558401	32.366
2	LIFT	-9.91313	-5.01876	11.1112	-153.148
2	MOMENT	-.786022	-6.27628	6.32531	-97.138
2	X-CP	.568254	.472004	.738715	39.714
3	LIFT	-6.76970	7.52965	10.1254	131.958
3	MOMENT	-13.3370	.224304E-02	13.3370	179.990
3	X-CP	1.13081	.979352	1.49595	40.895
4	LIFT	-13.5648	-3.77175	14.0794	-164.461
4	MOMENT	-6.27720	-.119256E-01	6.27721	-179.891
4	X-CP	.679774	-.118621	.690046	-9.899
5	LIFT	-13.5511	8.80183	16.1588	146.995
5	MOMENT	-18.8494	.920512E-03	18.8494	179.997
5	X-CP	1.22830	.635361	1.38289	27.351

COMPARISON WITH THE KUESSNER-SCHWARZ SOLUTION USING ETAH = 300
77/06/14. 10.41.12. PAGE 8

GENERALIZED AERODYNAMIC FORCES

ROW 1	2.50990	-3.38758	-9.91313	-5.01876
	-6.76970	7.52965	-13.5648	-3.77175
	-13.5511	8.80183		
ROW 2	-1.88183	6.77412	18.2542	-2.51504
	-13.1345	-15.0548	14.5752	7.51964
	-10.5964	-17.6018		
ROW 3	-1.25484	-6.77551	-15.1216	15.0644
	39.2777	2.51067	-40.7266	-7.48823
	35.7489	17.5809		
ROW 4	1.25551	6.77921	13.5613	-15.0695
	-37.7213	10.0253	79.1556	-5.05180
	-74.1779	-17.5537		
ROW 5	-1.25751	-6.77809	-13.5587	15.0776
	36.6959	-10.0346	-78.1295	17.5789
	124.989	5.02429		

1. Report No.	2. Government Accession No.	3. Recipient's Catalog No.
NASA CR-2967		

4. Title and Subtitle	5. Report Date
Unsteady Two Dimensional Airloads Acting on Oscillating Thin Airfoils in Subsonic Ventilated Wind Tunnels	May 1978
	6. Performing Organization Code
7. Author(s)	8. Performing Organization Report No.
Joseph Fromme and Michael Golberg	
9. Performing Organization Name and Address	10. Work Unit No.
University of Nevada at Las Vegas Las Vegas, Nevada 89154	11. Contract or Grant No.
	NSG-2140
12. Sponsoring Agency Name and Address	13. Type of Report and Period Covered
National Aeronautics and Space Administration	Contractor Report
	14. Sponsoring Agency Code

15. Supplementary Notes

16. Abstract

The numerical calculation of unsteady two dimensional airloads which act upon thin airfoils in subsonic ventilated wind tunnels is studied. Neglecting certain quadrature errors, Bland's collocation method is rigorously proved to converge to the mathematically exact solution of Bland's integral equation, and a new three-way equivalence is established between collocation, Galerkin's method and least squares whenever the collocation points are chosen to be the nodes of the quadrature rule used for Galerkin's method. The computer program displays remarkable convergence with respect to the number of pressure basis functions employed, and agreement with known special cases is demonstrated. New results are obtained for the combined effects of wind tunnel wall ventilation and wind tunnel depth to airfoil chord ratio, and for acoustic resonance between the airfoil and wind tunnel walls. A new boundary condition is proposed for permeable walls through which mass flow rate is proportional to pressure jump, and promising research areas for further work are discussed.

17. Key Words (Suggested by Author(s))	18. Distribution Statement
Unsteady aerodynamics, ventilated wind tunnels, subsonic flow, aero-elasticity, structural dynamics, two dimensional aerodynamics, integral equations, computational fluid dynamics	UNCLASSIFIED-UNLIMITED STAR Category - 02

19. Security Classif. (of this report)	20. Security Classif. (of this page)	21. No. of Pages	22. Price*
UNCLASSIFIED	UNCLASSIFIED	137	$4.75

*For sale by the National Technical Information Service, Springfield, Virginia 22161

NASA-Langley, 1978

END

9. 19. 78